UNIWERSYTET ŚLĄSKI
W KATOWICACH

Instytut Fizyki
im. Augusta Chełkowskiego

ZAKŁAD BIOFIZYKI I FIZYKI MOLEKULARNEJ

PRACA DOKTORSKA:

Badanie kinetyki reakcji polimeryzacji w różnych warunkach termodynamicznych (*T*, *p*)

mgr Magdalena Tarnacka

promotor pracy:
dr hab. Kamil Kamiński

KATOWICE 2016

Chciałabym serdecznie podziękować
dr hab. Kamilowi Kamińskiemu za wskazanie interesującej tematyki, życzliwość, poświęcony czas oraz ogromne wsparcie merytoryczne, a także pomoc przy redagowaniu niniejszej pracy.

Składam również serdecznie podziękowania panu prof. dr hab. Marianowi Paluchowi za umożliwienie prowadzenia badań na Zakładzie Biofizyki i Fizyki Molekularnej, a także cenne uwagi i wszechstronną pomoc.

Ponadto chciałabym podziękować całej grupie badawczej za owocną współpracę i czas poświęcony na wykonanie eksperymentów.

Do powstania niniejszej rozprawy doktorskiej w znaczącym stopniu przyczyniło się stypendium, otrzymane przeze mnie w ramach programu „DoktoRIS – Program stypendialny na rzecz innowacyjnego Śląska" współfinansowanego przez Unię Europejską w ramach Europejskiego Funduszu Społecznego.

Ponadto temat niniejszej rozprawy doktorskiej był realizowany w ramach programu SONATA Narodowego Centrum Nauki pt. „*Polimeryzacja wysokociśnieniowa. Badania nad kinetyką procesu*." na podstawie decyzji DEC-2012/05/D/ST4/00326.

KAPITAŁ LUDZKI
NARODOWA STRATEGIA SPÓJNOŚCI

UNIA EUROPEJSKA
EUROPEJSKI
FUNDUSZ SPOŁECZNY

Streszczenie

Praca zawiera wyniki systematycznych badań nad kinetyką reakcji polimeryzacji prowadzonych w warunkach podwyższonego ciśnienia oraz układach ograniczonych przestrzennie monitorowanych za pomocą szerokopasmowej spektroskopii dielektrycznej. Polimeryzacje indukowane ciśnieniem stanowią innowacyjne rozwiązanie problemu uzyskania polimerów o bardzo wysokich masach cząsteczkowych lub określonej konfiguracji. Ciśnienie wywierane na reagujący układ pozwala na maksymalne uproszczenie jego elementów oraz prowadzenie reakcji polimeryzacji bez potrzeby stosowania rozpuszczalników, inicjatorów oraz katalizatorów bardzo często o skomplikowanych strukturach i złożonych mechanizmach działania. Ponadto również reakcje prowadzone w warunkach ograniczenia przestrzennego wyznaczają nowy kierunek badań rozwijających możliwość syntezy materiałów o całkowicie kontrolowanej morfologii tzw. nanodrutów, nanowłókien, o unikalnych własnościach fizykochemicznych, które w znaczącym stopniu mogą przyczynić się do rozwoju nanotechnologii.

W pracy zaprezentowano wpływ ciśnienia na przebieg dwóch typów reakcji: (*i*) polimeryzacji jonowej glicydolu oraz (*ii*) polimeryzacji żywic epoksydowych i różnych amin pierwszorzędowych. Przeprowadzone badania jednoznacznie wykazały wyraźną korelację między wartością przyłożonego na reagujący układ ciśnienia a szybkością reakcji, wartością objętości aktywacji (ΔV) oraz właściwościami powstającego polimeru (takimi jak: rozkład mas cząsteczkowych, temperaturę zeszklenia). Zaobserwowano również, że wartości ΔV zmienia się wraz z warunkami termodynamicznymi procesu powodując zmianę ścieżki kinetycznej reakcji chemicznej i eliminacje reakcji pobocznych (takich jak m.in. makrocyklizacja). Ponadto w przypadku reakcji prowadzonych w układach ograniczonych przestrzennie, szybkość badanego procesu wzrasta wraz ze zwiększeniem ograniczenia geometrii reagującego układu. Mimo, iż energia aktywacji procesu jest stała i niezależna od zastosowanego ograniczenia przestrzennego.

Uzyskane wyniki niosą za sobą bardzo duży walor poznawczy z uwagi na fakt, że w literaturze brak jest systematycznych badań w danej tematyce. Ponadto w szerszej perspektywie pozwolą one na lepsze i bardziej świadome kontrolowanie przebiegu reakcji chemicznych, co w przyszłości może zaowocować nowymi metodami syntezy polimerów, jak i nowatorskimi zastosowaniami nanomateriałów w przemyśle, głównie nanotechnologii.

Niniejsza rozprawa doktorska pt. **„Badanie kinetyki reakcji polimeryzacji w różnych warunkach termodynamicznych (*T, p*)"** stanowi zbiór czterech artykułów naukowych opublikowanych w recenzowanych czasopismach, znajdujących się na liście filadelfijskiej:

Lp.	Publikacja	str.	aktualny Impact Factor czasopisma	aktualna liczna punktów MNiSW czasopisma
A1.	M. Tarnacka, T. Flak, M. Dulski, S. Pawlus, K. Adrjanowicz, A. Swinarew, K. Kaminski, M. Paluch, **High Pressure Polymerization of Glicydol. Kinetics Studies**, *Polymer* 2014, **55**, 1984-1990	28	3.562	40
A2.	M. Tarnacka, O. Madejczyk, M. Dulski, M. Wikarek, S. Pawlus, K. Adrjanowicz, K. Kaminski, and M. Paluch, **Kinetics and Dynamics of the Curing System. High Pressure Studies**, *Macromolecules* 2014, **47,** 4288–4297	36	5.800	45
A3.	M. Tarnacka, M. Wikarek, S. Pawlus, K. Kaminski, M. Paluch, **Impact of high pressure on the progress of polymerization of DGEBA cured with different amine hardeners. Dielectric and DSC Studies**, *RSC Advances* 2015**, 5**, 105934-105942	47	3.840	35
A4.	M. Tarnacka, M. Dulski, S. Starzonek, K. Adrjanowicz, E. U. Mapesa, K. Kaminski, M. Paluch, **Following Kinetics and Dynamics of DGEBA-aniline Polymerization in Nanoporous Native Alumina Oxide Membranes - FTIR and Dielectric Studies**, *Polymer* 2015, **68**, 253-261	57	3.562	40

Spis treści

Wstęp

Zgodnie z nomenklaturą Międzynarodowej Unii Chemii Czystej i Stosowanej (ang. *International Union of Pure and Applied Chemistry*, *IUPAC*), polimerem jest substancja złożona z makrocząsteczek i powstająca w wyniku procesu polimeryzacji, będącej procesem przemiany monomeru lub mieszaniny monomerów [1,2]. Warto jednak wspomnieć, że reakcje polimeryzacji są bardzo zróżnicowane, czego wynikiem jest wiele występujących w literaturze prób ich klasyfikacji. Jedna z głównych i obowiązujących od lat 50. XX wieku bierze pod uwagę: (*i*) sposób reagowania cząsteczek monomeru między sobą oraz (*ii*) zależność pomiędzy stopniem polimeryzacji a stopniem konwersji monomeru, dzieląc reakcje polimeryzacji na biegnące stopniowo lub łańcuchowo.

Polimeryzacja stopniowa (ang. *step-growth polymerization*) jest procesem charakteryzującym się sukcesywnym wzrostem stopnia polimeryzacji w trakcie trwania procesu. A długie łańcuchy polimerowe otrzymuje się dopiero przy bardzo wysokich stopniach konwersji. Reakcja ta zachodzi na skutek reakcji grup funkcyjnych występujących w monomerach i bardzo często towarzyszy jej wydzielenie małocząsteczkowego produktu ubocznego. Do polimeryzacji stopniowej zalicza się polikondensację oraz poliaddycję.

Polimeryzacja łańcuchowa (ang. *chain-growth polymerization*) zakłada powstawanie polimeru w wyniku trzech zachodzących kolejno etapów: inicjacji, propagacji oraz terminacji. Do zapoczątkowania reakcji niezbędny staje się układ inicjujący (inicjator lub katalizator), który reaguje z monomerem tworząc centra aktywne. W trakcie trwania procesu kolejne cząsteczki monomeru przyłączają się do powstałego centrum, powodując wzrost łańcucha powstającego polimeru. Etap propagacji trwa aż do momentu, w którym nie nastąpi dezaktywacja centrów aktywnych wyznaczająca zakończenie reakcji. W przeciwieństwie do polimeryzacji stopniowej, już przy niewielkim stopniu przereagowania w układzie znajdują się polimery o wysokim stopniu polimeryzacji [3,4]. W zależności od sposobów generowania centrów aktywnych w układzie reagującym, reakcje te można podzielić na 3 główne grupy polimeryzacji [5]: (*i*) rodnikową, (*ii*) jonową (kationową i anionową) oraz (*iii*) koordynacyjną. Z czego najlepiej poznane są łańcuchowe polimeryzacje rodnikowe, które odgrywają dominująca rolę w przemyśle produkcji związków wielkocząsteczkowych [6].

Należy jednak podkreślić, że dynamiczny rozwój przemysłu wymaga produkcji materiałów o ściśle zdefiniowanej budowie oraz właściwościach, czego owocem jest intensywny rozwoju syntezy organicznej umożliwiający swobodne kontrolowanie procesu polimeryzacji, a także otrzymywanie zaplanowanych struktur polimerów. W ciągu ostatnich lat zostało zaprojektowane wiele nowych metod chemicznych, z których niewątpliwie najważniejszymi są:

a) polimeryzacja z trwałym wolnym rodnikiem (ang. *Stable Free Radical Polymerization – SFRP* [7,8,9]);
b) polimeryzacja rodnikowa z przeniesieniem atomu (ang. *Atom Transfer Radical Polymerization – ATRP* [10,11,12]);
c) polimeryzacja z odwracalnym addycyjno-fragmentacyjnym przeniesieniem łańcucha (ang. *Reversible Addition-Fragmentation Chain Transfer Polymerizatin - RAFT* [13,14,15]).

Jak można zaobserwować głównym narzędziem zwiększającym kontrole nad przebiegiem reakcji polimeryzacji jest modyfikacja chemiczna reagujących układów. Jednak ważnym czynnikiem przyspieszającym lub wręcz inicjującym reakcję polimeryzacji może być również kompresja układu. Metoda ta została zaproponowana przez Percy'iego W. Brigmanna, który po raz pierwszy wykorzystał warunki wysokiego ciśnienia (12 000 atm) do polimeryzacji izoprenu otrzymując twarde, transparentne ciało stałe podobne do gumy (*rubber-like*) ze 100% wydajnością. Ponadto za wynalezienie aparatury do wytwarzania skrajnie wysokich ciśnień i za odkrycia, których dokonał przy jej użyciu w dziedzinie fizyki wysokich ciśnień została mu przyznana w roku 1946 nagroda Nobla. Pomimo, iż przez wiele lat tematyka kompresji reakcji chemicznych była prawie w ogóle nieporuszana to ostatnie doniesienia literaturowe pokazują, że w warunkach wysokiego ciśnienia możliwe jest otrzymanie polimerów o konkretnej strukturze przy jednoczesnym maksymalnym uproszczeniu metody ich syntezy, co zostało pokazane na przykładzie polimeryzacji etylenu [16] i 1,3-butadienu [17].

Przemysłowo polimeryzację etylenu prowadzi się w reaktorach rurowych lub typu autoklawowego przy zastosowaniu odpowiednich inicjatorów (zwykle wodorotlenki), katalizatorów (tlenku chromu (VI), osadzonego na nośniku zbudowanym z tlenku krzemu i tlenku glinu) oraz rozpuszczalników (m.in. węglowodorów alifatycznych) w wyniku wielu kolejnych cykli zawracania nieprzereagowanego monomeru (wydajność jednego cyklu

wynosi ok. 20 %). Podobne wyniki uzyskano dla polimeryzacji etylenu prowadzonej wyłącznie w warunkach wysokiego ciśnienia (3.3 GPa oraz 5.4 GPa), która przebiega bardzo powoli przy niewielkim stopniu przereagowania monomeru powodując powstanie polietylenu o małej gęstości (ang. *low-density polyethylene, LDPE*). Jednak obniżenie ciśnienia (do 0.7-1.4 GPa) oraz naświetlanie reagującego układu promieniowaniem laserowym o różnej długości fali spowodowało znaczący wzrost szybkości oraz wydajności badanego procesu. Zaobserwowano istotną korelację między długością wykorzystanego promieniowania a szybkością procesu. Najlepsze wyniki zostały uzyskane dla układów naświetlanych promieniowaniem o jednej długości λ = 468 nm oraz jednoczesnym naświetlaniu dwoma długościami fali λ=351+364 nm. Odpowiedni dobór warunków ciśnienia oraz długości fali wykorzystanego promieniowania umożliwił otrzymanie polietylenu o dużej gęstości (ang. *high-density polyethylene, HDPE*) w bardzo krótkim czasie, który pod ciśnieniem 1.4 GPa wynosił 2 godziny przy całkowitej konwersji monomeru [16].

W przypadku 1,3-butadienu sytuacja jest jeszcze trudniejsza, gdyż monomer ten niebywale szybko ulega reakcji dimeryzacji, których produkt jest uzależniony od mechanizmu reakcji i tak możliwej jest otrzymanie: (*i*) 1,2- diwinylocyklobutan w wyniku cykloaddycji [2π +2π]; (*ii*) 4-winylocyklohensen poprzez cykloaddycję [4π +2π] oraz (*iii*) 1,5- cyklooktadien w wyniku reakcji Dielsa-Aldera [4π +4π]) [18]. Dlatego też proces jego polimeryzacji wymaga bardzo restrykcyjnych warunków i prowadzi do powstania mieszaniny izomerów *cis*- i *trans*-butadienu. Jednak przy odpowiednich warunkach ciśnienia (p = 0.8 GPa) oraz naświetlaniu próbki promieniowaniem o długości fali λ = 488 nm możliwe jest całkowite zahamowanie reakcji dimeryzacji 1,3-butadienu oraz skierowanie reakcji wyłącznie w kierunku powstania czystego *trans*-polibutadienu [17].

Podobną, choć już nie tak spektakularną selektywność reakcji indukowanej ciśnieniem zaobserwowano również w przypadku izoprenu [19], gdzie przyłożone na reagujący układ ciśnienie faworyzuje albo proces polimeryzacji albo reakcje dimeryzacji (prowadzące do powstania 7 różnych produktów [20]) w zależności od wartości. Dla procesu indukowanego wyłącznie ciśnieniem w zakresie p = 1.1 – 1.5 GPa uprzywilejowane stają się dimeryzację, które w powyższych warunkach są niezwykle selektywne prowadząc do powstania jedynie jednego produktu – sylwestrenu. Natomiast zastosowanie promieniowania o długości fali λ = 458 nm ponownie powoduje całkowite zahamowanie

tworzenia dimerów. Ponadto badana reakcja znacznie przyspiesza wraz z kompresją układu w stosunkowo niskim zakresie ciśnień (do 2 GPa). Jednak dalszy wzrost ciśnienia powoduje jej zwolnienia i ostatecznie zahamowanie w ciśnieniu powyżej 3 GPa. Zachowanie to dyskutowane jest w literaturze w kontekście zmiany wartości objętości aktywacji procesu, opisującej mechanizm zachodzącej reakcji. Zaobserwowano, że wzrasta ona wraz ze wzrostem ciśnienia – od -24.3 cm^3/mol w warunkach atmosferycznych do -7.9 cm^3/mol w ciśnieniu 2 GPa [19]. Warto wspomnieć, że zgodnie z teorią stanów przejściowych (ang. *the transition-state theory*), objętość aktywacji jest różnicą obojętności między stanem przejściowym ($V^{\#}$) a reagentami (V^R) i może zostać wyznaczony z danych eksperymentalnych zgodnie z poniższym równaniem:

$$\Delta V = RT\left(\frac{\partial \ln k}{\partial p}\right)_T = V^{\#} - V^R, \qquad (1)$$

gdzie R to stała gazowa, T – temperatura, a k – stała szybkości reakcji. W syntezie organicznej, wielkość ta umożliwia zrozumienie mechanizmu reakcji chemicznej, który określany jest poprzez konkretne wartości ΔV (np. dla reakcji otwarcia pierścienia epoksydowego wynosi ona ok. - 15 cm^3/mol). W tym kontekście powyższe badania nad kinetyką reakcji oraz objętością aktywacji wydają się niezbędne do zrozumienia mechanizmu polimeryzacji indukowanej ciśnieniem oraz określeniem wpływ p na szybkość oraz kierunek badanego procesu. Tym bardziej, że jak zostało zaobserwowane wartość ΔV w znaczący sposób zależy od warunków termodynamicznych wpływając tym samym na ścieżki kinetyczne polimeryzacji i eliminując reakcje uboczne [19]. Przedstawione powyżej wyniki badań pokazują wyraźnie, że ciśnienie może być tym parametrem, który zapewnia selektywność reakcji i prowadzić w konsekwencji do otrzymania makrocząsteczek o ściśle określonej strukturze chemicznej, której nie można uzyskać poprzez standardowe metody polimeryzacji.

Polimeryzacje indukowane ciśnieniem stanowią innowacyjne rozwiązanie problemu uzyskania polimerów o bardzo wysokich masach cząsteczkowych lub określonej konfiguracji. Ciśnienie wywierane na reagujący układ pozwala na maksymalne uproszczenie jego elementów oraz prowadzenie reakcji polimeryzacji bez potrzeby stosowania rozpuszczalników, inicjatorów oraz katalizatorów bardzo często o skomplikowanych strukturach i złożonych mechanizmach działania. Choć wyraźne

walory ekonomiczne oraz ekologiczne polimeryzacji indukowanej ciśnieniem świadczą o jej wielkim potencjale gospodarczym, to trzeba jednak wspomnieć, że zakres ciśnień jakim obecnie dysponuje przemysł wciąż uniemożliwia jej wykorzystanie w skali globalnej. Niemniej jednak należy pamiętać, że perspektywa odpowiednich reaktorów ciśnieniowych w kontekście obecnego niezwykle dynamicznego rozwoju techniki to zapewne nieodległa przyszłość, tym bardziej, że warunki wysokiego ciśnienia są już z powodzeniem wykorzystywane w przemyśle spożywczym m.in. do konserwacji soków owocowych.

Pomimo, iż reakcje indukowane ciśnieniem stanowią nowatorską metodę polimeryzacji to wciąż brakuje systematycznych badań nad ich mechanizmem oraz kinetyką. Jak można zauważyć szybkość procesu polimeryzacji określonych monomerów na ogromne znaczenia technologiczne, ponieważ jej znajomość pozwala na określenie czasu potrzebnego do wytworzenia produktu polimerowego o pożądanej średniej długości łańcucha, dlatego szybkość reakcji i jej zależność od warunków prowadzenia wciąż pozostaje przedmiotem wielu pomiarów wykonywanych w laboratoriach naukowych. Prowadzone badania mają na celu określenie prawidłowości, które rządzą procesem i oznaczenie charakteryzujących go wielkości fizycznych, takich np. objętość czy energia aktywacji [21].

Monitorowanie postępu reakcji polimeryzacji możliwe jest za pomocą wielu różnorodnych technik eksperymentalnych, m.in spektroskopii jądrowego rezonansu magnetycznego (NMR), spektroskopii w podczerwieni (IR), spektroskopii Ramana, czy skaningowej kalorymetrii różnicowej (DSC) [22,23,24,25]. Warto jednak również wspomnieć, że alternatywną metodą badawczą z powodzeniem wykorzystywaną w badaniach dynamiki materiałów szklistych [26,27] oraz do monitorowania takich procesów jak: polimeryzacja [28], krystalizacja [29], mutarotacja [30,31], czy też tautomeryzacja [32] jest szerokopasmowa spektroskopia dielektryczna (ang. *Broadband Dielectric Spectroscopy, BDS*). Metoda ta pozwala na obserwowanie zjawisk związanych z reorientacją molekuł obdarzonych trwałym momentem dipolowym w bardzo szerokim zakresie częstości pomiarowych (10^{-2} -10^{9} Hz), w różnych warunkach temperatury i ciśnienia. Jednak pomimo, że metoda ta jest powszechnie wykorzystywana to w literaturze wciąż trwa otwarta dyskusja na temat zależności miedzy mierzonymi wielkościami a przebiegiem monitorowanego procesu oraz właściwościami powstającego polimeru m.in. jego masą cząsteczkową, temperaturą zeszklenia, lepkością. Należy

wspomnieć, że zwykle kinetyka reakcji monitorowana jest najczęściej poprzez zmianę: (*i*) przewodnictwa stałoprądowego (σ_{dc}) oraz (ii) zachowania relaksacji strukturalnej i drugorzędowej [33,34], w zależności od właściwości oraz kompleksowości badanych układów.

Zmiany w przewodnictwie stałoprądowym spowodowane są poprzez: (*i*) zmniejszenie populacji i mobilności jonów obecnych w układzie wraz ze wzrostem konwersji substratów oraz (*ii*) niszczenie wiązań wodorowych obecnych w układzie, jak to zostało przedstawione na przykładzie reakcji mieszaniny 2,2'-di (4-(2,3-epoksypropoksy)fenylo) propanu (DGEBA) i cykloheksyloaminy [25]. Natomiast zmiana położenia piku relaksacyjnego w trakcie trwania reakcji wywołana jest wzrostem lepkości układu w wyniku powstawania polimeru o coraz dłuższych łańcuchach, czego konsekwencją jest również wzrost temperatury przejścia do stanu szklistego (T_g) tworzonych makrocząsteczek. Zmiana ta była monitorowana dla reakcji DGEBY z butyloaminą [28], gdzie zaobserwowano, że maksimum piku relaksacyjnego przesuwa się w kierunku niższych wartości częstotliwości w trakcie trwania reakcji (co jest zachowaniem typowych dla reakcji epoksydowo-aminowych). Ponadto można było również zauważyć wyraźny spadek wartości epsilona statycznego (ε_0) wraz z czasem trwania reakcji i stopniem konwersji substratów, który opisany jest relacją Onsagera-Kirkwoda-Frohlicha:

$$\varepsilon_0 = \frac{(\varepsilon_s - \varepsilon_\infty)(2\varepsilon_s - \varepsilon_\infty)}{\varepsilon_s(\varepsilon_\infty + 2)^2} = \frac{4\pi}{9k_BT}\sum N_i\left\langle \mu_i^2 \right\rangle, \qquad (2)$$

gdzie: *N* to ilość dipoli w jednostce objętości, μ^2- kwadrat momentu dipolowego molekuły, k_B- stała Boltzmanna. Jak można zauważyć zmiana wartości ε_0 wywołana jest zmianą ilości dipoli oraz momentu dipolowego mieszaniny reagującej, wynikającymi z powstawania coraz dłuższych łańcuchów polimerowych oraz zastąpienia grup epoksydowych i aminowych poprzez grupy hydroksylowe (-OH) powstające w wyniku reakcji.

Przebieg reakcji chemicznych można opisać za pomocą wielu różnych modeli kinetycznych, które najogólniej można sklasyfikować jako opisy: (*i*) fenomenologiczne oraz (*ii*) bazujące na mechanizmie reakcji. Modele fenomenologiczne opisują tylko główne cechy przebiegu reakcji, traktując badany proces jako całość i nie uwzględniając różnorodności poszczególnych jego etapów. Przykładem jest model Avramiego [35]

z powodzeniem wykorzystywanym do opisu kinetyki procesu krystalizacji, jak również polimeryzacji:

$$1-\alpha = \exp(-kt)^n, \qquad (3)$$

gdzie α oznacza konwersje układu, a n jest tzn. parametrem Avramiego określającym mechanizm badanego procesu. Natomiast modele kinetyczne oparte na mechanizmie reakcji starają się szczegółowo opisać wszystkie etapy badanego procesu uwzględniając również zmianę stężenia poszczególnych substratów w trakcie jego trwania (np. model zaproponowany przez K. Horie'ego i współpracowników [36] lub M. R. Kamala [37]). Należy jednak wspomnieć, że pomimo często bardzo dobrej precyzji opisu danych modele te nie są możliwe do zastosowania w przypadku bardzo złożonych procesów, jak np. reakcje epoksydowo-aminowe [38]. Dodatkowo modele te „zawodzą", kiedy reakcja przechodzi do obszaru kontrolowanego przez dyfuzję, jak również w przypadku kiedy badany proces jest prowadzony w warunkach wysokiego ciśnienia za pomocą którego można swobodnie sterować mechanizmem procesu. Dlatego też bardzo często opisu przebiegu reakcji dokonuje się za pomocą prostych modeli fenomenologicznych, które mogą być z powodzeniem wykorzystywane w różnych warunkach termodynamicznych.

Celem niniejszej pracy doktorskiej pt. **„Badanie kinetyki reakcji polimeryzacji w różnych warunkach termodynamicznych (T, p)”** było:

1. opracowanie odpowiedniej metody analizy danych dielektrycznych uzyskanych w warunkach wysokiego ciśnienia pozwalającej na poprawny opis kinetyki badanych reakcji polimeryzacji,
2. określenie wpływu podwyższonego ciśnienia na kinetykę polimeryzacji jonowej glicydolu oraz właściwości otrzymanego produktu reakcji,
3. scharakteryzowanie kinetyki reakcji polimeryzacji żywic epoksydowych i amin pierwszorzędowych w różnych warunkach termodynamicznych,
4. określenie wpływu ograniczenia przestrzennego na przebieg poliaddycji aniliny do 2,2'-di(4-(2,3-epoksypropoksy)fenylo)propanu.

Rezultaty prowadzonych badań opublikowano w następujących pracach:

A1. M. Tarnacka, T. Flak, M. Dulski, S. Pawlus, K. Adrjanowicz, A. Swinarew, K. Kaminski, M. Paluch, **High Pressure Polymerization of Glicydol. Kinetics Studies**, *Polymer* 2014, **55**, 1984-1990

A2. M. Tarnacka, O. Madejczyk, M. Dulski, M. Wikarek, S. Pawlus, K. Adrjanowicz, K. Kaminski, and M. Paluch, **Kinetics and Dynamics of the Curing System. High Pressure Studies**, *Macromolecules* 2014, **47,** 4288−4297

A3. M. Tarnacka, M. Wikarek, S. Pawlus, K. Kaminski, M. Paluch, **Impact of high pressure on the progress of polymerization of DGEBA cured with different amine hardeners. Dielectric and DSC Studies**, *RSC Advances* 2015**, 5**, 105934-105942

A4. M. Tarnacka, M. Dulski, S. Starzonek, K. Adrjanowicz, E. U. Mapesa, K. Kaminski, M. Paluch, **Following Kinetics and Dynamics of DGEBA-aniline Polymerization in Nanoporous Native Alumina Oxide Membranes - FTIR and Dielectric Studies**, *Polymer* 2015, **68**, 253-261

Treść wyżej wymienionych publikacji można zaleźć w Rozdziale 2. Publikacje naukowe stanowiące podstawę rozprawy doktorskiej. Ponadto jestem również współautorem poniższych 16 artykułów, których tematyka nie jest bezpośrednio związana z problematyką niniejszej pracy:

1. K. Adrjanowicz, D. Zakowiecki, K. Kaminski, L. Hawelek, K. Grzybowska, M. Tarnacka, M. Paluch, and K. Call, **Molecular Dynamics in Supercooled Liquid and Glassy States of Antibiotics: Azithromycin, Clarithromycin and Roxithromycin**

Studied by Dielectric Spectroscopy. Advantages Given by the Amorphous State, *Mol. Pharm*. 2012, **9**, 1748−1763

2. K. Kaminski, K. Adrjanowicz, D. Zakowiecki, E. Kaminska, P. Wlodarczyk, M. Paluch, J. Pilch, and M. Tarnacka, **Dielectric Studies on Molecular Dynamics of Two Important Disaccharides: Sucrose and Trehalose**, *Mol. Pharm*. 2012, **9**, 1559−1569
3. K. Kaminski, K. Adrjanowicz, E. Kaminska, K. Grzybowska, L. Hawelek, M. Paluch, M. Tarnacka, I. Gruszka, and A. Kasprzycka, **Impact of water on molecular dynamics of amorphous α-, β-, and γ -cyclodextrins studied by dielectric spectroscopy**, *Phys. Rev. E* 2012, 86, 031506
4. E. Kaminska, K. Adrjanowicz, K. Kaminski, P. Wlodarczyk, L. Hawelek, K. Kolodziejczyk, M. Tarnacka, D. Zakowiecki, I. Kaczmarczyk-Sedlak, J. Pilch, and M. Paluch, **A New Way of Stabilization of Furosemide upon Cryogenic Grinding by Using Acylated Saccharides Matrices. The Role of Hydrogen Bonds in Decomposition Mechanism**, *Mol. Pharm.* 2013, **10**, 1824−1835
5. K. Adrjanowicz, K. Kaminski, P. Wlodarczyk, K. Grzybowska, M. Tarnacka, D. Zakowiecki, G. Garbacz, M. Paluch, S. Jurga, **Molecular Dynamics of Supercooled Pharmaceutical Agent Posaconazole Studied via Differential Scanning Calorimetry, Dielectric and Mechanical Spectroscopies**, *Mol. Pharm*. 2013, **10**, 3934−3945
6. M. Tarnacka, K. Adrjanowicz, E. Kaminska, K. Kaminski, K. Grzybowska, K. Kolodziejczyk, P. Wlodarczyk, L. Hawelek, G. Garbacz and A. Kocot, M. Paluch, **Molecular dynamics of itraconazole at ambient and high pressure,** *Phys. Chem. Chem. Phys.* 2013,**15**, 20742-2075
7. W. Kossack, K. Adrjanowicz, M. Tarnacka, W. K. Kipnusu, M. Dulski, E. U. Mapesa, K. Kaminski, S. Pawlus, M. Paluch and F. Kremer, **Glassy dynamics and physical aging in fucose saccharides as studied by infrared- and broadband dielectric spectroscopy**, *Phys. Chem. Chem. Phys.* 2013,**15**, 20641-20650
8. E. Kaminska, K. Adrjanowicz, D. Zakowiecki, B. Milanowski, M. Tarnacka, L. Hawelek, M. Dulski, J. Pilch, W. Smolka, I. Kaczmarczyk-Sedlak, K. Kaminski, **Enhancement of the Physical Stability of Amorphous Indomethacin by Mixing it with Octaacetylmaltose. Inter and Intra Molecular Studies**, *Pharm. Res.* 2014, **31**, 2887-2903
9. E. U. Mapesa, M. Tarnacka, E. Kaminska, K. Adrjanowicz, M. Dulski, W. Kossack, M. Tress, W. K. Kipnusu, K. Kaminski and F. Kremera, **Molecular dynamics of itraconazole confined in thin supported layers**, *RSC Adv*. 2014,**4,**28432−28438
10. E. Kaminska, K. Adrjanowicz, M. Tarnacka, K. Kolodziejczyk, M. Dulski, E. U. Mapesa, D. Zakowiecki, L. Hawelek, I. Kaczmarczyk-Sedlak, and K. Kaminski, **Impact of Inter-**

and Intramolecular Interactions on the Physical Stability of Indomethacin Dispersed in Acetylated Saccharides, *Mol. Pharm.* 2014, **11**, 2935−2947

11. E. Kaminska, M. Tarnacka, K. Kolodziejczyk, M. Dulski, D. Zakowiecki, L. Hawelek, K. Adrjanowicz, M. Zych, G. Garbacz, K. Kaminski, **Impact of low molecular weight excipient octaacetylmaltose on the liquid crystalline ordering and molecular dynamics in the supercooled liquid and glassy state of itraconazole**, *Eur. J. Pharm. Biopharm.* 2014, **88**, 1094–1104
12. K. Adrjanowicz, K. Kolodziejczyk, W. K. Kipnusu, M. Tarnacka, E. U. Mapesa, E. Kaminska, S. Pawlus, K. Kaminski and M. Paluch, **Decoupling between Interfacial and Core Molecular Dynamics of Salol in 2D Confinement,** *J. Phys. Chem. C* 2015, **119**, 14366–14374
13. M. Tarnacka, O. Madejczyk, K. Adrjanowicz, J.Pionteck, E. Kaminska, K. Kamiński and M.Paluch, **Thermodynamic Scaling of Molecular Dynamics in Supercooled Liquid State of Pharmaceuticals: Itraconazole and Ketoconazole**, *J. Chem. Phys.* 2015, **142**, 224507
14. E. Kaminska, M. Tarnacka, P. Włodarczyk, K. Jurkiewicz, K. Kołodziejczyk, M. Dulski, D. Haznar-Garbacz, L. Hawelek, K. Kaminski, A. Wlodarczyk, and M. Paluch, **Studying the impact of modified saccharides on the molecular dynamics and crystallization tendencies of model API nifedipine**, *Mol. Pharm.* 2015, **12**, 3007–3019
15. E. Kaminska, M. Tarnacka, K. Kaminski, K. L. Ngai, M. Paluch, **Changes in dynamics of the glass-forming pharmaceutical nifedipine in binary mixtures with octaacetymaltose**, *Eur. J. Pharm. Biopharm.* 2015, **97**, 185-191
16. E. Kaminska, M. Tarnacka, K. Jurkiewicz, K. Kaminski, M. Paluch, **High Pressure Dielectric Studies on the Structural and Orientational Glass**, *J. Chem. Phys.* 2016, **144**, 054503

Wyniki przeprowadzonych badań były również prezentowane na międzynarodowych konferencjach naukowych w Barcelonie, Madrycie oraz Wiśle.

Badania, które dostarczyły wyników do niniejszej pracy doktorskiej finansowane były w ramach programu SONATA Narodowego Centrum Nauki pt. „*Polimeryzacja wysokociśnieniowa. Badania nad kinetyką procesu*." na podstawie decyzji DEC-2012/05/D/ST4/00326, a także w ramach programu „DoktoRIS – Program stypendialny na rzecz innowacyjnego Śląska" współfinansowanego przez Unię Europejską w ramach Europejskiego Funduszu Społecznego.

1. Otrzymane wyniki i ich dyskusja

W trakcie badań nad wpływem warunków wysokiego ciśnienia na kinetykę procesu polimeryzacji oraz właściwości otrzymanych produktów reakcji, skupiłam się głównie na następujących typach układów: (*a*) polimeryzacji jonowej glicydolu, (*b*) polimeryzacji żywic epoksydowych i różnych amin pierwszorzędowych, których nazwy oraz wzory zostały przedstawione w poniższej tabeli (Tabela 1.) oraz (*c*) poliaddycji aniliny do 2,2'-di(4-(2,3-epoksypropoksy)fenylo)propanu przeprowadzonej w warunkach ograniczenia przestrzennego wytworzonego za pomocą materiałów porowatych wykonanych z tlenku glinu.

Lp.	Nazwa związku	M_w [g/mol]	Wzór strukturalny
1.	Glicydol	74.08	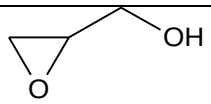
2.	2,2'-di (4-(2,3-epoksypropoksy)fenylo) propanu (DGEBA)	340.41	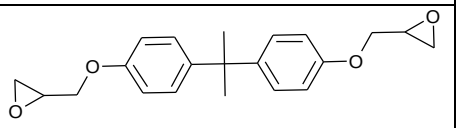
3.	2-etylheksyloamina	129.24	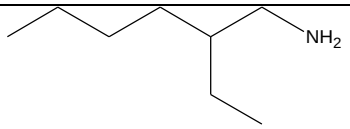
4.	Anilina	93.13	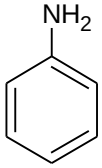
5.	cykloheksyloamina	98.13	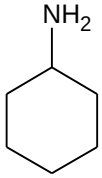

Tabela 1. Charakterystyka badanych substancji.

a) Wpływ wysokiego ciśnienia na kinetykę polimeryzacji jonowej

Pierwszym przebadanym układem była polimeryzacja jonowa glicydolu inicjowana wodorotlenkiem potasu (KOH) prowadzona w temperaturze pokojowej w zakresie ciśnień aż do 800 MPa. Jej przebieg w cały badanym zakresie warunków termodynamicznych

monitorowany był za pomocą szerokopasmowej spektroskopii dielektrycznej (BDS). Szczegółowa analiza została przedstawiona w treści artykułu A1 opublikowanego w czasopiśmie *Polymer* (str. 28).

Kinetyka polimeryzacji glicydolu była monitorowana za pomocą zmian dwóch wielkości: (*i*) przewodnictwa stałoprądowego (σ_{dc}) oraz (*ii*) rzeczywistej składowej przenikalności dielektrycznej (ε') mierzonych przy stałej częstotliwości f = 1 MHz. Badania nad kinetyką procesu polimeryzacji pozwalają na określenie prawidłowości, które rządzą procesem i oznaczenie charakteryzujących go wielkości fizycznych, takich jak stałe szybkości reakcji czy energia aktywacji. Parametry te w przypadku reakcji polimeryzacji określonych monomerów wykorzystywanych na skalę przemysłową mają ogromne znaczenia technologiczne, ponieważ ich znajomość pozwala na określenie czasu potrzebnego do wytworzenia produktu polimerowego o pożądanej średniej długości łańcucha, a przez to również ich właściwości.

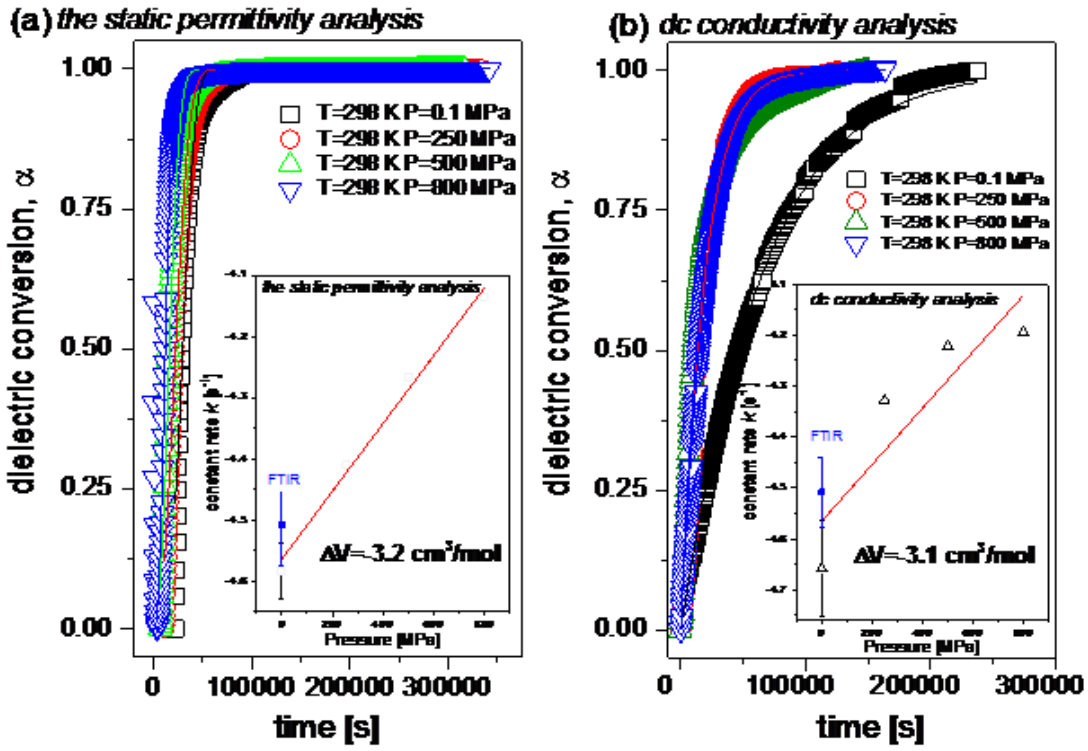

Rys. 1. Konwersja układu śledzona za pomocą zmiany stałej dielektrycznej (Panel a) oraz przewodnictwa (Panel b). Jako dodatkowe panele zostały przedstawione ciśnieniowe zależności stałych szybkości reakcji dla obu przeprowadzonych analiz.

Zaproponowana przez nas analiza danych dielektrycznych wykazała jednoznacznie, że wzrost ciśnienia powoduje wzrost szybkości reakcji oraz przesunięcie krzywych kinetycznych w stronę krótszych czasów reakcji wraz ze wzrostem wywieranego na układ ciśnienia (Rys. 1). Jednak kształt otrzymanych krzywych kinetycznych dla obu analizowanych wielkości (σ_{dc} oraz ε') jest wyraźnie różny. W przypadku przewodnictwa widać wyraźnie, że wzrost ciśnienia powyżej wartości 250 MPa praktycznie nie ma wpływu na wyznaczone krzywe, które są identyczne dla ciśnienia 500 MPa oraz 800 MPa, sugerując brak prostej korelacji pomiędzy przewodnictwem próbki a lepkością układu.

Stałe szybkości reakcji (k) wyznaczone dla obu analizowanych wielkości (σ_{dc} oraz ε') za pomocą modelu Avramiego bardzo dobrze korespondują (w zakresie niepewności pomiarowych) z wartościami k wyznaczonymi przy pomocy pomiarów IR, które zostały wykonane w celu walidacji przeprowadzonej analizy (Rys. 1). Jak można było zauważyć spektroskopia dielektryczna oraz proponowana metoda analizy danych mogą być z powodzeniem wykorzystywane jako alternatywny sposób monitorowania przebiegu procesu polimeryzacji.

Wykonane przez nas wysokociśnieniowe pomiary dielektryczne umożliwiły wyznaczenie wartości objętości aktywacji (ΔV), która wyniosła -3 cm^3/mol dla obu analizowanych wielkości (Rys. 1). Należy podkreślić, że wyznaczona przez nas ΔV jest znacząco wyższa niż wartość podawana zwykle w literaturze dla otwarcia pierścienia epoksydowego (-15 cm^3/mol) [39,40,41], co może być spowodowane użyciem przez nas KOH jako inicjatora reakcji. Warto wspomnieć, że na wartość objętości aktywacji duży wpływ ma wybór użytych substratów, rozpuszczalników, inicjatorów itp. [42]

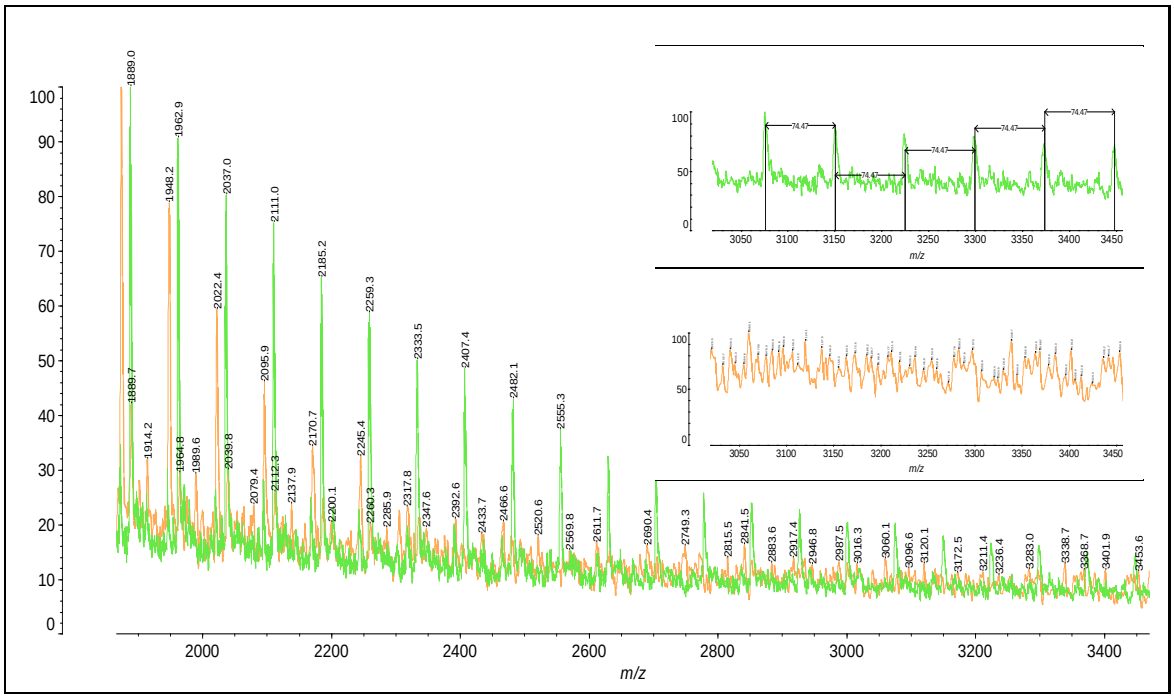

Rys. 2. Widma masowe uzyskane dla próbek otrzymanych pod ciśnieniem p=0.1 MPa (kolor pomarańczowy) oraz p=800 MPa (kolor zielony) za pomocną techniki MALDI ToF.

Charakterystyka otrzymanych produktów za pomocą techniki MALDI TOF potwierdziła pogląd, że podwyższone ciśnienie faworyzuje powstanie polimeru o wyższej masie cząsteczkowej (M_n). W przypadku produktu otrzymanego w warunkach atmosferycznych zostało zarejestrowanych dużo sygnałów w stosunkowo małym zakresie M_n, wskazujących na dużą dyspersyjność próbki (Rys. 2). Warto wspomnieć, że polimeryzacjom przebiegającym z otwarciem pierścienia (ang. *Ring Openig Polymerization*, ROP) towarzyszy szereg reakcji ubocznych (m.in. makrocyklizacja, deprotonacja), które powodują duży rozrzut mas cząsteczkowych powstającego produktu. Jednak reakcje te wydają się wyeliminowane przez przyłożone na reagujący układ ciśnienie, które powoduje powstanie produktu o większych masach cząsteczkowych i mniejszej dyspersyjności w porównaniu z warunkami atmosferycznymi (mniejsza ilość sygnałów w większym zakresie M_n – Rys. 2). Powodu takiej rozbieżności zgodnie z danymi literaturowymi należy dopatrywać się w zmianie ścieżki kinetycznej reakcji chemicznej wywołanej warunkami podwyższonego ciśnienia, w których uprzywilejowane są te przemiany o najwyższej wartości ΔV co zostało pokazane w przypadku 1,3-butadienu, etylenu oraz izoprenu [16,17,19].

b) Wpływ wysokiego ciśnienia na reakcje utwardzania żywic epoksydowych

W dalszej pracy naukowej badany był wpływ podwyższonego ciśnienia (w zakresie do 400 MPa) na przebieg reakcji polimeryzacji żywic epoksydowych z trzema różnymi aminami pierwszorzędowymi (aniliną, cykloheksyloaminą oraz 2-etyloheksyloaminą). Celem prowadzonych badań było scharakteryzowanie kinetyki badanej reakcji w różnych warunkach termodynamicznych za pomocną spektroskopii dielektrycznej, przy wykorzystaniu zaproponowanej przez nas metody analizy danych umożliwiającej poprawny opis kinetyki badanych reakcji w szerokim zakresie *T* i *p*. Szczegółowa analiza przebiegu powyższych reakcji stanowi treść dwóch artykułów A2 oraz A3 opublikowanych w czasopismach *Macromolecules* (str. 36) oraz *RSC Advances* (str. 47).

Kinetyka reakcji DGEBY z różnymi pierwszorzędowymi aminami była charakteryzowana za pomocą nowej metody analizy danych uwzględniającej zmiany rzeczywistej składowej przenikalności dielektrycznej (ε') monitorowanych za pomocą techniki BDS przy stałej wartości częstotliwości. W literaturze można znaleźć liczne przykłady zastosowań zarówno niskich (*Hz*) jak i wysokich (*GHz*) częstotliwości w charakterystyce reakcji żywic epoksydowych m.in. z pochodnymi aniliny i cykloheksyloaminy [43,44,45], oraz *n*- butyloaminy [27]. Jednak ze względu na polaryzacją elektrod oraz ograniczenia techniczne aparatury wysokociśnieniowej uniemożliwiające rejestrowanie reakcji, w naszych pomiarach została wybrana częstotliwości f = 0.3 MHz. Otrzymane wartości podstawowych parametrów kinetycznych takich jak: stałe szybkości reakcji oraz energia aktywacji wyznaczone przy pomocy zaproponowanej metody okazały się porównywalne (w zakresie błędu pomiarowego) z wynikami uzyskanymi z pomiarów IR oraz DSC przeprowadzonymi w celu jej walidacji. Warto podkreślić fakt, że pomimo, iż każda z powyższych metod badawczych zwraca inny kształt krzywych kinetycznych w związku z monitorowaniem innej własności reagującego układu to jednak wyznaczona szybkość reakcji jest taka sama dla każdej z nich. Energia aktywacji procesu wyznaczona dla wszystkich badanych układów oscyluje ok wartości 45 kJ/mol, niezależnie od rodzaju użytej aminy (Rys. 3).

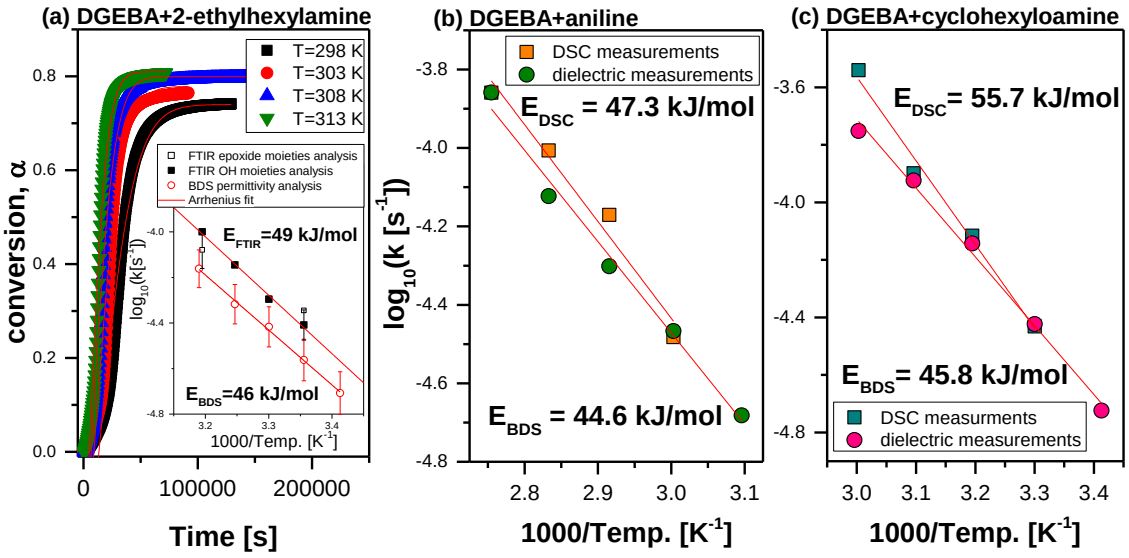

Rys. 3. (Panel a) Zmiana konwersji układu w funkcji czasu dla częstotliwości f=0.3 MHz; (Panel b) Stałe szybkości wyznaczone z pomiarów dielektrycznych w warunkach wysokiego ciśnienia w 293 K; (Panel c) Stałe szybkości wyznaczone w warunkach wysokiego ciśnienia dla układu DGEBA + anilina.

Ciśnienie przyłożone na reagujący układ powoduje przesunięcie otrzymanych krzywych w stronę krótszych czasów trwania reakcji – podobnie jak w przypadku polimeryzacji glicydolu. Jednak należy podkreślić, że wzrost ciśnienia ma znacząco większy wpływ na szybkość reakcji niż wzrost temperatury. Reakcja DGEBY z aniliną w warunkach ciśnienia atmosferycznego w temp. 293 K trwa aż 7 dni, podczas gdy pod ciśnieniem 400 MPa czas ten skraca się do ok 16 godzin. Dodatkowo przyłożone ciśnienie powoduje wzrost szybkości reakcji. Jednak w przypadku poliaddycji DGEBY z 2-etyloheksyloaminy zwiększenie ciśnienia powyżej 300 MPa spowodowało wyraźne odchylenie od obserwowanej liniowej zależności *k* co jest szczególnie widoczne w temp. 293 K (Rys. 4(a)). Odchylenie to związane jest ze zmianą lepkości próbki wywołaną dwoma czynnikami: (*i*) przyłożonym ciśnieniem oraz (*ii*) powstawaniem polimerów o coraz większych masach cząsteczkowych. Wzrost lepkości powoduje spadek dyfuzji nieprzereagowanych monomerów oraz spowolnienie reakcji. Tym samym możliwe jest obserwowanie zmiany obszaru kinetyki monitorowanego procesu z obszaru kontrolowanego przez masę (ang. *mass controlled*) przebiegającego szybko ze względu na duże stężenie reagujących monomerów oraz małą lepkością układu do obszaru determinowanego dyfuzją pozostałych w układzie monomerów (ang. *diffusion controlled*), który limituje

powstawanie polimerów o wyższych masach cząsteczkowych. Warto wspomnieć, że podobne zachowanie zostało również zaobserwowane w przypadku wysokociśnieniowej polimeryzacji izoprenu [19].

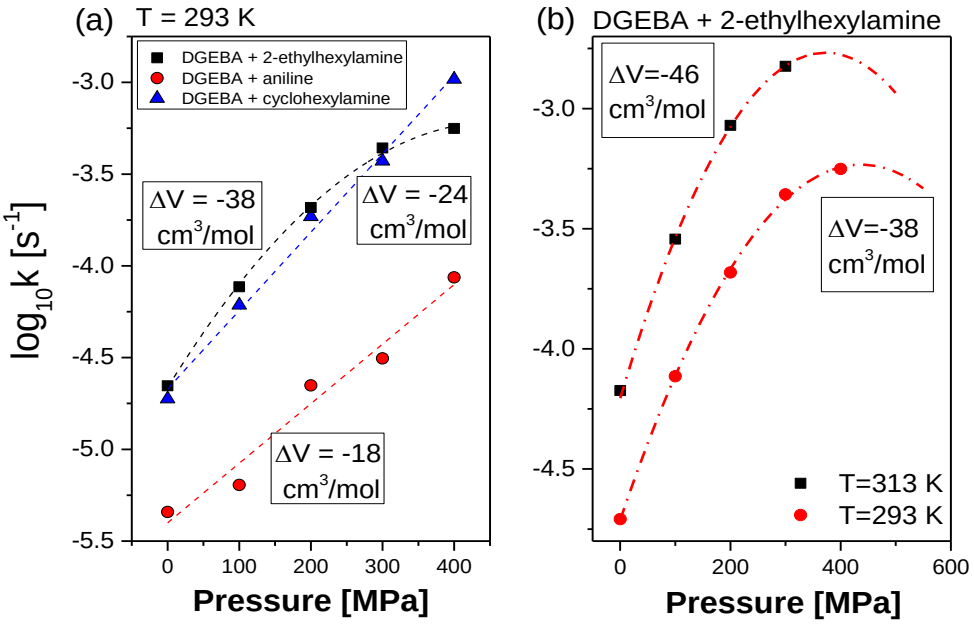

Rys. 4. (Panel a) Stałe szybkości wyznaczone z pomiarów dielektrycznych w warunkach wysokiego ciśnienia w 293 K; (Panel b) Stałe szybkości wyznaczone w warunkach wysokiego ciśnienia dla układu DGEBA + anilina.

Otrzymane wartości ΔV dla badanych reakcji wynosiły odpowiednio -18, -24 oraz -38 cm³/mol odpowiednio dla reakcji DGEBY z 2- etyloheksyloaminą, cykloheksyloaminą oraz aniliną(Rys. 4a). Otrzymane wartości różnią się od danych literaturowych podawanych dla reakcji otwarcia pierścienia epoksydowego (- 15 cm³/mol [39,40,41]), jednak różnica ta jest znacznie mniejsza niż w przypadku polimeryzacji glicydolu (-3 cm³/mol). Wartość ΔV nie tylko w znaczący sposób zależy od użytej aminy (największa i najmniejsza wartość została wyznaczona odpowiednio dla reakcji z aminą aromatyczną oraz alifatyczną), ale również od warunków termodynamicznych. Wzrost temperatury reakcji spowodował zmniejszenie ΔV. Objętość aktywacji dla reakcji DGEBY z 2-etyloheksyloaminą w warunkach podwyższonego ciśnienia w temp. 293 oraz 313 K wyniosła odpowiednio -38 oraz -46 cm³/mol (Rys. 4b).

Ponadto przyłożone ciśnienie ma znaczący wpływ na dwie wielkości: (*i*) stopnień konwersji monomeru oraz (*ii*) temperaturę zeszklenia (T_g) układu. Wartość α dla najwyższego ciśnienia przyłożonego na reagujący układ jest aż o 10 % mniejsza w porównaniu z danymi atmosferycznymi. Dodatkowo zaobserwowano wyraźną korelację między czasem trwania reakcji a stopniem konwersji – im wyższe ciśnienie wywierane na badany proces tym krócej on trwa oraz tym mniejsza jest konwersja reagujących monomerów. Podobną zależność zaobserwowano dla temperatury zeszklenia mieszaniny poreakcyjnej, gdzie zaobserwowano spadek wartości T_g nawet o 20 K w porównaniu z warunkami atmosferycznymi, w których T_g polimerów równe jest temperaturze reakcji.

Nasze dotychczasowe badania nad reakcjami epoksydowo-aminowymi wyraźnie pokazały, że ciśnienie w znaczącym stopniu wpływa na szybkość procesu, a także na lepkość, stopień konwersji, temperaturę zeszklenia produktu. W świetle powyższych wyników można zauważyć, że odpowiednia ciągła zmiana wartości przyłożonego ciśnienia w trakcie trwania polimeryzacji umożliwiłaby swobodne manipulowanie lepkością układu, a w konsekwencji własnościami otrzymanego produktu reakcji. Dlatego też tak niezwykle ważne wydają się dalsze systematyczne badania nad reakcjami prowadzonymi w warunkach podwyższonego ciśnienia mające na celu poznanie jego wpływu m.in. na lepkość układu czy obj. aktywacji reakcji, które umożliwią dobór optymalnych warunków reakcji pozwalając na otrzymanie polimerów o zaplanowanej strukturze i właściwościach.

c) Wpływ ograniczenia przestrzennego na przebieg polimeryzacji żywic epoksydowych

Ostatnim etapem mojej pracy doktorskiej było badanie wpływu dwuwymiarowego ograniczenia przestrzennego (ang. *2D confinement*) na przebieg reakcji polimeryzacji DGEBY i aniliny monitorowanej za pomocą techniki IR oraz BDS. W przeprowadzonym eksperymencie zostały wykorzystane materiały porowate wykonane z tlenku glinu (Al_2O_3) składające się z uniaksjalnych otworów o różnej średnicy (150nm, 73nm, 55nm oraz 35nm). Użyte membrany zostały zakupione do firmy Synkera Technologies, INC z siedzibą w Stanach Zjednoczonych, a ich charakterystyka została przedstawiona na Rys. 5 [46]. Jak zostało wspomniane – reakcja DGEBY z aniliną w warunkach pokojowych trwa aż 7 dni,

dlatego możliwe było opracowanie przez nas odpowiedniej procedury napełnienia membran. Wypracowana metoda, ze względu na odpowiedni dobór warunków termodynamicznych, pozwoliła na 12-godzinnne napełniane materiałów porowatych mieszaniną reakcyjną przy nieznacznej 2-4% konwersji substratów – co zostało potwierdzone za pomocą pomiarów IR. Należy podkreślić, że obecnie są to wciąż pionierskie badania i w literaturze można znaleźć bardzo niewiele prac poświęconym reakcjom prowadzonym w układach ograniczonych przestrzennie [47,48,49,50], a w szczególności układom epoksydowym [51]. Szczegółowa analiza danych została zamieszczona w artykule A4 opublikowanym w czasopiśmie *Polymer* (str. 57).

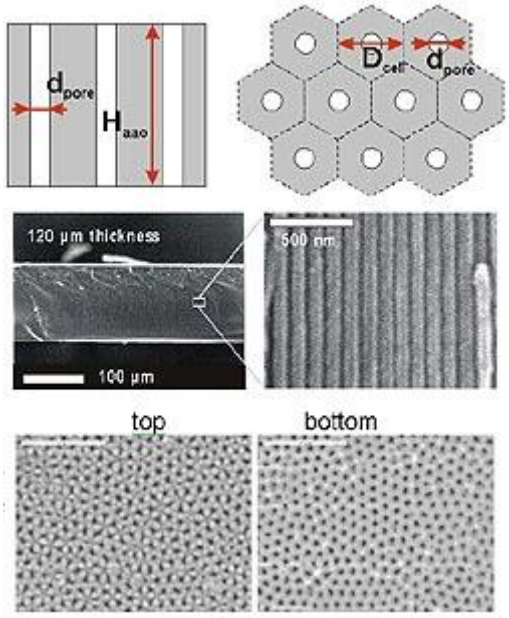

Rys. 5. Charakterystyka wykorzystanych membran wykonanych z tlenku glinu. Rysunki pochodzą ze strony producenta [46].

Analiza widm uzyskanych z pomiarów IR oraz pasm pochodzących od drgań grupy NH_2 pozwoliła na wyznaczenie wpływu stosowanych „nanoreaktorów" na szybkość reakcji badanego procesu. Wykorzystane ograniczenie przestrzenne znacząco przyśpieszyło przebieg reakcji w porównaniu do reakcji litych (ang. *bulk*). Jednak wyznaczona wartość energii aktywacji standardowego procesu wynosi ok 50 kJ/mol i jest porównywalna z wartościami E_a uzyskanymi dla wszystkich układów ograniczonych przestrzenie niezależnie od średnicy wykorzystanej membrany (Rys. 6b). Ponadto warto podkreślić, że badane układy charakteryzują się wysokim stopniem konwersji, który w temp. 353 K wynosił 86% oraz 93% dla reakcji prowadzonej w membranach aluminiowych o średnicy odpowiednio 150 nm oraz 35nm (Rys. 6a).

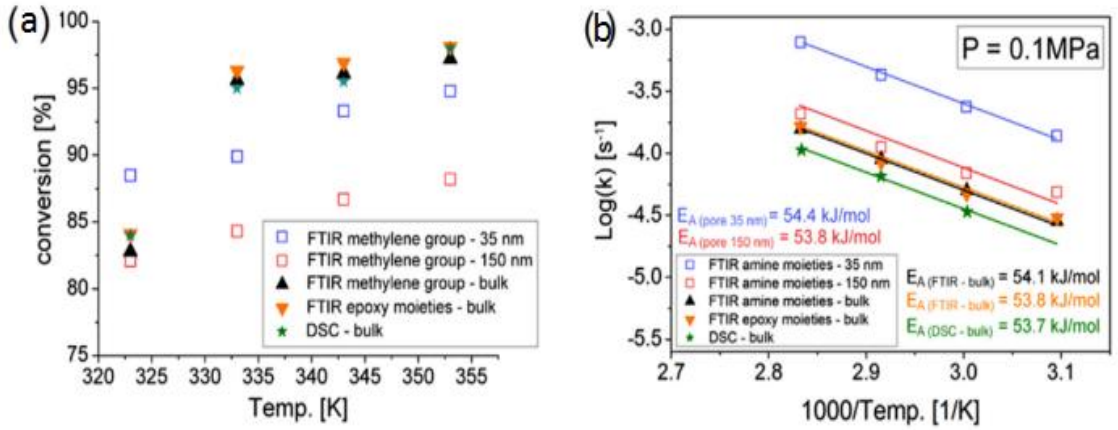

Rys. 6. (Panel a) Zależność stopnia konwersji układu od temperatury reakcji; (Panel b) Stałe szybkości wyznaczone z pomiarów FTIR oraz DSC w różnych warunkach termodynamicznych.

Ponadto układy te charakteryzują się innym kształtem wyznaczonych krzywych kinetycznych. Należy wspomnieć, że poliaddycja amin do żywic epoksydowych przebiega w pierwszym etapie reakcji wg mechanizmu autokatalitycznego ze względu na nowo powstające oligomery zakończone grupami –OH powodując charakterystyczny sigmoidalny kształt krzywych kinetycznych. Jednak w przypadku reakcji prowadzonej w aluminiowych membranach ten etap wydaje się zahamowany w związku z obecnością na ściankach kanałów grup –OH, które są dostępne w reagującym układzie od początki jego trwania powodując wzrost szybkości układu.

Dielektryczne pomiary dynamiki molekularnej badanych układów pozwoliły po raz pierwszy na zaobserwowanie odchylenia czasów relaksacji reakcji DGEBY z aniliną od typowej zależności obserwowanej dla polimeryzacji litych (Rys. 7a). Należy podkreślić, że podobne odchylenie zostało również zaobserwowane w przypadku materiałów szklistych umieszczonych w materiałach porowatych. W literaturze zachowanie to tłumaczone jest heterogenicznością badanego układu, wynikającą z obecności w nim różnych frakcji molekuł o niejednakowej (wolniejszej i szybszej) dynamice [52,53]. Nasze ostatnie badania pozwoliły na potwierdzenie powyższego poglądu oraz zaobserwowanie na przykładzie salolu (umieszczonego w aluminiowych membranach o różnej średnicy) różnej mobilności molekuł znajdujących się przy ściankach porów oraz w ich centrum charakteryzujących się całkowicie odmienną dynamiką [54]. Dalsze badania wykazały, ze witryfikacja frakcji przyściankowej zamraża gęstość układu, który można traktować jako izochoryczny. Zachowanie to zostało wytłumaczone generowaniem w układzie ujemnych ciśnień, które

w istotny sposób wpływają na dynamikę układu oraz jego temperaturę zeszklenia [57]. Ponadto zaobserwowano również znaczne poszerzenie piku relaksacyjnego wraz ze zmniejszeniem średnicy wykorzystanych membran zwłaszcza w zakresie niskich częstotliwości, co sugeruje silne oddziaływania pomiędzy powstającą makrocząsteczką oraz ściankami użytych porów (Rys. 7b). Należy podkreślić, że podobne zachowanie zostało również zaobserwowane w przypadku materiałów szklistych oraz polimerów ograniczonych przestrzennie w różnych materiałach [55,56].

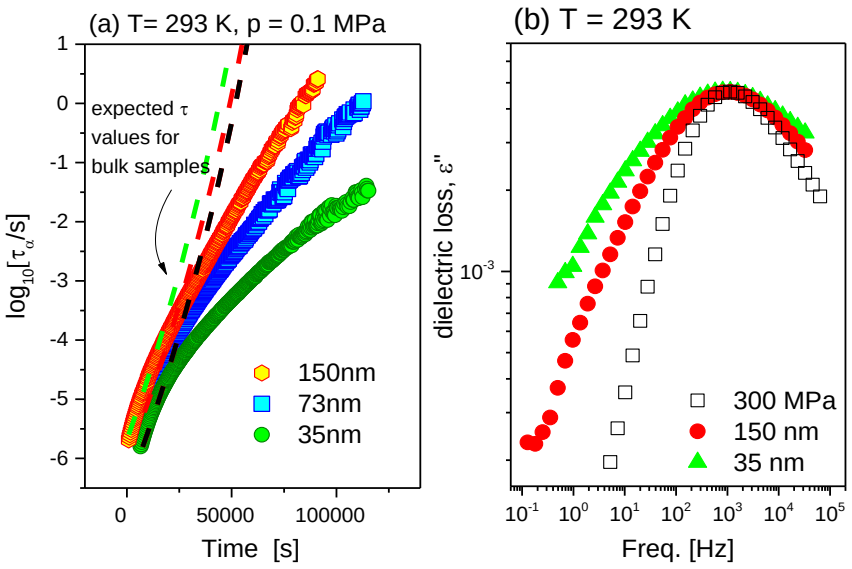

Rys. 7. (Panel a) Ewolucja wyznaczonych czasów relaksacji w trakcie trwania reakcji; (Panel b) Porównanie kształtu procesu relaksacji segmentalnej dla reakcji litej oraz przeprowadzonej w membranach o średnicy 35nm oraz 150nm.

Jednak ze względu na innowacyjność prowadzenia reakcji polimeryzacji w układach ograniczonych przestrzennie – temat ten wymaga dalszych systematycznych badań.

2. Publikacje naukowe stanowiące podstawę rozprawy doktorskiej

A1. High Pressure Polymerization of Glicydol. Kinetics Studies.

Autorzy: M. Tarnacka, T. Flak, M. Dulski, S. Pawlus, K. Adrjanowicz, A. Swinarew, K. Kaminski, M. Paluch

Referencja: *Polymer* 2014, **55**, 1984-1990

Mój udział w poniższym artykule polegał na zaplanowaniu i koordynowaniu eksperymentu, wykonaniu pomiarów dielektrycznych, analizie otrzymanych wyników oraz przygotowaniu artykułu. Natomiast wkład pozostałych autorów pracy wyglądał następująco:

- mgr Tomasz Flak przygotował mieszaninę reakcyjną oraz pomógł umieścić ją w aparaturze badawczej,
- dr Mateusz Dulski wykonał pomiary IR oraz przeanalizował otrzymane wyniki,
- dr Sebastian Pawlus przygotował stanowisko do pomiarów wysokociśnieniowych oraz brał udział w dyskusji wyników,
- dr Karolina Adrjanowicz pomogła w analizie danych dielektrycznych oraz brała udział w dyskusji otrzymanych wyników,
- dr hab. Kamil Kamiński jest kierownikiem grantu SONATA przyznanego przez Narodowe Centrum Nauki w ramach którego realizowano tematykę niniejszej pracy doktorskiej, brał udział w dyskusji wyników oraz poprawił treść manuskryptu,
- prof. dr hab. Marian Paluch brał udział w dyskusji wyników.

Polymer 55 (2014) 1984–1990

Contents lists available at ScienceDirect

Polymer

journal homepage: www.elsevier.com/locate/polymer

High pressure polymerization of glycidol. Kinetics studies

M. Tarnacka [a,*], T. Flak [b], M. Dulski [a], S. Pawlus [a], K. Adrjanowicz [c], A. Swinarew [b], K. Kaminski [a], M. Paluch [a]

[a] Institute of Physics, University of Silesia, Uniwersytecka 4, 40-007 Katowice, Poland
[b] Institute of Materials Science, University of Silesia, 75 Pulk Piechoty 1, 41-500 Chorzow, Poland
[c] NanoBioMedical Centre, Adam Mickiewicz University, Umultowska 85, 61-614 Poznan, Poland

ARTICLE INFO

Article history:
Received 28 November 2013
Received in revised form
22 January 2014
Accepted 21 February 2014
Available online 1 March 2014

Keywords:
High pressure
Polymerization
Constant rate

ABSTRACT

High pressure polymerization of glycidol was carried out at four different pressures ranging from $p = 0.1$ MPa up to $p = 800$ MPa at room temperature ($T = 298$ K). To monitor polymerization kinetics at high pressure dielectric spectroscopy was employed. Constant rates of polymerization at given thermodynamic conditions were determined form the analysis of dc conductivity as well as variation of the static dielectric permittivity. To be sure that both quantities can be used to monitor progress of the polymerization reaction, complementary FTIR studies were carried out at ambient pressure. The vibration of the C–O–C epoxy rings assigned to the band in the 760–880 cm^{-1} range was chosen to follow progress of the monomer conversion. The rate constant "*k*" determined from the Fourier Transform Infrared data analysis, was found to be in good correlation with dielectric data. Furthermore, having rate constant obtained for polymerization carried out at different pressures and constant temperature the activation volume was determined $\Delta V = -3$ cm^3/mol. Finally, analysis with the use of MALDI-TOF^2 MS^2 equipment showed that high pressure favors formation of polymers of greater molecular weight. Moreover, it was found that mechanism of polymerization at high pressure is quite different with respect to the reaction carried out at ambient pressure. It turned out that side reaction occurring upon polymerization of glycidol are completely eliminated at high compression.

1. Introduction

Effective polymerization of common monomers usually involves the use of initiators (chemical or physical), catalysts and high temperature [1–4], with the reaction often carried out in a solvent (e.g., ethylene, isoprene, etc.) [2]. The use of a given initiator, catalyst or other agent affecting kinetics of the polymerization enable to obtain polymers having well defined geometry, physical and chemical properties and narrow polydispersity. One of the most known controlled radical polymerization method is Atomic Transfer Radical Polymerization (ATRP), that enables to synthesize complex polymeric architectures such as block copolymers, star polymers, polymer brushes, gradient copolymers, and others [5–9]. ATRP has been has been carried out with various transition metals, including Cu, Ru, Fe, Ni, or Os, as catalysts at ambient as well as at high pressure [10–14]. It was shown that application of high pressure yields macromolecules of very high molecular weight M_w, not attainable at ambient pressure [15,16]. Moreover, compression enhanced the rate of polymerization and enabled to use very low amount of catalyst to reach targeted molecular weight [13].

Current trends in pressure synthesis of polymers focus on either production of new materials, not obtainable at ambient pressure [17,18] or on preparation those ones having well defined structure. Until now, polymerization under pressure has been carried out for acetylene [19–21], propylene [22], paracyanogen [23], styrene [24–27], isoprene [3,28–30], ethylene [31], 1,3-butadiene [32,33], phenoxyethyl acrylate [34], and TEGDMA [35]. For ethylene and 1,3-butadiene it was shown that compression assisted with the laser irradiation of the compressed monomers leads to formation of the pure transpolybutadiene [33] and HDPE [36], respectively. This seems to be very promising for the development of new strategies for the production of these polymers.

There are many experimental techniques that can be applied to track the polymerization reaction. Among them Fourier Transform Infrared (FTIR) spectroscopy is probably one of the best method to provide an insight into intramolecular interactions as well as progress of reaction, degree of polymerization etc. Besides of FTIR spectroscopy, dielectric spectroscopy has been demonstrated to be

* Corresponding author.
E-mail address: mtarnacka@us.edu.pl (M. Tarnacka).

http://dx.doi.org/10.1016/j.polymer.2014.02.051
0032-3861/

another very useful technique to monitor polymerization reaction. As presented in the past, by analyzing the static permittivity, shape parameters of the structural process or even dc conductivity it is possible to monitor polymerization progress [37–41]. Casalini et al. [42] reported very good agreement between dielectric conversion and the one determined from the calorimetry. Moreover, basing solely on dielectric data they were able to detect switching of the reaction from the mass controlled regime into the diffusion one. However, mentioned above studies were carried out only at ambient pressure, whereas high pressure experiments are still very infrequent and unique [38].

In this paper, we report high pressure dielectric studies on the polymerization of glycidol initiated by KOH. To describe kinetics of polymerization reaction dc conductivity as well as static dielectric permittivity (ε') were analyzed. In addition, we have carried out complementary FTIR measurements on glycidol at room temperature to follow the reaction progress and determine constant rate (k). We have established that there is a good agreement between k obtained from FTIR and dielectric spectroscopies. Dielectric measurements performed at high pressure have indicated that polymerization slightly speeds up with increasing pressure. Estimated activation volume for this kind of polymerization was found to be equal to -3 cm^3/mol. Further studies with the use of MALDI-TOF MS have confirmed that compression favors formation of polymers having greater molecular weight. Moreover, it was shown that application of pressure affects mechanism of polymerization. MALDI-TOF spectra revealed that side reactions are limited or totally terminated. As a consequence of that alkyl moieties, cyclic oligomers are not formed during polymerization process.

2. Experimental section

Glycidol was supplied from Sigma Aldrich. The purity was higher than 99.5%. In each course of polymerization the same amount of KOH was added as initiator. Prior to reaction glycidol was distilled to eliminate oligomers. The chemical structure of glycidol is presented in Scheme 1.

The reaction mixture (monomer + initiator) as well as high pressure cell were prepared in the glove box filled by argon to avoid any contact with the air, oxygen and humidity. The dielectric cell with liquid sample was placed into a Teflon bellows mounted in the high pressure chamber. Hydrostatic pressure was generated by displacing the piston by means of a hydraulic press. Pressure was measured by a Nova Swiss tensometric meter, which had an accuracy of 10 MPa [43,44]. The temperature was controlled within 0.1 K by means of liquid flow from a thermostatic bath.

FTIR measurements were performed using a Bio-Rad FTS-6000 spectrometer equipped with a KBr beam splitter, a standard source and a DTGS Peltier-cooled detector. The MIRacle diamond accessory with KRS5 prism was applied to collect spectra in the range 380–4000 cm^{-1}, with a spectral resolution 2 cm^{-1}. The time dependent measurements were made at room temperature. Spectra were collected each 2 min.

MALDI-TOF spectra were recorded on a Shimadzu AXIMA Performance MALDI-TOF^2 MS instrument equipped with 50 Hz nitrogen laser. A laser power ranged from 61 to 140 arbitrary units.

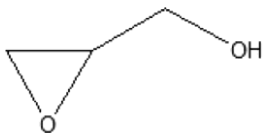

Scheme 1. The chemical structure of glycidol.

Dithranol (1,8,9-trihydroxyanthracene) and DHB (dihydroxybenzoic acid) were used as matrixes. PG (1 mg) dissolved in isopropanol and the matrix (1 mg) dissolved in tetrahydrofuran (0.6 cm^3) were stepwise spreaded on an analytical stage in the amount of 1.5 μL for one measuring point. Each sample was analyzed three times. In one series of experiments isopropanol solution of PG (2 mg/cm^3) was mixed with DHB tetrahydrofuran solution (10 mg/cm^3) and with $AgNO_3$ tetrahydrofuran solution (17 mg/cm^3) in 10:10:1 volume ratio.

3. Results and discussion

Glycidol is a bifunctional monomer consisted of epoxide and hydroxyl groups which make it very special material for different kind of industrial applications. When stored at 298 K it undergoes very slow oligomerization process. As an effect of this reaction dimmers, trimmers and cyclic moieties can be formed. On the other hand achieving greater degree of polymerization of this monomer is rather challenging problem. Many attempts have been done to obtain glycidol of higher molecular weight. However, despite of the use of different catalyst, initiators and other more sophisticated methods no progress in this subject was achieved.

In this paper we decided to carry out high pressure polymerization of glycidol initialized by KOH to investigate effect of pressure on the kinetics of reaction as well as molecular weight of produced macromolecules. The dielectric spectroscopy (DS) was used to monitor the reaction progress. It should be stressed that this technique can be applied mainly in the case of reaction where the concentration or permanent dipole moment of the initial material changes. Since glycidol polymerizes via the ring opening, DS seems to be perfect tool to follow polymerization of this kind of monomer. One can add that kinetics of the epoxide polymerization were investigated by many groups in the past [37,40,41].

In Fig. 1 representative dielectric dispersion as well as loss spectra obtained during polymerization of glycidol at different thermodynamic conditions are presented. In the dispersion spectra, two regions can be observed: (i) the plateau at high frequencies that is connected to the static permittivity of the system and (ii) the second region at lower frequencies that can be assigned to the electrode polarization effect which results from the accumulation of the ions at the sample–electrode interface. It is well visible that as reaction proceeds the electrode polarization effect shifts to the lower frequencies. At the same time decrease in the static permittivity is noted. It is quite surprising observation since densification of the sample should induce an increase in ε_0. As shown in literature decrease in the static permittivity is a common situation for the polymerized systems. In most cases reacting polar groups are being replaced by less polar or non-polar units. Consequently, dipole moment of newly formed macromolecule is smaller than the initial monomer.

In the loss spectra presented in Fig. 1 mainly dc conductivity, that is related to the charge transport, can be observed. Just as in the case of polarization dc conductivity shifts to the lower frequencies with the time of reaction. This is due to the viscosity increase caused by the formation of polymers having greater molecular weight. It should be noted that we do not observe structural relaxation process coming into experimental window as it was usually reported in case of epoxy amine polymerization [37,42]. However, one should bear in mind that KOH was used to initialize reaction in glycidol. Thus, dielectric loss spectra are dominated by the large dc conductivity contribution due to ions coming from dissociation of the initiator, masking the structural relaxation peak in the dielectric loss spectra.

In the inset in Fig. 2 time evolution of dc conductivity and static permittivity measured at $f = 1$ MHz upon polymerization of

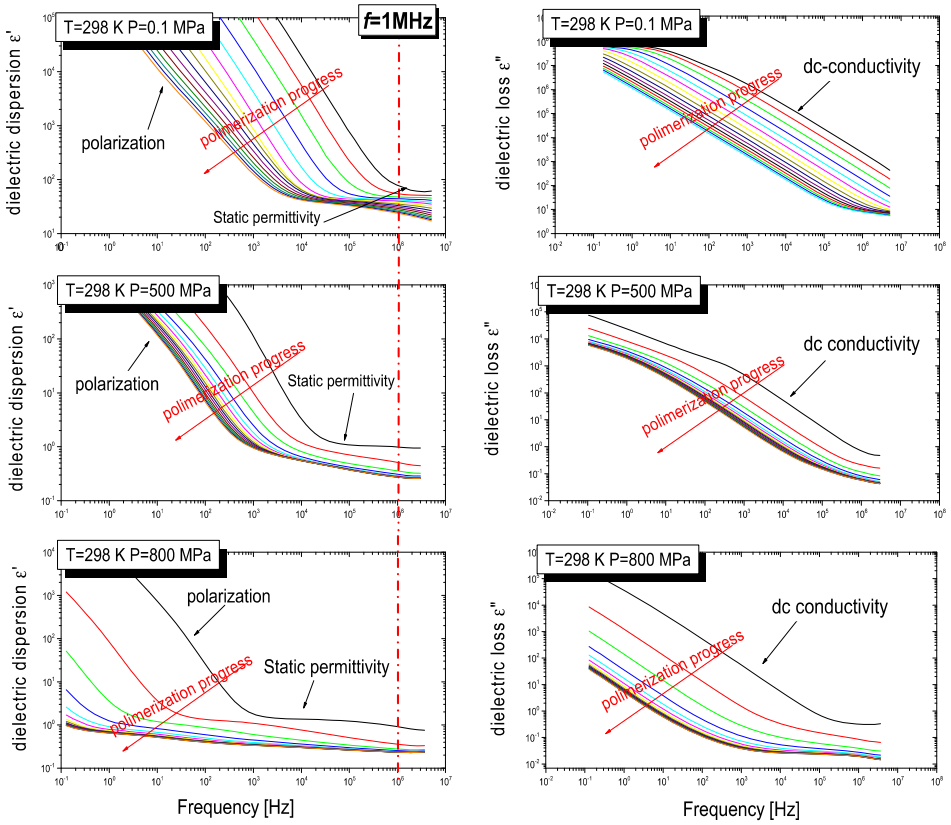

Fig. 1. Time evolution of dielectric dispersion and loss spectra measured upon polymerization of glycidol at indicated thermodynamic conditions.

glycidol at $p = 250$ MPa and 500 MPa at $T = 298$ is shown. As discussed above in each run of polymerization experiment, the drop in ε_0 was observed. It is worth to mention that unlike the ambient pressure polymerization, significant drop of the static permittivity was preceded by increase at the initial stages of the reaction carried out at high pressure. However, at the moment it is difficult to state what is the origin of this unexpected increase.

In the inset in the right panel of Fig. 2 dc conductivity evolution in polymerizing glycidol is shown. It can be seen that in case of polymerization carried out at $p = 250$ MPa and $p = 500$ MPa four decades shift of dc conductivity is observed. Taking into account that far above the glass transition temperature dc conductivity is usually inversely proportional to the viscosity and additionally assuming that concentration of the ions does not change as reaction proceeds, we can conclude that polymerization of glycidol is accompanied by the four decade increase in viscosity.

To describe kinetics of polymerizing systems few different approaches were developed and proposed. One can recall that usually variation of the static permittivity, dc conductivity or resistance of the polymerized sample is used to describe kinetics of chemical reactions [39,45]. One should also note that among of three mentioned herein methods the one based on the analysis of dc conductivity seems to be risky. It is mainly connected to the fact that there is lack of deep understanding of the fundamental basics of measured conductivity and its relation to the chemorheological properties of polymerized systems. However, it should be noted that these reasons do not disqualify this kind of analysis to describe polymerization reaction.

Thus, to study kinetics of polymerization of glycidol at ambient and elevated pressures two methods based on variation of the static permittivity and dc conductivity were applied. Accordingly to the Onsager–Kirchwood–Frohlich equation (1) [46]:

$$\varepsilon_0 = \frac{(\varepsilon_s - \varepsilon_\infty)(2\varepsilon_s - \varepsilon_\infty)}{\varepsilon_s(\varepsilon_\infty + 2)^2} = \frac{4\pi}{9kT}\sum N_i\left\langle \mu_i^2 \right\rangle \quad (1)$$

where: ε_0 is linearly proportional to the concentration of the given dipoles (N_i) and to the mean square of dipole moment (μ^2). Upon glycidol polymerization dipolar charge distribution is modified due to the consumption of the epoxide moieties. As a consequence of that right side of equation (1) is likely to change. Hence, using ε_0 as the parameter to follow kinetics of reaction seems to be well grounded theoretically.

In left panel of Fig. 2 plot of dielectric conversion $\alpha_{\varepsilon 0}$ versus time of reaction for each course of polymerization carried out at four different pressure conditions is presented. It should be stressed that this parameter was evaluated from equation (2):

$$\alpha_{\varepsilon 0} = \frac{\varepsilon'(0) - \varepsilon'(t)}{\varepsilon'(0) - \varepsilon'(\infty)} \quad (2)$$

where $\varepsilon'(0)$ and $\varepsilon'(\infty)$ are the initial and final values of the static permittivity measured upon reaction. It is obvious that polymerization becomes faster at higher pressure, although the change in speed seems to be rather small.

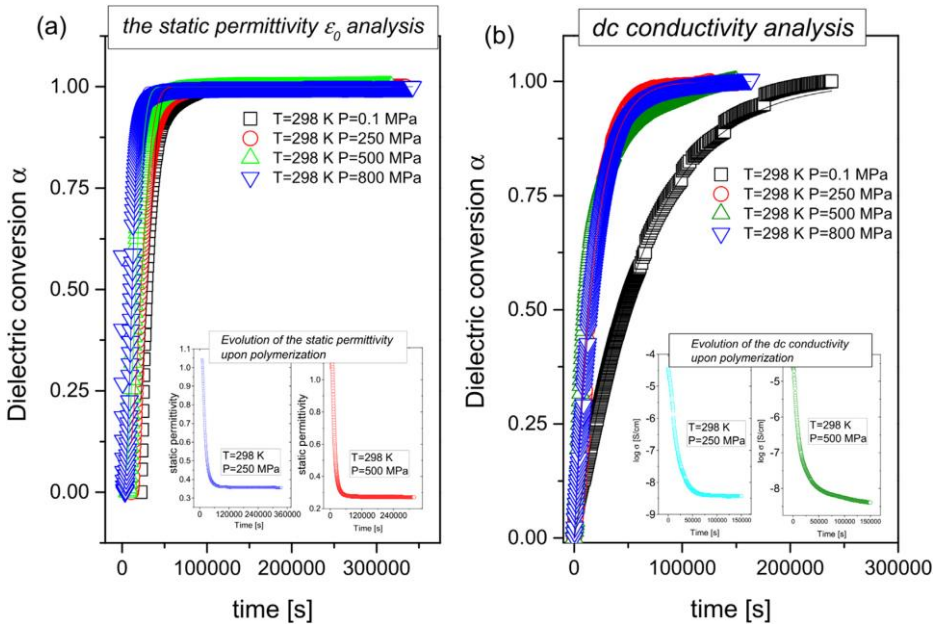

Fig. 2. Dielectric conversion calculated from equation (2) for the evolution of (a) the static permittivity and (b) dc conductivity upon glycidol polymerization at various thermodynamic conditions. In the inset evolution of the static permittivity and dc conductivity upon polymerization of glycidol measured at indicated thermodynamic conditions $T = 298$ K $p = 250$ MPa, $T = 298$ K, $p = 500$ MPa is presented.

The same procedure of analysis was applied in case of dc conductivity data. To calculate dielectric conversion for dc conductivity α_{dc} static epsilon in equation (2) was replaced by dc conductivity. As it can be deduced form the kinetic curves depicted in right panel of Fig. 2 reaction speeds up with compression. Although, at higher pressures $p = 500$ MPa and 800 MPa, kinetic curves almost collapse, indicating saturation of reaction. However, one should be very careful to interpret this observation in this way, because at very high pressures ($p > 500$ MPa) dc conductivity may decouple from the viscosity. Consequently, the wrong conclusion can be drawn based only on dc conductivity analysis.

In order to obtain rates of polymerization carried out at different thermodynamic conditions kinetic curves were analyzed with the use of Avrami equation [47]:

$$1 - \alpha = \exp(-kt^n) \tag{3}$$

where: α is the dielectric conversion, k is a constant rate of reaction and n is the Avrami exponent that can be related to the mechanism of crystallization or reaction.

From the analysis of the kinetic curves in term of the Avrami model, we obtained that polymerization becomes faster as pressure increases. Moreover, constant rate determined from both independent approaches applied herein were almost the same within the uncertainty. By plotting pressure dependence of the rate constant k (see Fig. 3) activation volume was evaluated from the following formula:

$$\Delta V = -RT\left(\frac{\partial \ln k}{\partial p}\right)_T \tag{4}$$

Accordingly to the transition-state theory, activation volume can be correlated to the difference in volumes of transition states and substrates. Since the volumes of reactants are available experimentally, the activation volume seems to be a direct measure of the transition-state volumes. Moreover, this quantity can be used for the qualitative discussion on possible mechanism of the reaction. It is worth to note that estimated activation volume for the KOH initialized polymerization of glycidol is equal to ~ -3 cm^3/mol, which is much higher than −15 cm^3/mol reported in the literature for the epoxide ring opening reactions [48]. This discrepancy between our data and the literature ones can be explained as due to the effect of initiator, which can affect the activation barrier as well as activation volume for the reaction. In this context it is worth to add that Kiselev et al. [49] reported that viscosity as well as polarity of solvent may have significant impact on the activation volume of the reaction.

In addition we also included pressure dependence of the parameter n from the Avrami equation into Fig. 3. One can see that at ambient pressure n is around 3. Thus, by the analogy to the crystallization, polymerization process can be regarded as the three dimensional growth by instantaneous nucleation. With increasing pressure n becomes lower. The same pattern of behavior is reported in literature [50,51]. To explain this observation one can note that compression leads to the significant densification of the polymerizing system. Consequently, reaction becomes more diffusion controlled at high pressure. On the other hand decrease of n can be correlated to the change in direction of the polymerization. As it will be shown later on there are many different products of polymerization for the reaction carried out at ambient pressure while in case of the high compressions only one macromolecule of given structure is produced.

To be sure that analysis carried out for the dielectric data is correct, we have performed complementary time-dependent FTIR measurements during glycidol polymerization at $T = 298$ K and ambient pressure (see Fig. 4). As demonstrated, upon polymerization continuous changes in the integral intensities as well as wavenumber of some bands are observed. The most significant

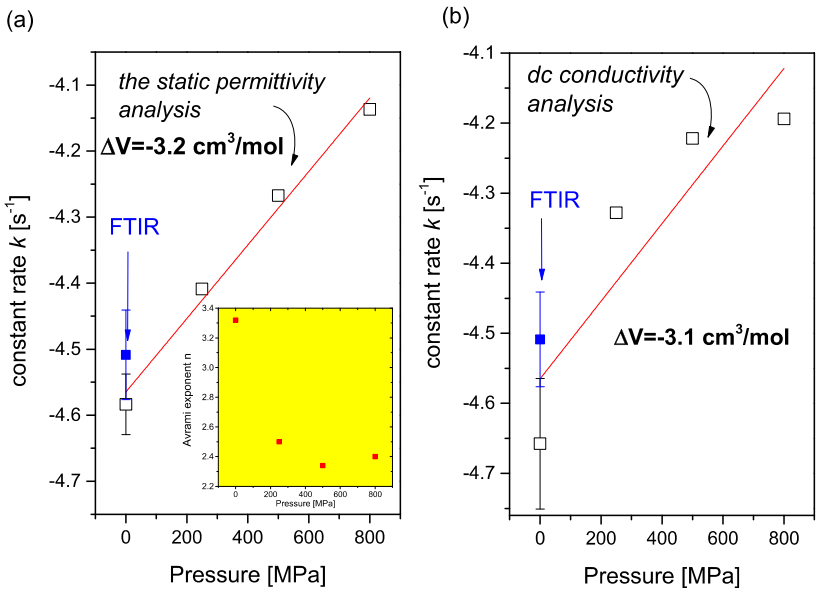

Fig. 3. Dependence of the constant rate k determined from the analysis of (a) the static permittivity and (b) dc conductivity. Red lines are the best fits to the Eq. (4). (For interpretation of the references to color in this figure legend, the reader is referred to the web version of this article.)

ones are observed in the 760–880 cm^{-1} as well as in 2900–3800 cm^{-1} regions (see Fig. 5). The first wavelength region can be associated with the vibration of C–O–C in epoxide ring while the second one is related to the stretching vibration of hydroxyl units. Since polymerization of glycidol proceeds via opening of the epoxide ring, the time dependent integral intensity analysis of the C–O–C band and O–H band were carried out to follow the kinetics of the investigated reaction. As polymerization progresses the shift of hydroxyl bands to the lower wavenumber is noted. It is due to increase of interactions between molecules (see Fig. 5). The integral intensity analysis has revealed simultaneous decrease of C–O–C band and increase of O–H band (see Fig. 5). From the time dependencies of the infrared integral intensities of both examined bands rate constants have been calculated, it turns out that they are comparable to the one previously estimated from dielectric data. This is well demonstrated in Fig. 3. From the results given above one can conclude that, indeed, the analysis of dielectric data provide the same quantitative information about kinetics of glycidol polymerization as FTIR spectroscopy, and both can be used in some cases interchangeably.

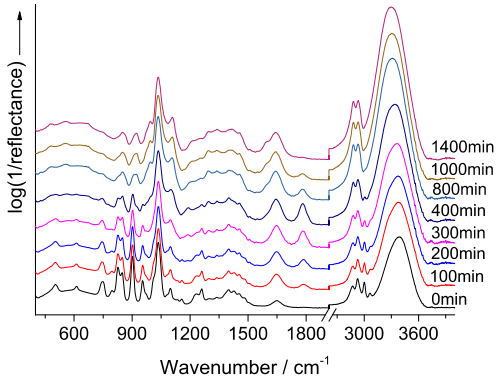

Fig. 4. Time dependent isothermal infrared spectra collected upon polymerization of glycidol at $T = 298$ K and $p = 0.1$ MPa.

Finally, we have also performed additional measurements with the use of MALDI-TOF MS technique to study pressure effect on the molecular weight of formed polymers (see Fig. 6). One should note that only data obtained for the polymerization carried out at ambient and at $p = 800$ MPa were presented to make this figure more readable. From the spectra presented in Fig. 6, it can be observed that elevated pressure favors formation of polyglycidol of higher molecular weight. It is well illustrated in the inset to Fig. 6 where region of higher molecular masses is zoomed. There are visible peaks indicating formation of polymers having M_n even greater than 3000 for the reaction carried out at elevated pressure while in case of ambient pressure polymerization there are no such signals registered.

Moreover, MALDI-TOF^2-MS^2 spectra registered in the (CID) mode revealed also information useful to discussion about the structure and possible mechanism of the reaction at high pressure. As it is well known polymerization of glycidol initialized by KOH proceeds accordingly to the classical Ring Opening Polymerization (ROP) scheme. However, it is also discussed in literature that beside of the main pathway of the reaction there are also side ones such as transesterification, macrocyclization, deprotonation leading to degradation of the polymer chains, formation of the cyclic oligomers, or unsaturated species [52]. The products of these undesired reactions have strong influence on broadening of the molecular weight distribution and deterioration of the mechanical properties of the recovered material. As it can be observed in the spectrum recorded for the polyglycidol produced at $T = 298$ K and $p = 0.1$ MPa (see Fig. 6), there are a lot of peaks located close to each other indicating formation of polymers having different structures. Thus, one can argue that side reactions play rather significant role upon ambient pressure polymerization of glycidol. On the other hand there are only strong single peaks for the polymer obtained at

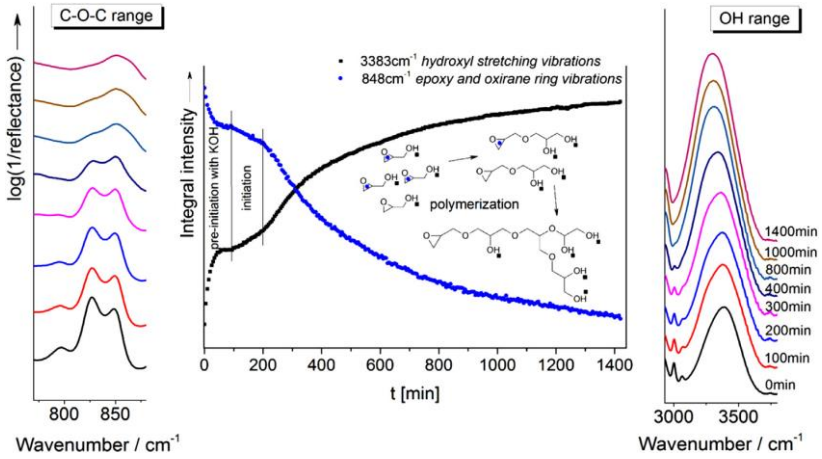

Fig. 5. Time-dependent isothermal infrared spectra in two spectral regions upon polymerization progress of glycidol at atmospheric conditions: a) 760–880 cm^{-1}, c) 2980–3800 cm^{-1} and b) polymerization kinetics based on integral intensity analysis of bands associated with hydroxyl and epoxy groups.

elevated pressure. Such finding means that the main pathway of the ROP reaction is highly promoted and side reactions are completely eliminated. Thus, polymers of well-defined structure and large molecular mass can be formed. One can add that the main series of signals presented on the MALDI-TOF spectra lying within the range 1000–7500 m/z represents the macromolecules with hydroxyl terminal moieties consisted of 12–100 repetitive monomer units with double potassium adducts.

4. Conclusions

High pressure studies on the polymerization kinetics of glycidol were carried out. As demonstrated dielectric spectroscopy can be successfully applied to follow the reaction progress and obtain appropriate rate constant k at elevated pressure. Two independent analysis based on dc conductivity and the static permittivity evolution upon polymerization progress were performed and provide comparable values of k that agrees quite well with the one obtained from the FTIR investigation. It was also demonstrated that high pressure speeds up slightly the polymerization progress.

From the pressure dependence of the rate constant the activation volume, being very important parameter describing chemical reactions, was estimated. We have found out that ΔV for polymerization of glycidol under compression is equaled to ~ -3 cm^3/mol. This value is almost 5 times higher than activation volume reported in the literature for the reaction involving opening of the epoxide ring ($\Delta V = -15$ cm^3/mol). However, it should be stressed that we have carried out polymerization of glycidol initialized by KOH. We conjecture that addition of potassium base should affect activation volume for the chemical reaction proceeding via opening of the epoxide ring and lowering the difference between transition states and substrates volumes.

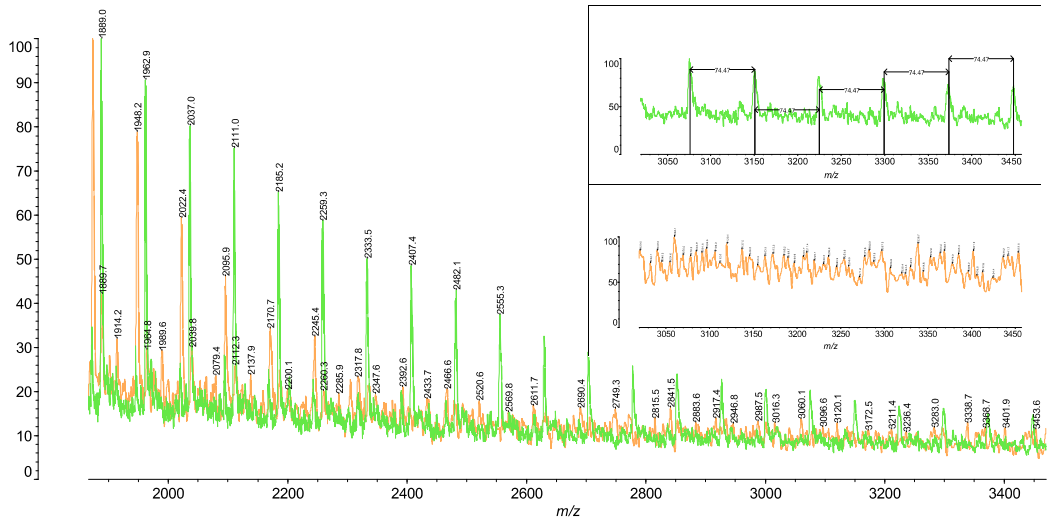

Fig. 6. Mass spectra of polyglycidols obtained at ambient pressure (brown spectra) and under pressure 800 MPa (green spectra). (For interpretation of the references to color in this figure legend, the reader is referred to the web version of this article.)

Finally, we have also shown that polymers of higher molecular masses and well-defined structure can be formed at elevated pressure due to complete elimination of the side reactions.

Acknowledgments

K.K, K.A, S.P, M.T gratefully acknowledge financial support from the Polish National Science Centre within the program Sonata 2 entitled “High pressure polymerization. The kinetic studies” based on decision DEC-2012/05/D/ST4/00326.

References

[1] Bhowmick A, Vijayabaskar V. Rubber Chem Technol 2006;9:402.
[2] Miller GH. J Polym Sci 1960;43:517.
[3] Conant JB, Tongberg CO. J Am Chem Soc 1930;52:1659.
[4] Chang CC, Halasa AF, Miller Jr JW. J Appl Pol Sci 1993;47:1589–99.
[5] Wang JS, Matyjaszewski K. J Am Chem Soc 1995;117:5614.
[6] Matyjaszewski K, Xia JH. Chem Rev 2001;101:2921.
[7] Tsarevsky NV, Matyjaszewski K. Chem Rev 2007;107:227.
[8] Matyjaszewski K. Macromolecules 2012;45:401.
[9] Matyjaszewski K, Spanswick J. Polymer scienceIn A comprehensive reference, vol. 3. Amsterdam: Elsevier; 2012.
[10] di Lena F, Matyjaszewski K. Prog Polym Sci 2010;35:95.
[11] Poli R. Eur J Inorg Chem 2011;2011:1513.
[12] Allan LEN, Perry MR, Shaver MP. Prog Polym Sci 2012;37:12.
[13] Wang Y, Schroeder H, Morick J, Buback M, Matyjaszewski K. Macromol Rapid Commun 2013;34:604–9.
[14] Morick J, Buback M, Matyjaszewski K. Macromol Chem Phys 2011;212:2423.
[15] Mueller L, Jakubowski W, Matyjaszewski K, Pietrasik J, Kwiatkowski P, Chaladaj W, et al. Eur Polym J 2011;47:730.
[16] Kwiatkowski P, Jurczak J, Pietrasik J, Mueller L, Matyjaszewski K. Macromolecules 2008;41:106.
[17] Iota V, Yoo CS, Cynn H. Science 1999;283:1510–3.
[18] Goncharov AF, Gregoryanz E, Mao H, Liu Z, Hemley RJ. Phys Rev Lett 2000;85:1262–5.
[19] Ceppatelli M, Santoro M, Bini R, Schettino V. J Chem Phys 2000;113:5991.
[20] Aoki K, Usuba S, Yoshida M, Kakudate Y, Tanaka K, Fijiwara S. J Chem Phys 1988;89:529.
[21] Sakashita M, Yamawaki H, Aoki K. J Phys Chem 1996;100:9943.
[22] Citroni M, Ceppatelli M, Bini R, Schettino V. J Chem Phys 2005;123:194510.
[23] Yoo CS, Nicol M. J Phys Chem 1986;90:6732.
[24] Gourdain D, Chervin JC, Pruzan Ph. J Chem Phys 1996;105:9040.
[25] Bridgman PW. Proc Am Acad Arts Sci 1949;77:129.
[26] Kobeko PP, Kuvshinskii EV, Semenova AS. Zh Fiz Khim 1950;24:345.
[27] Zharov AA. In: Kovarskii AL, editor. In high-pressure and physics and polymers. Boca Raton, FL: Chemical Rubber; 1994. p. 267.
[28] Bridgman PW, Conant JB. Proc Natl Acad Sci 1929;15:680.
[29] Abdi-Oskoui H, Jenner G, Brun O. Makromol Chem 1972;164:149.
[30] Walling C, Peisach J. J Am Chem Soc 1958;80:5819.
[31] Chelazzi D, Ceppatelli M, Santoro M, Bini R, Schettino V. J Phys Chem B 2005;109:21658.
[32] Citroni M, Ceppatelli M, Bini R, Schettino V. J Chem Phys 2003;118:1815.
[33] Citroni M, Ceppatelli M, Bini R, Schettino V. Science 2002;295:2058.
[34] Kaminski K, Wrzalik R, Paluch M, Ziolo J, Roland CM. J Phys Condens Matter 2008;20:244121.
[35] Kaminski K, Paluch M, Wrzalik R, Ziolo J, Bogoslovov R, Roland CM. J Polym Sci Pol Chem 2008;46:3795.
[36] Chelazzi D, Ceppatelli M, Santoro M, Bini R, Schettino V. Nat Mater 2004;3:470–5.
[37] Tombari E, Salvetti G, Johari GP. J Chem Phys 2000;113:6957.
[38] Johari GP, McAnanama JG, Wasylyshyn DA. J Chem Phys 1996;105:10621.
[39] Mijović J. Dielectric relaxation spectroscopy in reactive polymers. invited chapter in. In: Kremer F, Schonals A, editors. Dielectric relaxation spectroscopy; fundamentals and applications. Berlin: Springer-Verlag; 2002. pp. 349–84. Ch. 9.
[40] Fitz B, Mijović J. J Phys Chem 2000;104:12215.
[41] Gallone G, Capaccioli S, Levita G, Rolla P, Corezzi S. Polym Int 2001;50:545–51.
[42] Casalini R, Corezzi S, Livi A, Levita G, . Rolla PA. J Appl Polym Sci 1997;65:17–25.
[43] Johari GP, Whalley E. Faraday Symp Chem Soc 1972;6:23.
[44] Roland CM, Hensel-Bielowka S, Paluch M, Casalini R. Rep Prog Phys 1405;68:2005.
[45] Jovan Mijovic & et al. Dielectric spectroscopy of reactive polymers, novocontrol, application note dielectrics – 2.
[46] Kremer F, Schonhals A, editors. Berlin: Springer; 2003.
[47] Avrami M. J Chem Phys 1939;7. 1103; 1940, 8, 212; 1941, 9, 177.
[48] Wiebe H, Spooner J, Boon N, Deglint E, Edwards E, Dance P, et al. J Phys Chem C 2012;116:2240–5.
[49] Kiselev VD, Shikhaab MS, Iskhakova GG, Konovalov AI. Russ J General Chem 2002;72(1):98–104.
[50] Ceppatelli M, Santoro M, Bini R, Schettino V. J Chem Phys 2000;113:5991–6000.
[51] Chelazzi D, Ceppatelli M, Santoro M, Bini R, Schettino V. J Phys Chem B 2005;109:21658–63.
[52] Spassky N. Ring opening polymerization, vol. 8. Rapra Technology LTD; 1995.

A2. Kinetics and Dynamics of the Curing System. High Pressure Studies.

Autorzy: M. Tarnacka, O. Madejczyk, M. Dulski, M. Wikarek, S. Pawlus, K. Adrjanowicz, K. Kaminski, and M. Paluch

Referencja: *Macromolecules* 2014, **47**, 4288−4297

Mój udział w poniższym artykule polegał na zaplanowaniu i koordynowaniu eksperymentu, wykonaniu pomiarów dielektrycznych oraz kalorymetrycznych, analizie otrzymanych wyników i ich dyskusji oraz przygotowaniu artykułu. Natomiast wkład pozostałych autorów pracy wyglądał następująco:

- mgr Olga Madejczyk pomogła w wykonaniu pomiarów dielektrycznych w warunkach atmosferycznych,
- dr Mateusz Dulski wykonał pomiary IR oraz przeanalizował otrzymane wyniki,
- mgr Michał Wikarek pomógł w wykonaniu pomiarów dielektrycznych w warunkach podwyższonego ciśnienia,
- dr Sebastian Pawlus przygotował stanowisko do pomiarów wysokociśnieniowych oraz brał udział w dyskusji wyników,
- dr Karolina Adrjanowicz brała udział w dyskusji otrzymanych wyników oraz korekcji treści manuskryptu,
- dr hab. Kamil Kamiński brał udział w dyskusji wyników,
- prof. dr hab. Marian Paluch brał udział w dyskusji wyników.

Macromolecules

Article

pubs.acs.org/Macromolecules

Kinetics and Dynamics of the Curing System. High Pressure Studies

M. Tarnacka,[†,‡] O. Madejczyk,[†,‡] M. Dulski,[†,‡] M. Wikarek,[†,‡] S. Pawlus,[†,‡] K. Adrjanowicz,[§] K. Kaminski,*[,†,‡] and M. Paluch[†,‡]

[†]Institute of Physics, University of Silesia, ul. Uniwersytecka 4, 40-007 Katowice, Poland

[‡]Silesian Center of Education and Interdisciplinary Research, University of Silesia, ul. 75 Pulku Piechoty 1A, 41-500 Chorzów, Poland

[§]NanoBioMedical Centre, Adam Mickiewicz University, ul. Umultowska 85, 61-614 Poznan, Poland

Supporting Information

ABSTRACT: Broadband dielectric and Fourier transform infrared spectroscopies were applied to study dynamics and kinetics upon polymerization of bisphenol A diglycidyl ether (DGEBA) and 2-ethylhexylamine under different thermodynamic conditions. We found out that polymerization constant rates as well as activation barriers determined from both methods are almost the same (within the experimental uncertainty). High pressure studies have enabled to calculate the activation volume which was found $\Delta V = -38$ cm^3/mol and -46 cm^3/mol in the limit of low pressure for two independent isothermal experiments. This finding shows that the activation volume is not constant, but varies with thermodynamic conditions. As a result, polymerization reaction cannot be described with the use of only one given activation volume, as it is usually reported in literature. It should be also noted that ΔV increases with compression and tends to be positive above $P = 430$ and 370 MPa for the reaction carried out at $T = 293$ K and $T = 313$ K, respectively. This is strongly related to the diffusion mechanism that starts to control the polymerization reaction under higher compression. Finally, we have also verified the validity of the time−temperature−pressure superposition (TTP) rule with respect to the structural relaxation process that seems to be crucial point in the context of the proposed protocol of the data analysis.

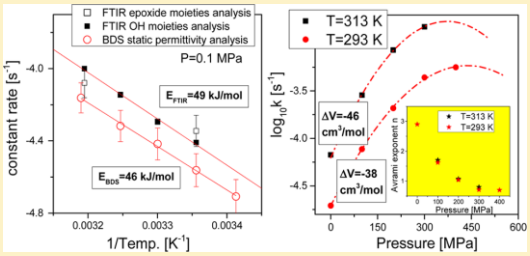

INTRODUCTION

Polymers, are now widely utilized in different fields of technology, i.e., electronic and aerospace industries.[1−3] Variety of their applications relies on excellent chemical and mechanical properties, such as high processability, stability, heat distortion temperatures, and good chemical resistance. The advantages of polymeric materials imply continuous increasing demand for improved their physicochemical properties which is inseparably associated with development of new synthesis methods. In the literature, one can find numerous examples of that, including: (i) "living" radical polymerization,[4,5], (ii) the usage of completely new catalysts or initiators, and (iii) varying thermodynamic conditions of the reaction, to optimize and control the whole process. Among different approaches listed above variation with thermodynamic conditions (temperature and pressure) in the course of polymerization seems to be the very interesting. Systematic studies carried out by Bini's group indicated that high pressure can be used to trigger as well as to control selectively pathways of the reaction. Such scenario was observed in 1,3-butadiene,[6] for which formation of a highly stereoregular polymer was obtained. Moreover, it was possible to control synthesis of low-density or high-density polyethylene by varying with the level of monomer compression.[7] In this context, it is also worth adding that upon high pressure polymerization of glycidol initialized by potassium hydroxide (KOH) all side reactions such as deprotonation, macrocylcization, transesterification, etc. were completely eliminated and only one product of the well-defined structure was recovered.[8] Such selectivity of the high pressure synthesis is strongly related to the activation volume. It should be mentioned that under compression chemical transformations of the highest negative activation volume are favored.[9−15]

The other very intriguing aspect is the impact of pressure on the polymerization kinetics. It should be noted that this is quite complicated issue as the reaction kinetics strongly depends on the viscosity of polymerizing system. If the viscosity is low, the system is in mass-controlled regime where compression accelerates the polymerization due to density increase. On the other hand, at higher viscosities polymerization is solely controlled by diffusion of molecules (diffusion-controlled regime). Thus, application of pressure significantly slows down the reaction rate, since mass transport within polymerized sample is highly limited.[16,17] Such scenario was reported to occur in the case of high pressure ($p = 1.15−2.6$ GPa) polymerization of isoprene.[18] Additionally, it turned out that the activation volume increases with compression from

Received: April 16, 2014
Revised: June 5, 2014
Published: June 16, 2014

Scheme 1. Chemical Structures of DGEBA, 2-Ethylhexylamine, and Polymerization Scheme between an Epoxide and Amine Groups

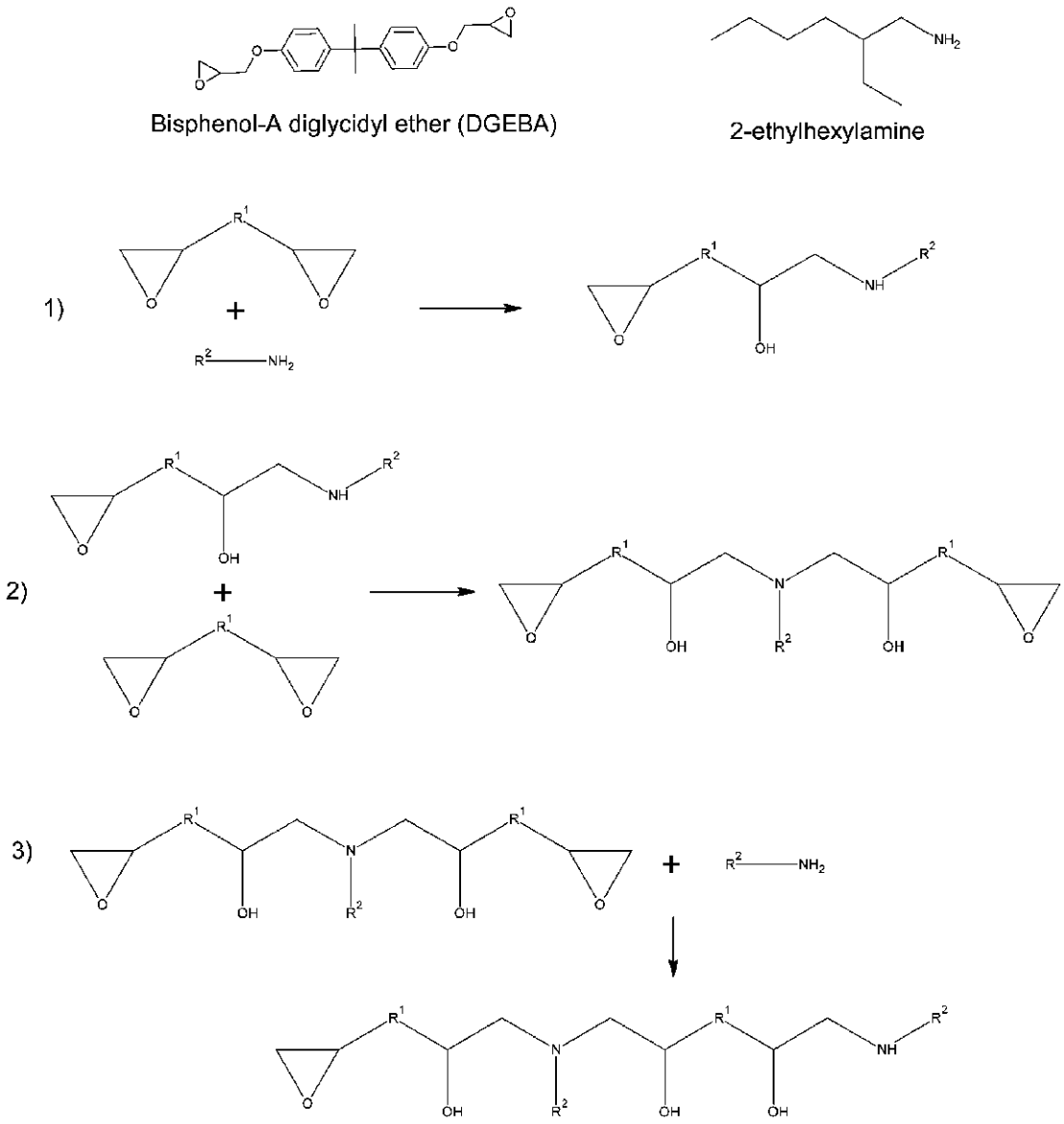

−25 to −7.9 cm^3/mol. Hence, it becomes evident that the activation volume reported in the literature is not constant in the whole range of studied pressures, and changes significantly with thermodynamic conditions at which reaction is carried out.

In this work, we present high pressure studies on the polymerization of epoxy resin (DGEBA) and primary amine (2-ethylhexylamine). Polymerization progress was monitored by using broadband dielectric spectroscopy (BDS). In the past, the reaction kinetics of epoxy resin polymerized with the use of various curing agents was investigated at atmospheric pressure. For this purpose, differential scanning calorimetry (DSC), Fourier transform infrared (FTIR), Raman, BDS, and NMR spectroscopies were employed.[19−25] It is worth noting that, by using dielectric spectroscopy, one can get simultaneous direct insight into kinetics and dynamics of the curing system which seems to be the greatest advantage of this experimental technique over other ones. Our studies have indicated that high pressure accelerates the reaction. However, above a certain pressures (P = 370 and 440 MPa for the reaction carried out at temperatures T = 313 K and T = 293 K, respectively), polymerization of epoxy resin slows down indicating dominant role of diffusion that starts to control the kinetics. Additionally,

dx.doi.org/10.1021/ma500802g | Macromolecules 2014, 47, 4288−4297

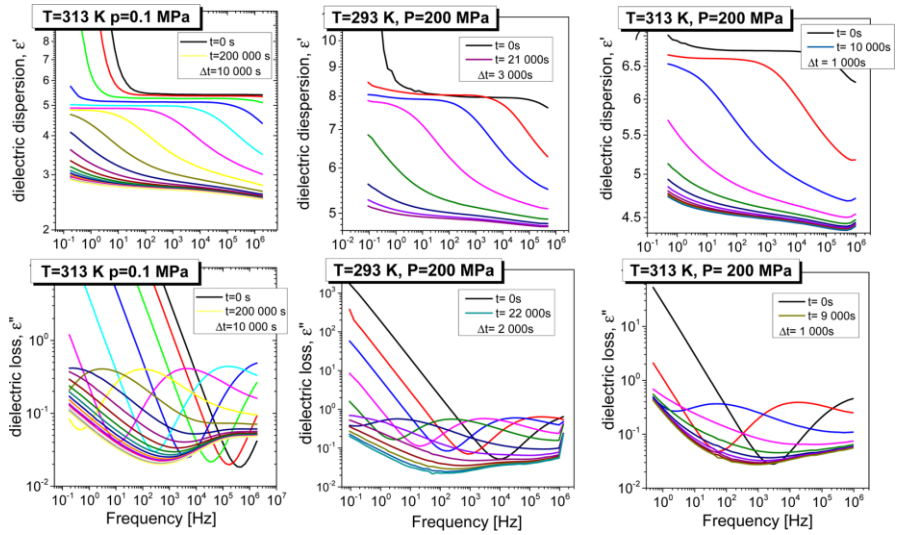

Figure 1. Dielectric loss and dispersion spectra measured upon polymerization of DGEBA and 2-ethylhexylamine at indicated thermodynamic conditions.

we have carried out FTIR measurements to verify and validate results extracted from dielectric studies. The degree of monomer conversion evaluated for the ambient pressure data is α = 73%–81%. Finally, we have tested time–temperature–pressure (TTP) superposition rule concerning scaling of the structural relaxation process for the curing system in the vicinity of the glass transition.

EXPERIMENTAL SECTION

Bisphenol-A diglycidyl ether (known as EPON 828 or DGEBA) and 2-ethylhexylamine of purity higher than 99% were supplied from the Sigma-Aldrich. These two compounds were mixed with molar ratio 1:1. The chemical structures of investigated systems were presented in Scheme 1 together with the sketch of polymerization reaction.

Dielectric Measurements. Isobaric measurements of the dielectric permittivity $\varepsilon^*(\omega) = \varepsilon'(\omega) - i\varepsilon''(\omega)$ at ambient pressure were performed using the impedance analyzer (Novocontrol Alpha) over a frequency range from 1×10^{-2} to 3×10^6 Hz. Investigated samples were placed between two stainless-steel electrodes (diameter, 20 mm; gap, 0.14 mm) and mounted inside a cryostat. During measurement each sample was maintained under dry nitrogen gas flow. The temperature was controlled by Quatro Cryosystem using a nitrogen gas cryostat, with stability better than 0.1 K. The time dependent dielectric measurement of curing system were carried at five different temperatures (293, 298, 303, 308, and 313 K).

For dielectric measurements at elevated pressure high pressure chamber with a special homemade flat parallel capacitor was used. Thin Teflon spacers were used to maintain a fixed distance between the plates. The sample capacitor was sealed and mounted inside a Teflon capsule to separate it from the silicon liquid used for pressurization. Pressure was measured by a Nova Swiss tensometric meter with a resolution of 0.1 MPa. Temperature was adjusted with a precision of 0.1 K by means of refrigerated and heating circulator. Complex dielectric permittivity was measured within the frequency range form 10^{-2} up to 10^6 Hz.

FTIR Measurements. IR measurements were performed using a Agilent Cary 660 FTIR spectrometer equipped with a standard source and a DTGS Peltier-cooled detector. The spectra have been collected using GladiATR diamond accessory (Pike Technologies) in the 4000–400 cm^{-1} range. All spectra were accumulated with spectral resolution of 4 cm^{-1} and recorded by accumulation of 16 scans. The time dependent measurements were made at four temperatures (298, 303, 308, and 313 K). Spectra were collected each 2 min.

RESULTS AND DISCUSSION

I. Kinetic Analysis. DGEBA is a bisfunctional monomer consisted of two epoxide groups. Upon the curing process, the amine group of the curing agent (being a primary amine) breaks the epoxy ring. And the covalent bond between the amines nitrogen atom and the terminal atom of epoxide molecule as well as the –OH group are formed. In a consequence, the primary amine becomes a secondary one. This newly formed secondary amine reacts further; i.e., it breaks the epoxy ring and forms two additional covalent bonds. As a result, the nitrogen atom from the curing agent links two epoxide molecules. Accordingly to this mechanism, polymer structure grows in –A–B–A–B– sequence. The sketch of DGEBA and 2-ethylhexylamine polymerization is illustrated in Scheme 1.

In Figure 1, dielectric dispersion as well as loss spectra measured for the curing system at indicated thermodynamic conditions are presented. It can be seen that dielectric response undergoes continuous and systematic changes with polymerization progress. The most important ones are the shift of dc-conductivity and structural relaxation to lower frequencies. This is connected to the increase of viscosity caused by formation of polymer chains having greater molecular weights, and therefore higher glass transition temperature. Simultaneously, upon polymerization progress a decrease of static permittivity increment due to consumption of the very polar epoxide group is observed (see dispersion spectra ε' in Figure 1).

As the main goal of this paper is to describe the kinetics of the polymerization reaction carried out at ambient and elevated pressure, it is very important to work out the appropriate procedure of analyzing dielectric data. Different approaches were proposed and developed in the past to monitor chemical reactions by means of broadband dielectric spectroscopy.

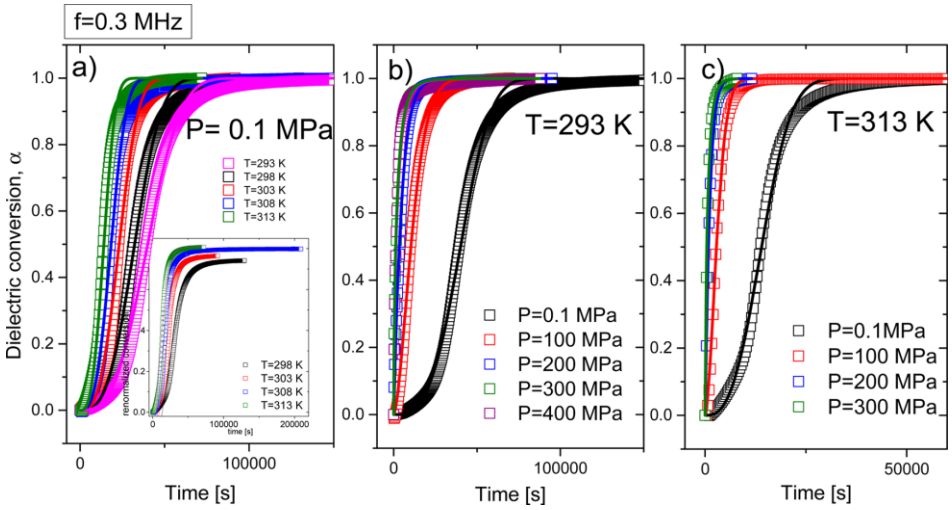

Figure 2. Time evolution of dielectric conversion obtained after renormalization of the permittivity ε' measured at f = 0.3 MHz accordingly to eq 2 for the polymerization carried out at different thermodynamic conditions, as indicated. Solid lines represent the best fit to the Avrami equation, eq 3. The insert in panel a presents kinetic curves obtained after renormalization accordingly to the modified Avrami equation, eq 5

Usually, the variation of structural relaxation time, static permittivity, resistance, or dc-conductivity is used to describe kinetics of the sample undergoing a chemical reaction.[26] It is worth noting that the analysis of dc-conductivity changes upon polymerization progress seems to be the most risky one, due to the lack of deep understanding of the fundamental basics of measured conductivity and its relation to the chemo-rheological properties of polymerized systems.

As demonstrated many times in the literature, dielectric spectroscopy was successfully applied to study the kinetics of mutarotation or tautomerization[27−32] by following time-dependent changes in the structural relaxation time. For both types of reactions, the shift in the relaxation time was not significant (typically it does not exceed three decades) so it was possible to monitor the entire reaction progress by recording the variation of the α-relaxation time (interlinked with the viscosity) within the experimentally accessible frequency window. However, dielectric loss spectra presented in Figure 1 revealed that structural relaxation process shifts more than 10 decades upon polymerization of DGEBA. Consequently, it is not possible to determine the initial and final positions of the segmental relaxation peaks as they are located at much higher and lower frequencies regions, respectively. Thus, kinetic curves cannot be constructed and analyzed. Similar situation was also found to occur in case of the dc-conductivity and resistivity (ρ) of the sample.[26,33] Therefore, in order to analyze polymerization progress we have analyzed the real part of the complex dielectric permittivity function. Accordingly to the Onsager−Kirkwood−Fröhlich equation[34]

$$\varepsilon_0 = \frac{(\varepsilon_s - \varepsilon_\infty)(2\varepsilon_s - \varepsilon_\infty)}{\varepsilon_s(\varepsilon_\infty + 2)^2} = \frac{4\pi}{9kT}\sum N_i\langle\mu_i^2\rangle \quad (1)$$

where ε_0 and ε_∞ are static and infinity permittivity, respectively. Static permittivity (ε_0) is linearly proportional to the concentration of dipoles (N_i) and mean square of dipole moment (μ^2). Upon DGEBA and 2-ethylhexylamine polymerization dipolar charge distribution is modified due to the consumption of epoxide moieties. As a consequence, the right-hand side of eq 1 changed. Hence, by using ε_0 one can follow polymerization progress. However, due to the huge shift of the structural relaxation process upon reaction, it was very difficult to find the exact frequency range that can be utilized to follow kinetics. One can try to select as low frequency as possible, but usually this frequency range is highly affected by polarization effects originating from the accumulation of the current on the surface of electrodes. To overcome this problem Casalini et al. have proposed to monitor evolution of permittivity at frequencies located at GHz region.[24] Since ε_∞ is closely related to the refractive index ($\varepsilon_\infty = n^2$), they were able to measure indirectly evolution of this quantity. Unfortunately, this approach cannot be applied at high pressure because of technical problems. Therefore, another procedure has to be worked out to describe polymerization of DGEBA and 2-ethylhexylamine at ambient and elevated pressures. For this purpose, we have chosen to follow the reaction progress by monitoring time-dependent changes in permittivity ε' at f = 0.3 MHz. At the first glance this analysis seems to be controversial due to segmental dispersion shifting through this frequency range upon polymerization. However, further studies with the use of FTIR spectroscopy verified and validated proposed approach. A similar kind of analysis was performed by Wasylyshyn et al.[19,20] for the DGEBA polymerized with different amine hardeners (i.e., aniline derivatives).

To construct kinetic curves, ε' measured at f = 0.3 MHz was renormalized accordingly to the following equation:

$$\alpha = \frac{\varepsilon'(0) - \varepsilon'(t)}{\varepsilon'(0) - \varepsilon'(\infty)} \quad (2)$$

where $\varepsilon'(0)$ and $\varepsilon'(\infty)$ are the initial and final values of the permittivity measured upon reaction. In Figure 2a, it is demonstrated that the obtained kinetic curves have sigmoidal shape. Additionally, it looks that polymerization becomes faster with increasing temperature, although the temperature effect on the kinetics is not significant.

dx.doi.org/10.1021/ma500802g | Macromolecules 2014, 47, 4288−4297

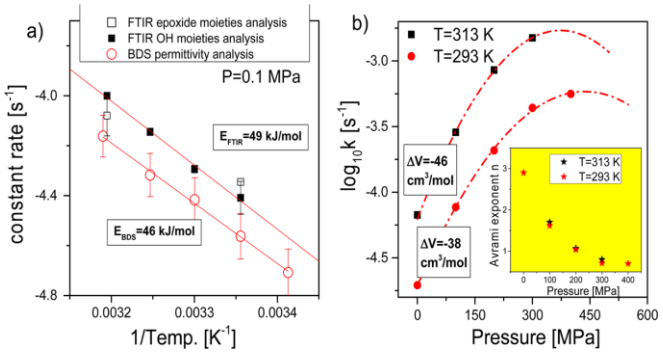

Figure 3. (a) Temperature dependence of polymerization constant rates obtained from dielectric (*open circles*) and FTIR (*filled and open squares*) measurements performed at ambient pressure. (b) Pressure dependence of the constant rates obtained from two isothermal dielectric measurements. Red lines in *panels a and b* represent the best fit to eq 5 and parabolic function, respectively. In the inset pressure dependence of Avrami exponent n is presented.

Constructed in this way, kinetic curves were analyzed with the use of the Avrami equation:[35]

$$1 - \alpha = \exp(-kt^n) \tag{3}$$

Here α is the dielectric conversion, k is a constant rate of reaction and n is the Avrami exponent that can be related to the mechanism of crystallization (or chemical reaction). Although, this model is phenomenological and does not take into account each step of reaction (initialization, elongation and termination), it is usually applied to describe kinetic data collected upon different chemical reactions.[36] It should be also stressed that the nomenclature "dielectric conversion (α)" was introduced just to call the progress of the reaction by means of dielectric spectroscopy. Thus, proposed data analysis protocol is just empirical in nature and cannot be regarded as a real conversion that was determined from FTIR measurements.

In Figure 2a, it can be seen that Avrami fits describe kinetic curves quite well, although some systematic deviation between fits and experimental data can be observed in the transition to the plateau region. As a result, determined constant rates can be slightly overestimated.

In Figure 3, error bars were depicted to show the uncertainty in estimation of constant rate k. After plotting k versus reciprocal temperature in Figure 3, the activation barrier for the polymerization of DGEBA and 2-ethylhexylamine was calculated from Arrhenius equation:

$$k = k_0 \exp(E_a/k_B T) \tag{4}$$

where k_0 is a pre-exponential factor, E_a is the activation barrier, and k_B is the Boltzmann constant. For investigated polymerization reaction we have obtained E_a = 46 kJ/mol at ambient pressure. It is worth noting that this value is similar to the activation barriers E_a= 59 and 73.3 kJ/mol that were estimated for the polymerization of DGEBA with 4,4′-diaminodicyclohexylmethane (PACM)[16] and 1-methylimidazole,[37] respectively.

We have performed analogous analysis for the lower frequencies (data not shown) and found that in the kinetic curves additional step connected to the segmental dispersion shifting through the given frequency region appears. Similar observation was made by Johari.[38]Therefore, analysis of the kinetic curves seems to be more complicated. However, by the use of low frequency data, it is possible to estimate constant rates that were systematically slower than those determined from the analysis of the permittivity measured at f = 0.3 MHz. Surprisingly, the activation barrier of the reaction remained the same independent of the frequency choice.

As the analysis of the polymerization progress with the use of dielectric spectroscopy seems to be far more complicated and controversial we have performed additional time-dependent FTIR measurements in the range of temperature 298−313 K and atmospheric pressure (see Figure 4). In the insets the

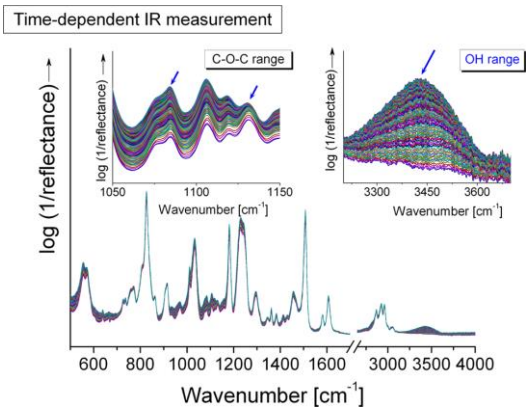

Figure 4. Time-dependent isothermal infrared spectra of bisphenol A diglycidyl (DGEBA) mixed with 2-ethylhexylamine in the whole range and two spectral regions 1000−1150 and 2980−3800 cm^{-1} (insets).

continuous changes in the integral intensities for some bands are illustrated. The most significant and useful ones are those observed in the range of 1050−1150 cm^{-1} as well as in the 3200−3700 cm^{-1} region (see Figure 5). In the first region, the vibration of C−O−C in epoxide ring can be detected, while the second one is related to the stretching vibration of hydroxyl moieties. Upon polymerization of DGEBA and 2-ethylhexylamine, epoxide rings are consumed and simultaneously OH units are formed. Thus, from the analysis of the time-dependence of integral intensities (TD-I_a) of both bands one

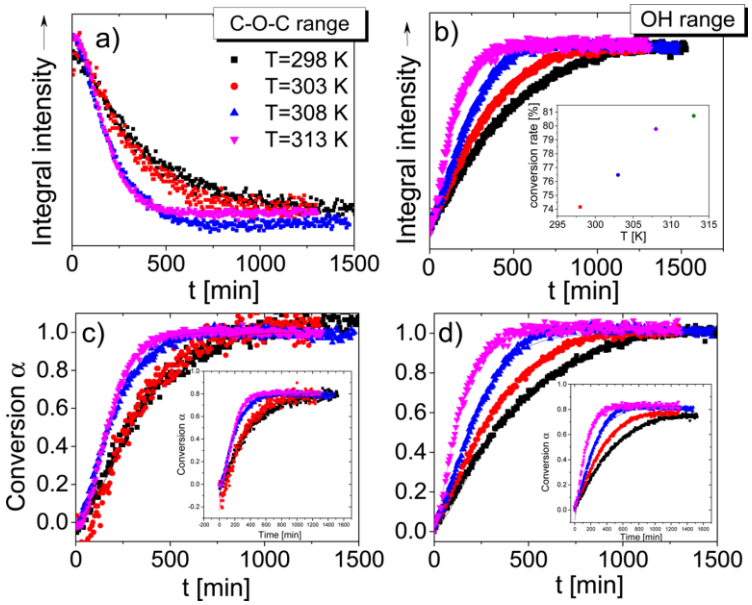

Figure 5. Integral intensities analysis of the C−O−C and OH bands that are consumed and formed upon polymerization of DGEBA and 2 ethylhexylamine (a, b). The kinetic curves obtained after renormalization of the data presented in the upper panel accordingly to eq 2. As inserts in panels c and d, the kinetic curves are obtained after renormalization according to the modified Avrami equation, eq 5

can determine constant rates of the polymerization at given temperature.

In Figure 5, TD-I_a of the bands connected to the vibration within epoxide rings as well as stretching vibration of hydroxyl moiety are presented. Significant decrease of integral intensity of the epoxide band and simultaneous grow up of the hydroxyl ones can be observed. After normalization procedure (analogous as that carried out for dielectric data), the time-dependence of the FTIR conversion, α_{FTIR}, was fitted to eq 3. It was found out that exponential function, or alternatively Avrami formula (with n ≈ 1), describes each kinetic curve very well. From the fitting, we have determined the reaction constant rates and plot them vs temperature (see panel a of Figure 3). It is clear that they are slightly faster than dielectric ones, but the difference is very small, lying within the experimental uncertainty. It should be noted that very recently similar finding was reported for the mutarotation of L-fucose.[39]

On the basis of infrared data, we have also calculated the activation barrier of the polymerization reaction, the value E_a = 49 kJ/mol is in almost perfect agreement to the one determined from dielectric measurements. Additionally, FTIR measurements have provided essential information about the degree of the monomer's conversion which was plotted versus temperature, as shown in the inset of Figure 5b. It is clearly demonstrated that, the efficiency of reaction becomes higher with the increasing temperature. At T = 313 K, the degree of monomer conversion reaches 81%, so as for DGEBA polymerized with ethylenediamine ($\alpha \approx 80\%$)[6] and with *n*-butylamine ($\alpha \approx 90\%$)[7].

Having degree of monomer conversion determined we have analyzed dielectric and FTIR data again (see insets in panels a and c in Figure 2 and Figure 5, respectively). Kinetic curves were reconstructed and fitted to the modified Avrami equation according to the following formula:

$$\frac{\alpha}{\alpha_m} = 1 - \exp(-kt^n) \tag{5}$$

Here α_m denotes maximum degree of monomer conversion. As it turned out, constant rates determined from eq 5 were slightly faster than those estimated originally (data not shown), while the activation energy for the polymerization was the same. This alternative way of data presentation indicates that initial analysis of dielectric results was correct and provides reliable information on the progress of reaction. This finding seems to be extremely important in context of the high pressure measurements for which degree of monomer conversion could not be estimated. Consequently, each kinetic curve has to be renormalized to the unity. Finally, one should also consider the shape of kinetic curves obtained from dielectric and FTIR spectroscopies which were found out to be not exactly the same. It can be also added that Avrami exponents determined from the global fitting of dielectric ($n \approx 3$) and FTIR data (n = 1) are significantly different. Such discrepancy can be related to the intrinsic mechanism of the reaction, specificity and basic physical features of the curing resin that are probed by dielectric and FTIR spectroscopies. In this context, it should be reminded that the latter technique enables to monitor conversion of the monomer at a given stage of the polymerization. On the other hand, decrease in permittivity at f = 0.3 MHz is mainly related to the shifting of the segmental dispersion caused by increase of the molecular weight upon formation of polymer chains. For living polymerization the increase of molecular weight is linearly correlated to the monomer conversion, while for the step growth polymerization (epoxy amine polymerization) such dependency does not exist.

dx.doi.org/10.1021/ma500802g | *Macromolecules* 2014, 47, 4288−4297

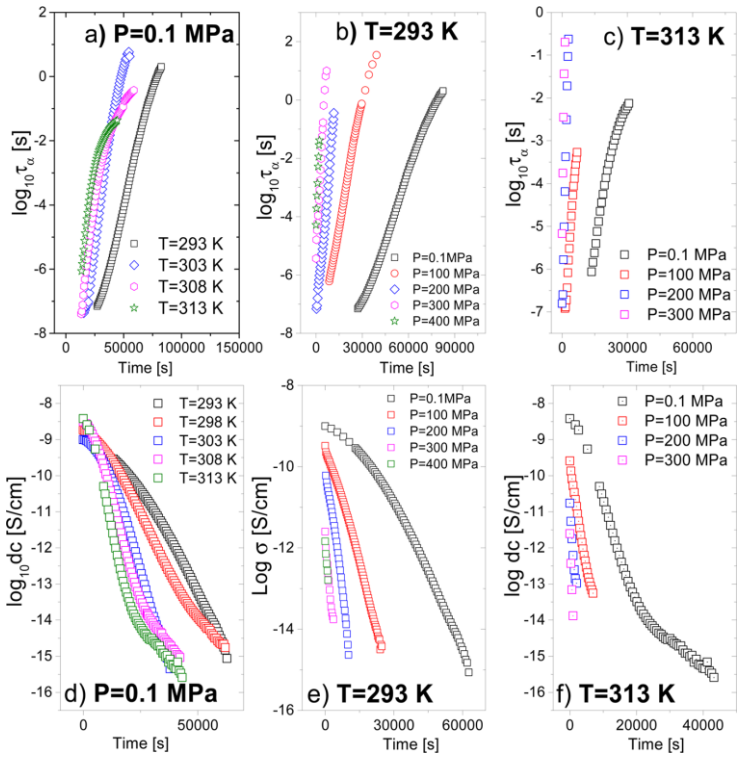

Figure 6. (a–c) Evolution of structural relaxation times vs time of polymerization. (d–f) Time dependence of the dc-conductivity in the curing system.

Thus, Avrami exponent determined from dielectric data does not have to be necessarily the same as the one estimated from FTIR measurements. However, it is important to note that fitting dielectric data presented in the inset to panel b in Figure 2 to eq 5 yields the Avrami exponent n = 1.5, which is highly expected for the linear polymerization.

In the next step, we have carried out high pressure studies to investigate the effect of compression on the reaction pace. For this purpose polymerization was carried out at five different pressures (0.1, 100, 200, 300, and 400 MPa) and at two temperatures (T = 293 and 313 K). Collected dielectric data were analyzed with the use of the same proven protocol as that given above. In Figure 2, dielectric conversion vs time of reaction was presented for the curing performed at T = 293 K (panel b) and T = 313 K (panel c) and different pressures. Upon compression polymerization speeds up significantly. To quantify these experimental findings kinetic curves were analyzed with the use of Avrami model. Then, polymerization constant rates k were plotted vs pressure (see panel b in Figure 3) and the activation volume of the reaction was calculated from the following formula:

$$\Delta V = -RT\left(\frac{\partial[\ln k]}{\partial p}\right)_T \tag{6}$$

It should be noted that we were not able to get reliable data for the polymerization at P = 400 MPa and T = 313 K, as the reaction proceeds faster than the time required to stabilize (T, p) conditions. One can mention that the first recorded spectrum indicated that the curing system just vitrified as segmental relaxation process moved out from the experimental window.

Accordingly to the transition-state theory, the activation volume is related to the difference in volumes of transition states and substrates. Thus, it can be used as a measure of the transition-state volumes. Typical ranges of the activation volume for different types of reaction are evaluated and available in the literature.[40] It is worth noting that ΔV for the epoxide ring-opening reaction is around −15 to −20 cm^3/mol. From the fitting analysis, presented in Figure 3b, we have obtained ΔV equal to −38 and −46 cm^3/mol for the polymerization carried out at T = 293 K and T = 313 K, respectively. After parametrization, the pressure dependence of constant rate with the use of quadratic functions we have obtained that above P = 370 MPa, T = 313 K and P = 440 MPa, T = 293 K the activation volume of polymerization becomes positive. This is a clear indication that at higher compression diffusion mechanism starts to play a dominant role in controlling polymerization leading to significant slowing down of the reaction. It is mainly due to the high density of the curing system as well as viscosity effects. In such cases, mass transport becomes a limiting factor of the overall process. However, our data have revealed also another very interesting finding which is in line with the results published by Bini's group.[18] The activation volume is not constant, but it varies significantly with thermodynamic conditions. Therefore, it

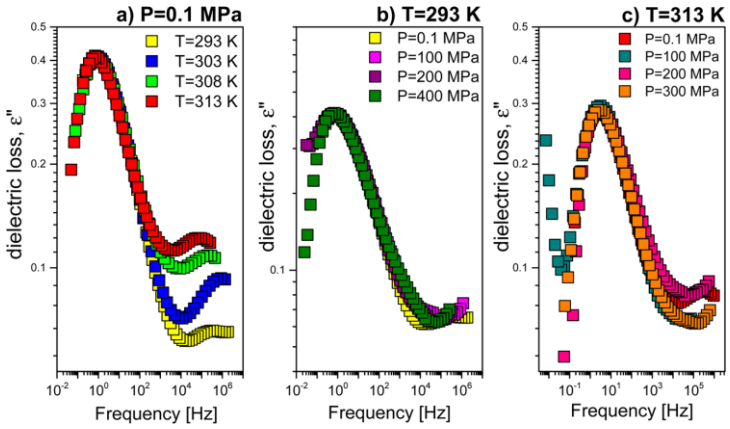

Figure 7. Segmental relaxation peaks collected in vicinity of the glass transition temperature for the polymerization carried out at indicated thermodynamic conditions.

seems to be rather inappropriate to describe given kind of the polymerization reaction by activation volume that varies within very narrow range. In this context, it is worthwhile to remind the reader that ΔV can be also affected by many factors such as substrates, initiators, solvents, etc.[41]

In the inset of Figure 3b, a pressure dependence of the Avrami exponent n is presented. As is discussed in the literature, this parameter can provide some information that can be used to get deeper insight into microscopic evolution of the reaction and describe the reaction regime as mass or diffusion-controlled.[36] It can be observed that n decreases below unity for the pressure higher than 200 MPa, which indicates that only diffusion-controlled growth takes place. Analogous situation was reported in the case of pressure-induced polymerization of acetylene and ethylene.[11,42]

II. Molecular Dynamics. In the next step, we have investigated polymerization induced changes in segmental relaxation times and dc-conductivity. To do that dielectric loss spectra, presented in Figure 1, were parametrized by using the Havriliak–Negami function with conductivity term[43]

$$\varepsilon(\varpi)'' = \frac{\sigma_{dc}}{\varepsilon_0 \varpi} + \mathrm{Im} \sum_{i=1}^{2} \left(\frac{\Delta\varepsilon_i}{[1 + (i\varpi\tau_i)^{\alpha_i}]^{\beta_i}} \right) \quad (7)$$

where α and β are the shape parameters representing the symmetric and asymmetric broadening of given relaxation peaks, $\Delta\varepsilon$ is the dielectric relaxation strength, τ is the relaxation time, ε_∞ is the high frequency limit permittivity, and ω is an angular frequency ($\omega = 2\pi f$). From fitting analysis, the evolution of segmental relaxation time and dc-conductivity were determined and presented in Figure 6.

As illustrated, a more than eight-decade-shift of the segmental relaxation time was observed, suggesting significant increase of viscosity. Moreover, it was also observed that pressure affects the evolution of segmental relaxation time and dc-conductivity upon polymerization process more significantly than temperature does. To quantify such difference one needs to compare how quickly the glass transition is reached by the curing system. As demonstrated in Figure 6(a), glass transition temperature T_g at ambient pressure was reached after around 30 h of keeping at T = 293 K, while at P = 400 MPa, it takes only 3 h. From that we can conclude that polymerization carried out at high pressure is even 10 times faster compared to the ambient conditions. Similar finding was also observed in case of dc-conductivity.

Finally, we would like to verify the validity of the time–temperature–pressure (TTP) rule for investigated curing systems. In the literature it was suggested that the shape of the structural relaxation process is governed by the relaxation time[44]. The only one exception from this phenomenological experimental observation is glass-forming with strongly interacting networks. In this specific case, the TTP rule breaks as different thermodynamic conditions affect population of hydrogen bonds in different way. At low pressures and temperatures, the formation of strong interactions is favored, while at higher temperatures and pressure hydrogen bonds tend to break. In Figure 7, we present segmental loss peaks measured in vicinity of the glass transition temperature for the polymerization carried out at different thermodynamic conditions. As can be seen the shape of the α-process is almost the same, so the TTP rule is satisfied. It should be stressed that validity of this rule seems to be very important in the context of the proposed protocol of the data analysis. We conjecture that this is the basic requirement that must be satisfied to analyze data at fixed frequency. Otherwise, kinetic curves will be affected by the changing shape of the segmental relaxation process and determined constant rates can be adulterated.

The other very interesting issue that can be addressed is the separation between structural and secondary relaxation as the glass transition temperature is approached. It is clear that, both modes become closer to each other with increasing temperature of the polymerization. Moreover, from Figure 7a, it can be deduced that the ratio between dielectric strength of the segmental and secondary modes is getting smaller. It should be also noted that in case of polymerization carried out at high pressures secondary relaxation stays out of the accessible frequency window indicating increasing separation between segmental and secondary relaxations. This result is not surprising taking into account the interpretation of the molecular origin of the secondary relaxation detected in DGEBA that was assigned to the reorientation of the side epoxide moieties.[45]

dx.doi.org/10.1021/ma500802g | *Macromolecules* 2014, 47, 4288–4297

CONCLUSIONS

Broadband dielectric spectroscopy was applied to follow kinetics as well as dynamics of DGEBA polymerized with 2-ethylhexylamine under different thermodynamic conditions. New way of analysis dielectric data upon polymerization reaction was proposed and validated by the complementary time-dependent FTIR measurements. It was demonstrated that polymerization constant rates and activation barriers determined from dielectric and FTIR studies are almost the same, even though the time evolution of dielectric conversion does not reproduce the exact kinetic curves obtained from the infrared. The activation volumes (ΔV = −38 and −46 cm^3/mol) determined for DGEBA and 2-ethylhexylamine polymerization were found out to be smaller than that obtained typically for the reaction involving epoxide ring-opening. However, it was shown that ΔV is not constant and significantly increases with pressure. Moreover, it tends to become positive above P = 370 and 440 MPa for the polymerization carried out at T = 313 K and T = 293 K, respectively. It is due to the diffusion effect, which becomes the most important parameter controlling polymerization. These results have questioned common practice to describe given kind of polymerization with the use of very narrow range or evens single constant value of activation volume. Finally, we have studied polymerization-induced changes in the molecular dynamics of the investigated curing systems, showing that TTP rule holds in the vicinity of the glass transition temperature.

ASSOCIATED CONTENT

Supporting Information

Test of Debye−Stokes−Einstein (DSE) relationship between segmental relaxation and the dc-conductivity close to the glass transition temperature for the curing carried out at different thermodynamic conditions. This material is available free of charge via the Internet at http://pubs.acs.org.

AUTHOR INFORMATION

Corresponding Author

*(K.K.) E-mail: kamil.kaminski@us.edu.pl.

Notes

The authors declare no competing financial interests.

ACKNOWLEDGMENTS

K.K, K.A, S.P, and M.T gratefully acknowledge financial support from the Polish National Science Centre within the program Sonata 2 entitled “High pressure polymerization. The kinetic studies” based on decision DEC-2012/05/D/ST4/00326.

REFERENCES

(1) Feldman, D.; Barbalata, A. *Synthetic polymers: technology, properties and applications*; Chapman and Hall: London, 1996.
(2) Knorr, D. B., Jr.; Yu, J. H.; Richardson, A. D.; Hindenlang, M. D.; McAninch, I. M.; La Scala, J. J. *Polymer* **2012**, *53*, 5917.
(3) Grujicic, M.; Pandurangan, B.; Koudela, K. L.; Cheeseman, B. A. *Appl. Surf. Sci.* **2006**, *253*, 730.
(4) Wang, J. S.; Matyjaszewski, K. *J. Am. Chem. Soc.* **1995**, *117*, 5614.
(5) Kamigaito, M.; Ando, T.; Sawamoto, M. *Chem. Rev.* **2001**, *101*, 3689.
(6) Citroni, M.; Ceppatelli, M.; Bini, R.; Schettino, V. *Science* **2002**, *295*, 2058.
(7) Chelazzi, D.; Ceppatelli, M.; Santoro, M.; Bini, R.; Schettino, V. *J. Phys. Chem. B* **2005**, *109*, 21658.
(8) Tarnacka, M.; Flak, T.; Dulski, M.; Pawlus, S.; Adrjanowicz, K.; Swinarew, A.; Kaminski, K.; Paluch, M. *Polymer* **2014**, *55*, 1984.
(9) Wurche, F.; Klarne, F. G. *High Pressure Chemistry*, van Eldik, R., Klarner, F. G., Eds.; Wiley: New York, 2002.
(10) Chelazzi, D.; Ceppatelli, M.; Santoro, M.; Bini, R.; Schettino, V. *J. Phys. Chem. B* **2005**, *109*, 21658.
(11) Ceppatelli, M.; Santoro, M.; Bini, R.; Schettino, V. *J. Chem. Phys.* **2000**, *113*, 5991.
(12) Citroni, M.; Ceppatelli, M.; Bini, R.; Schettino, V. *J. Chem. Phys.* **2003**, *118*, 1815.
(13) Gourdain, D.; Chervin, J. C.; Pruzan, P. *J. Chem. Phys.* **1996**, *105*, 9040.
(14) Bridgman, P. W.; Conant, J. B. *Proc. Natl. Acad. Sci. U.S.A.* **1929**, *15*, 680.
(15) Chelazzi, D.; Ceppatelli, M.; Santoro, M.; Bini, R.; Schettino, V. *Nat. Mater.* **2004**, *3*, 470.
(16) Fournier, J.; Williams, G.; Duch, C.; Aldridge, G. A. *Macromolecules* **1996**, *29*, 7097.
(17) Isaacs, N. S. *Liquid Phase High Pressure Chemistry*; Wiley: New York, 1981.
(18) Citroni, M.; Ceppatelli, M.; Bini, R.; Schettino, V. *J. Phys.Chem. B* **2007**, *111*, 3910.
(19) Wasylyshyn, D. A.; Johari, G. P. *J. Polym. Sci., Part B: Polym. Phys.* **1997**, *35*, 437.
(20) Wasylyshyn, D. A.; Johari, G. P. *J. Polym. Sci., Part B: Polym. Phys.* **1999**, *37*, 3071.
(21) Ricciardi, F.; Romanchick, W. A.; Joullie, M. M. *J. Polym. Sci., Part A: Polym. Chem.* **1983**, *21*, 1475.
(22) Levita, G.; Livi, A.; Rolla, P. A.; Culicchi, C. *J. of Polym. Sci.: Part B: Polym. Phys.* **1996**, *34*, 2731.
(23) Tombari, E.; Ferrari, C.; Salvetti, G.; Johari, G. P. *J. Phys.: Condens. Matter* **1997**, *9*, 7017.
(24) Casalini, R.; Corezzi, S.; Livi, A.; Levita, G.; Rolla, P. A. *J. Appl. Polym. Sci.* **1997**, *65*, 17.
(25) Galonne, G.; Capaccioli, S.; Levita, G.; Rolla, P. A.; Corezzi, S. *Polym. Int.* **2001**, *50*, 545.
(26) Mijovic, J., Fitz, B. D. *Dielectric Spectroscopy of Reactive Polymers: Application Note Dielectrics 2*; Novocontrol: Hundsangen, Germany, 1998; www.novocontrol.de/pdf_s/APND2.PDF.
(27) Wlodarczyk, P.; Kaminski, K.; Paluch, M.; Ziolo, J. *J. Phys. Chem. B* **2009**, *113*, 4379.
(28) Wlodarczyk, P.; Kaminski, K.; Haracz, S.; Dulski, M.; Paluch, M.; Ziolo, J.; Wygledowska-Kania, M. *J. Chem. Phys.* **2010**, *132*, 19510.
(29) Wlodarczyk, P.; Paluch, M.; Grzybowski, A.; Kaminski, K.; Cecotka, A.; Ziolo, J.; Markowski, J. *J. Chem. Phys.* **2012**, *137*, 124504.
(30) Wlodarczyk, P.; Paluch, M.; Hawelek, L.; Kaminski, K.; Pionteck, J. *J. Chem. Phys.* **2011**, *134*, 175102.
(31) Wlodarczyk, P.; Cecotka, A.; Adrjanowicz, K.; Kaminski, K.; Paluch, M. *J. Phys.: Condens. Matter* **2013**, *25*, 375101.
(32) Wojnarowska, Z.; Wlodarczyk, P.; Kaminski, K.; Grzybowska, K.; Hawelek, L.; Paluch, M. *J. Chem. Phys.* **2010**, *133*, 094507.
(33) Mijović, J. Dielectric relaxation spectroscopy in reactive polymers Invited Chapter in *Dielectric Relaxation Spectroscopy; Fundamentals and Applications*; Kremer, F., Schonals, A., Eds.; Springer-Verlag: Berlin, 2002.
(34) Kremer, F.; Schonhals, A. *Dielectric Relaxation Spectroscopy; Fundamentals and Applications*; Springer: Berlin, 2003.
(35) Avrami, M. *J. Chem. Phys.* **1939**, *7*, 1103; **1940**, *8*, 212; **1941**, *9*, 177.
(36) Schetitino, V.; Bini, R. *Chem. Soc. Rev.* **2007**, *36*, 869.
(37) Ooi, S. K.; Cook, D. W.; Simon, G. P.; Such, C. H. *Polymer* **2000**, *41*, 3639.
(38) Johari, G. P. *J. Chem. Soc. Faraday Trans.* **1994**, *90*, 883−888.
(39) Kossack, W.; Kipnusu, W. K.; Dulski, M.; Adrjanowicz, K.; Madejczyk, O.; Kaminska, E.; Mapesa, E. U.; Tress, M.; Kaminski, K.; Kremer, F. *J. Chem. Phys.* **2014**, *140*, 215101.
(40) Wiebe, H.; Spooner, J.; Boon, N.; Deglint, E.; Edwards, E.; Dance, P.; Weinberg, N. *J. Phys. Chem. C* **2012**, *116*, 2240.

(41) Kiselev, V. D.; Shikhaab, M. S.; Iskhakova, G. G.; Konovalov, A. I. *Russ. J. Gen. Chem.* **2002**, *72*, 983104.
(42) Ceppatelli, M.; Santoro, M.; Bini, R.; Schettino, V. *J. Chem. Phys.* **2000**, *113*, 5991.
(43) Havriliak, S.; Negami, S. *J. Polym. Sci. C* **1966**, *14*, 99.
(44) Ngai, K. L.; Casalini, R.; Capaccioli, S.; Paluch, M.; Roland, C. M. *J. Phys. Chem. B* **2005**, *109*, 17356.
(45) Sharifi, S.; Capaccioli, S.; Lucchesi, M.; Rolla, P. A.; Prevosto, D. *J. Chem. Phys.* **2011**, *134*, 044510.

A3. Impact of high pressure on the progress of polymerization of DGEBA cured with different amine hardeners. Dielectric and DSC Studies

Autorzy: M. Tarnacka, M. Wikarek, S. Pawlus, K. Kaminski, M. Paluch

Referencja: *RSC Advances 2015, **5**, 105934-105942*

Mój udział w poniższym artykule polegał na zaplanowaniu i koordynowaniu eksperymentu, wykonaniu pomiarów dielektrycznych oraz kalorymetrycznych, analizie otrzymanych wyników i ich dyskusji oraz przygotowaniu artykułu. Natomiast wkład pozostałych autorów pracy wyglądał następująco:

- mgr Michał Wikarek pomógł w wykonaniu pomiarów dielektrycznych w warunkach podwyższonego ciśnienia,
- dr Sebastian Pawlus przygotował stanowisko do pomiarów wysokociśnieniowych oraz brał udział w dyskusji wyników,
- dr hab. Kamil Kamiński brał udział w dyskusji wyników oraz korekcji treści manuskryptu,
- prof. dr hab. Marian Paluch brał udział w dyskusji wyników.

RSC Advances

PAPER

View Article Online
View Journal | View Issue

Cite this: *RSC Adv.*, 2015, **5**, 105934

Impact of high pressure on the progress of polymerization of DGEBA cured with different amine hardeners: dielectric and DSC studies

M. Tarnacka,*[ab] M. Wikarek,[ab] S. Pawlus,[ab] K. Kaminski[ab] and M. Paluch[ab]

Received 24th September 2015
Accepted 27th November 2015

DOI: 10.1039/c5ra19766j

www.rsc.org/advances

Kinetics and dynamics of the curing of bisphenol-A diglycidyl ether (DGEBA) with various agents *i.e.* cyclohexylamine, aniline and 2-ethylhexylamine, were investigated by means of Broadband Dielectric Spectroscopy (BDS) over a wide range of thermodynamic conditions. We proposed a novel method of dielectric data analysis to extract information on the progress of the curing reaction. This approach was validated by complementary calorimetry measurements. High pressure studies indicated that compression significantly reduces the time of the reaction. At the same time, a decrease in monomer conversion and the glass transition temperature of the recovered product was observed. This was due to vitrification of the system that occurs in a relatively short time. We found a linear correspondence between the time of the polymerization after which the investigated system undergoes glass transition and the degree of monomer conversion. Additionally, activation volumes for the investigated reactions were determined and found to lie in the range −18 and −38 $cm^3\ mol^{-1}$. The calculated values are lower than ΔV estimated for the ring opening reaction provided in the literature. However our data unquestionably showed that this quantity depends strongly on both the chemical structure of the substrates as well as thermodynamic conditions.

1. Introduction

In considering the effect of compression on polymerization, one needs to distinguish the impact of pressure on the reaction kinetics[1–5] from the reaction product.[3,6–10] Studies of kinetics studies at high pressure revealed that the polymerization rates can either increase or decrease due to compression of the system. It is directly related to the nature of the kinetics of polymerization, whether it is a mass- or diffusion-controlled regime. In the first case, pressure is expected to accelerate the process because it increases the number density of reacting molecules. On the other hand, as polymerization proceeds, viscosity increases as macromolecules of increasingly higher molecular weight are formed. Hence, further compression of the system may lead to a dramatic drop in the diffusion of the remaining monomers. Consequently, polymerization slows down or becomes suppressed. Such scenario was recently observed upon curing of epoxy resin with 2-ethylhexylamine[4] and the polymerization of isoprene[11] at ambient temperature above 440 MPa and 2.5 GPa, respectively.

As proposed by Waite[12] the nature of the kinetics can be described by the s parameter:

$$s = \exp\left[\frac{E_D - E_R}{RT}\right] \quad (1)$$

where: E_R is the activation energy of the reaction and E_D is the activation energy for the diffusion of the reacting molecules. It was shown that this parameter reaches value lower and higher than 1 for the mass- and diffusion-controlled regime, respectively. Unfortunately, the s parameter does not describe conditions between these two regimes.

The application of elevated pressure might also increase the selectivity and tune the reaction toward the formation of macromolecules of well-defined chemical structure. It might be related to the activation volume of competing reaction pathways. It was suggested that at higher compression, the reaction pathway of the smallest activation volume is promoted.[8] In fact, such scenario was observed for 1,3-butadiene[9] and ethylene,[10] where the elimination of side reactions (dimerization) and the formation of a highly stereoregular product with full conversion of the monomer were reported. A similar situation was observed also in the case of glycidol,[3] where it was demonstrated that side reactions connected to the macrocyclization and deprotonation were suppressed, and one polymer of given structure was recovered from the polymerization carried out at high pressures. The other obvious benefit of applying pressure during the

[a]*Institute of Physics, University of Silesia, Uniwersytecka 4, 40-007 Katowice, Poland. E-mail: sebastian.pawlus@us.edu.pl*

[b]*Silesian Center of Education and Interdisciplinary Research, University of Silesia, 75 Pulku Piechoty 1A, 41-500 Chorzow, Poland*

course of polymerization is the possibility of producing macromolecules of very high molecular weight not attainable at ambient pressures.[13,14] Moreover at high compression, the control over the reaction is enhanced leading to production of polymers of lower polydispersity index (PDI) relative to ambient pressure polymerization.

Other than the activation energy barrier, the activation volume (ΔV) seems to be another key parameter governing the kinetics of the chemical reaction under consideration. According to the transition state theory,[15] the activation volume is a difference between the volumes of the transition state $V^{\#}$ and the reactants V^{R}:

$$\Delta V = V^{\#} - V^{R} \quad (2)$$

It can be determined experimentally from the pressure dependence of the rate constant:

$$\left(\frac{\partial \ln k}{\partial P}\right)_T = -\frac{\Delta V}{RT} \quad (3)$$

The activation volume is often used in the discussion of the reaction mechanisms. In the literature there are concrete cases, where the activation volume was assigned to a given chemical transformations or polymerization.[16–18] It is also worthwhile to mention that the value of ΔV can be affected by many factors including the property of substrates, initiators and solvents (mostly by their polarity).[19] However, recent high pressure studies revealed that the value of the activation volume changes with the thermodynamic conditions. In the case of isoprene,[11] the increase in pressure increases the value of the activation volume from -24.3 cm^3 mol^{-1} to -7.9 cm^3 mol^{-1} in the pressure range from 0.1 MPa to 2.6 GPa. Interesting results were also reported for the curing of DGEBA with 2-ethylhexylamine,[4] where the activation volume determined by high pressure measurements carried out at 293 and 313 K have different values of -38 cm^3 mol^{-1} and -46 cm^3 mol^{-1}, respectively.

In this paper, we present high pressure studies on the curing of the epoxy resin (DGEBA) with different primary amines: cycloaliphatic (cyclohexylamine) and aromatic (aniline) in comparison to the aliphatic one (2-ethylhexylamine) studied before.[4] The progress of polymerization was monitored by means of Differential Scanning Calorimetry (DSC) as well as Broadband Dielectric Spectroscopy (BDS) in a wide ranges of temperature and pressure. From the dielectric data, the activation barrier was determined to be 44.6 and 45.8 kJ mol^{-1} respectively for the curing system with cyclohexylamine and aniline. The obtained values are in good agreement to those determined from DSC measurements (47.3 and 55.7 kJ mol^{-1}, respectively). Moreover, the isothermal pressure dependence of the rate constant and the respective activation volumes for the studied reactions was evaluated. High pressure studies revealed that the activation volume depends on the chemical structure of the substrates and increases from -38 cm^3 mol^{-1} to -18 cm^3 mol^{-1} for DGEBA polymerized with 2-ethylhexyl amine and aniline, respectively.

2. Experimental section

2.1 Materials

Bisphenol-A diglycidyl ether (known as EPON 828 or DGEBA, M_w = 340.41 g mol^{-1}), aniline (M_w = 93.13 g mol^{-1}) and cyclohexylamine (M_w = 99.17 g mol^{-1}) of purity higher than 99% were purchased from Sigma Aldrich. The epoxy resin and curing agent were mixed with molar ratio 1 : 1. In every measurement, we used 5 g of DGEBA with 1.37 g or 1.45 g of aniline or cyclohexylamine, respectively. All samples were prepared in a glove box in an identical manner. Immediately after preparation, the samples were measured by means of BDS and DSC techniques. The chemical structures of investigated systems were presented in Scheme 1. The sketch of polymerization reaction can be found in ref. 4 and 20.

2.2 Methods

BDS measurements. Dielectric permittivity $\varepsilon^*(\omega) = \varepsilon'(\omega) - i\varepsilon''(\omega)$ values at ambient pressure were measured by using the impedance analyzer (Novocontrol Alpha) over a frequency range from 1×10^{-1} to 3×10^6 Hz. The samples were placed between two stainless-steel electrodes (diameter: 15 mm, gap: 0.14 mm) and mounted inside a cryostat. During the measurement, each sample was maintained under dry nitrogen gas flow. The temperature was controlled by Quatro Cryosystem using a nitrogen gas cryostat, with stability better than 0.1 K. The time dependent dielectric measurements of curing system were carried out at different temperatures in the range from 293 to 363 K.

High pressure dielectric measurements were performed by using the high pressure chamber with a special homemade flat parallel capacitor. Thin Teflon spacers (0.1 mm) were used to maintain a fixed distance between the plates. The sample capacitor was sealed and mounted inside a Teflon capsule to separate it from the silicone liquid used for elevating pressure. Pressure was measured by a Nova Swiss tensometric meter with a resolution of 0.1 MPa. Temperature was adjusted with a precision of 0.1 K by means of refrigerated and heating circulator. Complex dielectric permittivity was measured within the frequency range from 1×10^{-1} to 3×10^6 Hz.

Bisphenol-A diglycidyl ether (DGEBA) aniline cyclohexylamine

Scheme 1 The chemical structures of DGEBA, aniline and cyclohexylamine.

DSC measurements. Calorimetric measurements of the isothermal curing of DGEBA were carried out by Mettler-Toledo DSC apparatus equipped with a liquid nitrogen cooling accessory and an HSS8 ceramic sensor (heat flux sensor with 120 thermocouples). Temperature and enthalpy calibrations were performed by using indium and zinc standards. The sample was prepared in an open aluminum crucible (40 μL) outside the DSC apparatus. Samples were scanned at various temperatures at constant heating rate of 10 K min^{-1}. After the polymerization, samples were measured on heating from 273 K to 523 K at constant heating rate of 10 K min^{-1}. Each measurement at a given temperature was repeated 3 times. For each experiment a new sample was prepared.

3. Results and discussion

3.1 Ambient pressure condition

The curing of epoxy resin with primary amines occurs accordingly to the step-growth polymerization mechanism. The process involves the opening of epoxide rings, addition of amine groups and formation of covalent bonds with the nitrogen and hydrogen.[20] The chemical structures of the substrates are presented in Scheme 1, while the mechanism of the process can be found in ref. 4.

The formation of polymer chains is connected with continuous changes in its molecular weight, glass transition temperature, viscosity and dipole moments distribution, enabling one to monitor the reaction by means of dielectric spectroscopy. It should be added that the recent reports show that beside of standard techniques such as Fourier Transform Infrared (FTIR) spectroscopy, Raman spectroscopy, Nuclear Magnetic Resonance (NMR) and DSC,[2,21–26] BDS can also be successfully applied to follow the polymerization reaction and might provide simultaneous insight into the dynamics and kinetics of the chemical reaction.

In Fig. 1, dielectric dispersion and loss spectra collected upon curing of DGEBA with various curing agents are presented at a number of temperatures. One can observe that the static permittivity (Fig. 1(a) and (b)) decreases for each sample due to decreasing concentration of the polar epoxide rings. Moreover, segmental relaxation and dc-conductivity move toward lower frequency and eventually out of the experimental window, due to the formation of longer polymer chains (Fig. 1(c) and (d)). It should be stressed that the variation of segmental relaxation and static permittivity, as well as the dc-conductivity can be utilized to analyze the progress of the chemical reaction monitored by BDS spectroscopy.[27] However, in the case of the curing of epoxy resin, the proper way to analyze dielectric data is not certain and, is currently a matter of some debate. This is due to the lack of deep understanding of the fundamental relationship between measured quantities and their connections to the monomer conversion for the investigated reaction.

A promising way to follow the progress of reaction is to monitor the dielectric constant. The static permittivity (ε_0) is linearly proportional to the concentration of dipoles (N_i) and the mean square dipole moment (μ^2) according to the Onsager–Kirkwood–Frohlich equation:

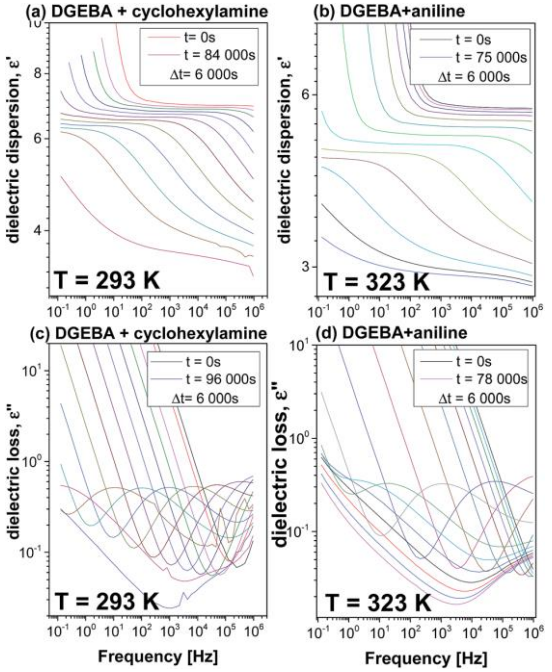

Fig. 1 Dielectric dispersion (panels (a) and (b)) and loss spectra (panels (c) and (d)) measured upon polymerization of DGEBA with different curing agents: aniline and cyclohexylamine at indicated thermodynamic conditions (at ambient pressure).

$$\varepsilon_0 = \frac{(\varepsilon_S - \varepsilon_\infty)(2\varepsilon_S - \varepsilon_\infty)}{\varepsilon_S(\varepsilon_\infty + 2)^2} = \frac{4\pi}{9kT}\sum N_i\langle\mu_i^2\rangle \quad (4)$$

where ε_0 and ε_∞ are static and infinity permittivity, respectively. As mentioned above, the epoxy ring concentration and dipole moment distribution is modified during the course of the reaction. As a consequence, one can obtain information on the progress of polymerization by following this variable. However, due to vitrification of the curing system and parasitic polarization contributions, it is not possible to utilize this way to analyze the dielectric data. Hence, it was proposed to analyze permittivity measured at either low or high frequency range. The former approach was used to follow the progress of curing of epoxy resin with aniline[24,25] and cyclohexylamine[28] derivatives. However, one should remember that the low frequency range is usually highly affected by electrode polarization effects originating from the accumulation of the current on the surface of electrodes. Moreover, the additional step originating from the shift of the segmental relaxation dispersion can be observed in the kinetic curves constructed from the data in the low frequency range. This artifact can be easily eliminated by considering higher frequency range. Casalini *et al.* showed that analysis of the permittivity measured at GHz region yields almost the same information on the rate of reaction as FTIR investigations.[29] For the purpose of this paper, we modified this approach and analyzed the real part of the permittivity recorded

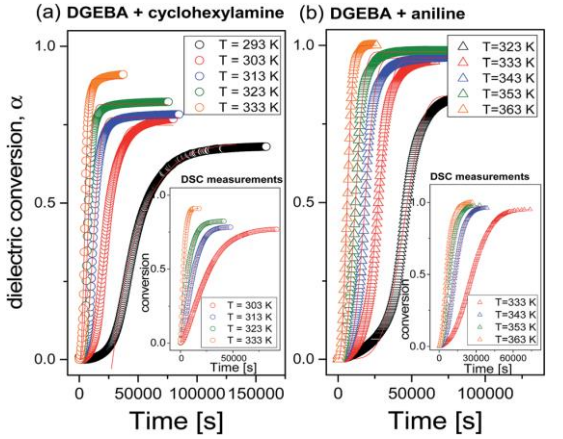

Fig. 2 Time evolution of dielectric conversion obtained after renormalization of the permittivity ε' measured at $f = 0.3$ MHz according to eqn (5) for the reaction carried out for different curing agents at various thermodynamic conditions. Solid lines represent the best fit to the Avrami equation [eqn (7)]. As insets in panels (a) and (b), time evaluations of DSC conversion of indicated systems are presented.

at $f = 0.3$ MHz. This approach was successfully verified and validated by FTIR measurements of DGEBA–2-ethylhexylamine system.[4]

The data collected were renormalized (see Fig. 2) in plotting the kinetic curves, according to the following equation:

$$\alpha_{\varepsilon_0} = \frac{\varepsilon'(0) - \varepsilon'(t)}{\varepsilon'(0) - \varepsilon'(\infty)} \quad (5)$$

where $\varepsilon'(0)$ and $\varepsilon'(\infty)$ are the initial and final values of the permittivity measured during the polymerization reaction. Here, it should be added that the dielectric conversion factor α does not reflect the monomer conversion and it is introduced to characterize the progress of the reaction by means of BDS. Furthermore, dielectric data were rescaled to the maximum value of the monomer conversion factor, which was determined from complementary DSC measurements. As it can be seen, increase in temperature accelerates the reaction for all studied samples. However, this effect is more significant in the case of the curing DGEBA with cyclohexylamine and aniline, when compared to 2-ethylhexylamine.[4] Since kinetic analysis based solely on dielectric data might not be unequivocal, complementary DSC measurements were carried out to verify the results from the proposed model of data analysis.

The raw calorimetric data obtained upon curing DGEBA with various amines are shown in Fig. 3(a) and (b). It can be seen that, the exothermic peak of polymerization shifts towards shorter times with increasing temperature of polymerization, which is a typical behavior of polymerization[30,31] carried out under isothermal conditions. One can add that a similar scenario is reported for the crystallization process.[32] It should be stressed that calorimetric studies enable one to obtain insight into the kinetics of the reactions, as well as to determine the degree of monomer conversion. For this purpose, time and temperature dependent DSC measurements were carried out. The progress of the reaction monitored by the application of the DSC method is presented by the insets in panels (b) and (c) in Fig. 2. The kinetic curves shown in Fig. 2 were obtained according to the equation:

$$\alpha_{\mathrm{DSC}} = \frac{\Delta H(t)}{\Delta H_{\mathrm{total}}} \quad (6)$$

where α_{DSC} is the DSC conversion, $\Delta H(t)$ is the enthalpy variation as a function of the time spent at a given temperature condition, $\Delta H_{\mathrm{total}}$ is the total heat of the reaction. It should be added that $\Delta H_{\mathrm{total}} = \Delta H(t) + \Delta H(T)$ is the sum of the isothermal enthalpy $\Delta H(t)$ (Fig. 3(a) and (b)) and the enthalpy of non-isothermal experiments $\Delta H(T)$ (Fig. 3(c)).[30,31,33,34] From the

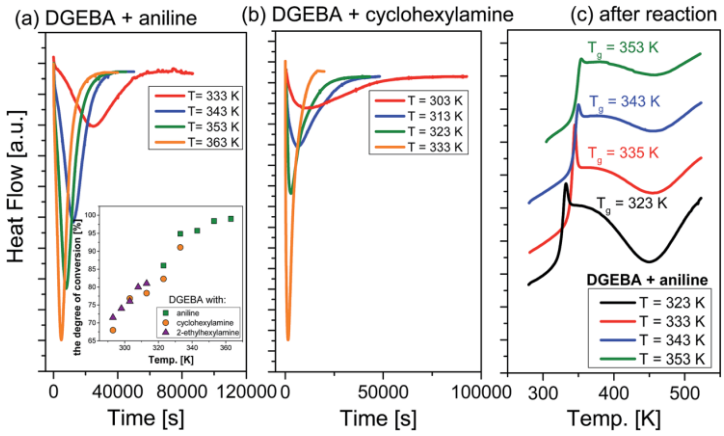

Fig. 3 Panels (a) and (b): raw calorimetric data obtained upon the curing of epoxy resin with aniline and cyclohexylamine, respectively. Panel (c): DSC thermograms obtained after the curing of DGEBA with aniline at indicated isothermal condition. As an inset in panel (a), the temperature dependency of the degree of conversion for all systems is presented.

presented kinetic curves (insets in Fig. 2), it is clear that the reaction gets faster with increasing temperature. Simultaneously, the degree of monomer conversion increases up to 91% and 98% for DGEBA polymerized with cyclohexylamine and aniline, respectively, at the highest temperatures. For comparison, α determined for the similar systems studied in literature varies between 80 and 90%.[4] In addition, our calorimetric data revealed that in each case, the curing system undergoes vitrification with the glass transition temperature located within experimental uncertainty at a temperature at which reaction was carried out.

The next step of the analysis was to model the cure kinetics and to determine the rate constants of the reaction. Due to complexity of the studied reaction, the curing kinetics of thermosetting materials can be analyzed by the application of three alternative models: (i) *n*-th order,[35] (ii) autocatalytic[36–38] and (iii) Avrami.[39] For the purpose of this paper, we decided to apply the last one, which is the commonly used approach in the literature to describe kinetics of step growth polymerization.[40–45] Although the Avrami equation is mostly used to model the kinetics of crystallization, it can be applied also successfully to describe the kinetics of polymerization. As the reaction continues, the formation of many molecular aggregates (microgels) or high-molecular weight particles can be observed as a result of curing.[46] A similar scenario can also be observed in the case of crystallization, where the nucleation also proceeds with time. Thus, it has been considered that, in a broad sense, crystallization can be considered as a physical form of polymerization.[41,47] The equation we applied reads as follows:[39]

$$\frac{\alpha}{\alpha_m} = 1 - \exp(-kt^n) \quad (7)$$

where α is the dielectric or DSC conversion, α_m is the maximum monomer conversion, k is the rate constant of the reaction, and n is the Avrami exponent that can be related to the mechanism of either crystallization or chemical reaction. As can be observed in Fig. 2, the Avrami model describes the kinetics data obtained for the various systems in the studied range of times and temperatures quite well, enabling accurate characterization of the rate constants.

In Fig. 4, the temperature dependent rate constants determined for both investigated systems are presented. It can be seen that the value of the rate constant increases with temperature. Moreover, it is worth noting that k determined from dielectric and calorimetric data is almost the same (within experimental uncertainty) in the studied range of temperatures. However, despite the good correspondence of the rate constants determined from BDS and DSC, clear differences in time evolution of the kinetic curves are observed. To explain these discrepancies, one should go to the fundamentals of the step growth polymerization. In this specific case, increasing molecular weight of the newly formed macromolecules is not linearly correlated with the monomer conversion. On the other hand, dielectric spectroscopy follows the shifting of the segmental relaxation process which is attributed to the increasing molecular weight of the formed macromolecules, while DSC traces the real monomer conversion upon polymerization. Hence, it is expected that kinetic curves constructed from the dielectric and calorimetric data should differ. Nevertheless, both techniques give almost the same information on the rate constant as is demonstrated in Fig. 4(a) and (b).

As a final point of this part of the paper, activation energies for the curing DGEBA with various amines were estimated using the Arrhenius function:

$$k = k_0 \exp(E_a/RT) \quad (8)$$

where k_0 is a pre-exponential factor, E_a is the activation barrier and R is the gas constant. The activation energy determined from the dielectric measurements was equaled to 44.6 and 45.8 kJ mol^{-1} for aniline and cyclohexylamine, respectively (Fig. 4(a) and (b)). The determined values are in good agreement

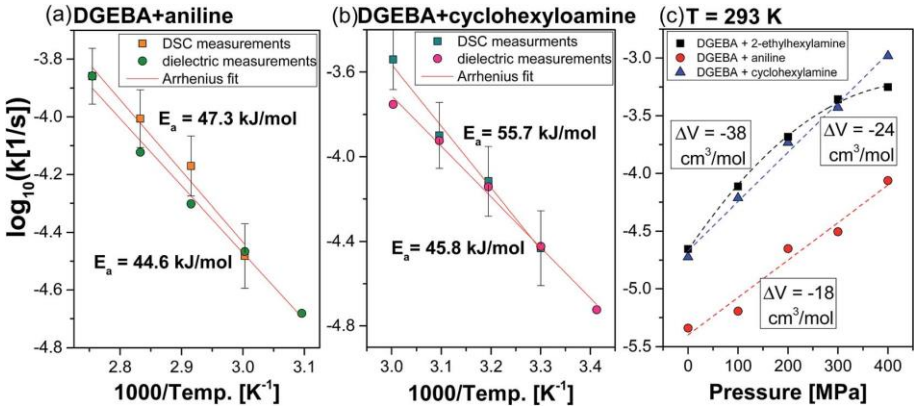

Fig. 4 Panels (a) and (b): temperature dependence of the rate constants obtained from dielectric (circles) and DSC (squares) measurements performed at ambient pressure for polymerization performed with two curing agents: aniline and cyclohexylamine, respectively. Red lines represent the best fit to eqn (7). Panel (c): pressure dependence of the rate constants obtained from dielectric measurements for different epoxy resin curing systems. Data for DGEBA–2-ethylhexylamine system are from ref. 4. Dashed lines represent the best fit to either the linear or parabolic equation.

with those determined from DSC measurements (47.3 and 55.7 kJ mol^{-1}, respectively). It should be stressed that similar value of the activation energy E_a = 46 and 59 kJ mol^{-1} was calculated for the curing of DGEBA with 2-ethylhexylamine[4] and 4,4′-diaminodicyclohexylmethane (PACM),[2] respectively.

3.2 Elevated pressure condition

Since it is well known that pressure accelerates progress of the majority of the chemical reactions, we decided to probe the impact of compression on the dynamics, properties of the formed polymers, as well as the monomer conversion and the kinetics of step growth polymerization. Unfortunately, we were not able to carry out calorimetric measurements at high pressure. Hence, all further analysis will be done, based mainly on the dielectric data.

As a first, dielectric loss spectra obtained during polymerization of DGEBA with aniline and cyclohexylamine performed at different thermodynamic conditions were analyzed with the use of the Havriliak–Negami function with a conductivity term added.[48] The fitting function is given by:

$$\varepsilon(\varpi)'' = \frac{\sigma_{dc}}{\varepsilon_0 \varpi} + \frac{\Delta\varepsilon}{[1 + (i\varpi\tau)^{\alpha}]^{\beta}} \quad (9)$$

where α and β are the shape parameters representing the symmetric and asymmetric broadening of given relaxation peaks, $\Delta\varepsilon$ is the dielectric relaxation strength, τ is the relaxation time, ε_0 is vacuum permittivity, and ω is an angular frequency ($\omega = 2\pi f$). In Fig. 5, the time evolution of the segmental relaxation times at ambient and elevated pressure is presented. One can observe the significant shift of τ_α over more than seven decades which is comparable to the data presented in literature.[4] Moreover, it is clear that the effect of pressure is more pronounced than the one induced by temperature variation. In this context, it is worth adding that the curing of DGEBA with aniline at 293 K at ambient pressure takes almost 7 days (data not shown).[49] The application of pressure of p = 100 MPa decreases the time of the reaction to almost 3 days, making the reaction more than two times faster with respect to the ambient conditions. Further compression up to 400 MPa reduces the time at which system undergoes vitrification down to less than 24 h. Hence when we compare this data to that obtained at ambient pressure, it will be clear that the time of the reaction was shortened by more than seven times. It should be stressed that the similar situation occurred in the case of pressure polymerization of DGEBA with cyclohexylamine and 2-ethylhexylamine.[4] Although the impact of pressure was not as pronounced as in the case of the DGEBA–aniline system.

In the next step, DSC measurements were carried out to determine the monomer conversion as well as the glass transition temperatures of macromolecules produced at high pressures. It should be stressed that these investigations were done immediately after pressure was released to avoid further curing of each system and water uptake. For this purpose, temperature dependent DSC measurements were carried out on the cured samples. These investigations enabled determination of the residual heat of polymerization $\Delta H(T)$. Thus,

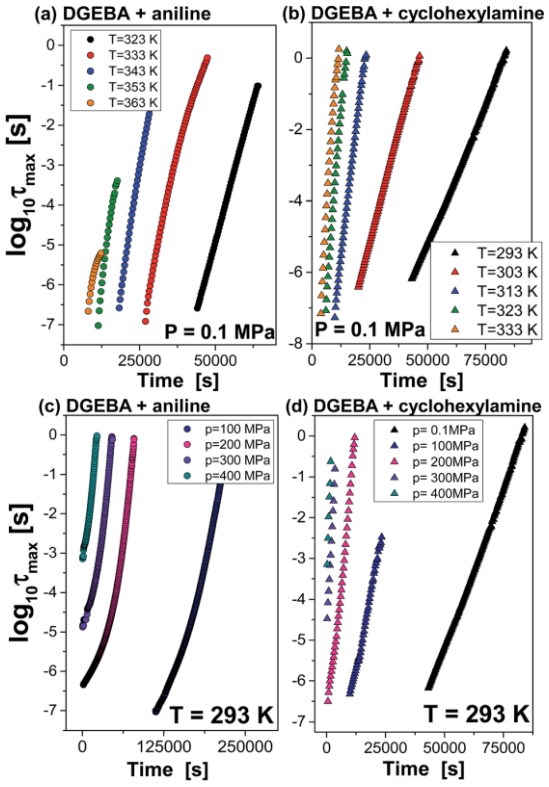

Fig. 5 Time evolution of structural relaxation times of polymerization performed at ambient ((a) and (b)) and elevated pressure conditions ((c) and (d)).

assuming ΔH_{total} to be pressure independent and applying eqn (6), we were able to evaluate the degree of monomer conversion for all examined systems polymerized at elevated pressures. In Fig. 6(a), the evolution of the degree of monomer conversion as a function of pressure is presented for each studied system. As it can be seen, α drops around 10% for the highest compression with respect to the ambient pressure polymerization and reaches approximately 62% and 54% for DGEBA cured with cyclohexylamine, 2-ethylhexylamine and aniline respectively. Additionally, the evolution of the glass transition temperature (T_g) of the polymers recovered at different thermodynamic conditions was shown in panel (b) in Fig. 6. It can be seen that T_g decreases with compression and falls within the range 273–280 K for the reactions carried out at T = 293 K and p = 400 MPa for all examined systems. Hence, the glass transition temperatures of the macromolecules recovered from the polymerization performed at high compression are 10–20 K lower than that of the reactions carried out at ambient conditions. This finding is quite surprising in the light of the literature data showing that at elevated pressures macromolecules of higher molecular weight and lower PDI index are obtained, and the degree of monomer conversion is usually significantly

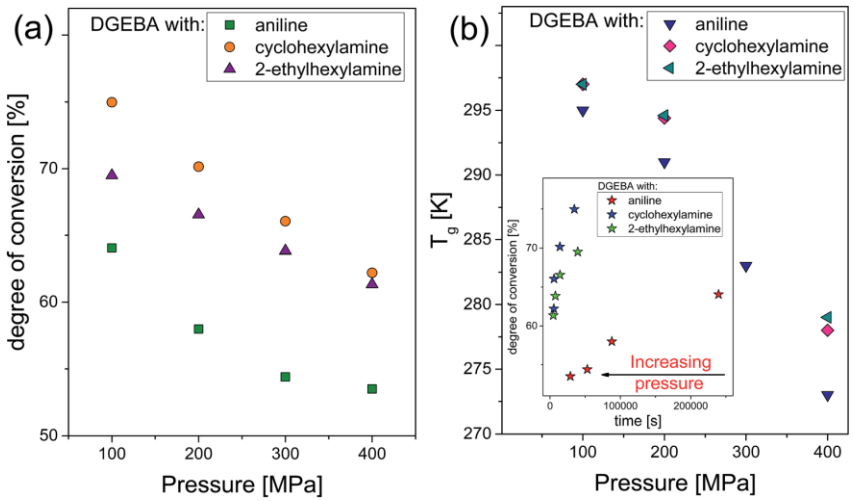

Fig. 6 Panel (a): the evolution of the degree of conversion of the curing of DGEBA with various curing agents as a function of pressure. Panel (b): the pressure dependency of the glass transition temperature of polymerized systems. As inset in panel (b), the time dependency of the degree of conversion of examined systems is presented.

higher. However, this situation is reported for systems with very low viscosity.[13,14]

On the other hand, in the case of the hardening of natural and synthetic resins, one should take into account also the chemical vitrification, which seems to have important influence on the kinetics of polymerization. This process assumes the ongoing polymerization of the constituent molecules is *via* the formation of irreversible chemical bonds, resulting in changes of the dynamics and the thermodynamic properties of the vitrified system.[50] Thus, once the curing system undergoes the glass transition, the reaction is essentially ended due to the immobilization of monomers. Therefore, further elongation of the chain is not possible. Hence, it seems that the time required for the system to reach the vitrification point is quite an important variable. In the inset to Fig. 6, we plot degree of monomer conversion *versus* time after which the polymerized samples undergo glass transition. It is well seen that there is linear dependency between both parameters indicating their interrelations.

As a final point of our discussion, we decided to utilize dielectric and calorimetric data obtained for the polymerization carried out at high pressures to evaluate rate constants and the activation volumes at different thermodynamic conditions for the investigated reactions. For this purpose, the same kind of analysis as the one described above was carried out and the kinetic curves constructed by normalizing the data with respect to the maximum degree of monomer conversion are presented in Fig. 7. Time dependences of α_{BDS} were fitted to the Avrami equation [eqn (7)]. This model describes experimental data very well enabling calculations of the rate constants, which were further plotted *vs.* pressure and presented in Fig. 4(c). It can be seen that the value of the rate constant increases with compression. However above 300 MPa, the slowing down of the reaction can be observed for the DGEBA–2-ethylhexylamine system.[4] This indicates that above this pressure, the viscosity of the system at the beginning of the reaction becomes too large and reduces the monomer diffusion. As a consequence, pressure acts as an inhibitor of polymerization. We believe that this effect is related to the sensitivity of viscosity or structural dynamics of the given system to the applied pressure. The increase in viscosity due to compression is the highest for the binary mixture consisting of 2-etyhexylamine and DGEBA. Hence, even at moderate pressures, this system becomes very viscous in a relatively short time. As a consequence, molecular diffusion and the pace of the reaction is slowed down, as shown

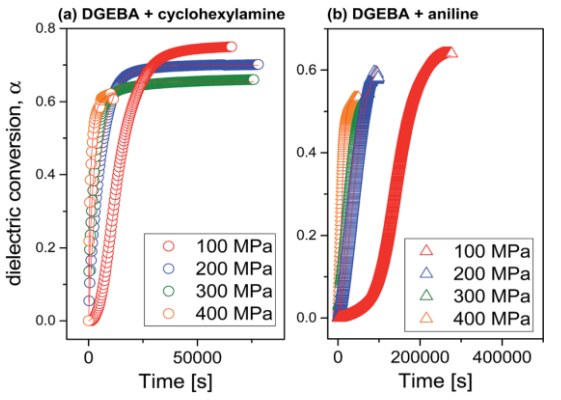

Fig. 7 Time evolution of dielectric conversion obtained after renormalization of the permittivity ε' measured at $f = 0.3$ MHz accordingly to eqn (5) for the reaction carried out for different curing agents at elevated pressure conditions. Solid lines represent the best fit to the Avrami equation [eqn (7)].

in Fig. 4(c). On the other hand, the impact of pressure on the viscosity in case of other examined herein samples is not so significant at the beginning of the reaction. Hence, polymerization is in the mass controlled regime in a wider range of pressures. It is worth adding that a similar scenario was also observed for the polymerization of isoprene, where similar slowing of the reaction was reported above 2 GPa.[11]

Additionally from the pressure dependency of the rate constants, activation volume of polymerization was calculated using eqn (3). It was found that in the limit of ambient pressure, ΔV varies significantly from −18, −24 up to −38 cm^3 mol^{-1} for DGEBA polymerized with aniline, cyclohexylamine and 2-ethylhexylamine respectively.[4] Hence, it seems to be quite obvious that activation volume is directly related to the structure of the amine used for the reactions with DGEBA. What is more, the ΔV was the greatest in the case of system consisting of DGEBA and aromatic amine. Herein, it should be noted that typical values of ΔV for the epoxide ring opening reactions is in the range −15 to −20 cm^3 mol^{-1}.[16–18] On the other hand, our data show that, dependent on the curing agent, the activation volume may change in much wider range. The other very interesting aspect is that activation volume tends to change and increase for DGEBA cured with 2-ethylhexylamine, while it stays constant in the range of studied pressures for DGEBA polymerized with aniline and cyclohexylamine. However, we are quite convinced that it is due to the range of compression applied in our studies. It is expected that for the reaction carried out at much higher pressures, activation volume will tend to increases even in the case of the latter systems.

4. Summary and conclusion

Kinetics and dynamics of the curing of DGEBA with various curing agents were measured by means of dielectric spectroscopy in wide ranges of temperatures and pressures. In addition, complementary DSC measurements were carried out to determine the degree of monomer conversion as well as glass transition temperatures for the samples polymerized at different thermodynamic conditions. It was found that compression enhances the rate of the reaction. Consequently, the reaction time was significantly reduced with respect to the ambient pressure polymerization procedure. However, due to quite fast vitrification of DGEBA cured with different amine hardeners, the degree of monomer conversion drops approximately 10% and the glass transition temperature of the recovered product is 10–20 K lower when compared to the reaction carried out at ambient pressure. Hence, it appears that in order to improve the degree of monomer conversion, increase the glass transition temperature of the macromolecules, and shorten the time of polymerization, one should change pressure continuously during polymerization. This will enable better control over viscosity, avoiding vitrification and allowing for the completion of the reaction. As a consequence, polymers of desired properties can be obtained during relatively short reaction times. In addition, activation volumes falling in the range −18 and −38 cm^3 mol^{-1} were determined for the studied systems. It can be stated that they are lower than the ΔV predicted in literature for the reaction involving opening of the epoxide ring. However, our studies clearly indicated that ΔV is a function of hardener as well as thermodynamic conditions. Thus, it can vary in much wider range than it is reported in literature.

Conflict of interest

The authors declare no competing financial interests.

Acknowledgements

K. K., S. P. and M. T. gratefully acknowledge financial support from the Polish National Science Centre within the program Sonata 2 entitled “High pressure polymerization. The kinetic studies” based on decision DEC-2012/05/D/ST4/00326. The authors thank K. L. Ngai and Philip J. Griffin for the language assistance during manuscript preparation.

References

1 N. S. Isaacs, *Liquid Phase High Pressure Chemistry*; Wiley, New 572 York, 1981.
2 J. Fournier, G. Williams, C. Duch and G. A. Aldridge, *Macromolecules*, 1996, **29**, 7097–7107.
3 M. Tarnacka, T. Flak, M. Dulski, S. Pawlus, K. Adrjanowicz, A. Swinarew, K. Kaminski and M. Paluch, *Polymer*, 2014, **55**, 1984–1990.
4 M. Tarnacka, O. Madejczyk, M. Dulski, M. Wikarek, S. Pawlus, K. Adrjanowicz, K. Kaminski and M. Paluch, *Macromolecules*, 2014, **47**, 4288–4297.
5 K. Kaminski, M. Paluch, R. Wrzalik, J. Ziolo, R. Bogoslovov and C. M. Roland, *J. Polym. Sci., Part A: Polym. Chem.*, 2008, **46**, 3795–3801.
6 P. W. Bridgman and J. B. Conant, *Proc. Natl. Acad. Sci. U. S. A.*, 1929, **15**, 680–683.
7 D. Gourdain, J. C. Chervin and P. Pruzan, *J. Chem. Phys.*, 1996, **105**, 9040–9045.
8 F. Wurche and F. G. Klarne, *High Pressure Chemistry*, ed. R. van Eldik and F. G. Klarner, Wiley, New York, 2002.
9 M. Citroni, M. Ceppatelli, R. Bini and V. Schettino, *Science*, 2002, **295**, 2058–2060.
10 D. Chelazzi, M. Ceppatelli, M. Santoro, R. Bini and V. Schettino, *J. Phys. Chem. B*, 2005, **109**, 21658–21663.
11 M. Citrini, M. Ceppatelli, R. Bini and V. Scettino, *J. Phys. Chem. B*, 2007, **111**, 3910–3917.
12 T. R. Waite, *Phys. Rev.*, 1957, **107**, 463–478.
13 L. Mueller, W. Jakubowski, K. Matyjaszewski, J. Pietrasik, P. Kwiatkowski, W. Chaladaj and J. Jurczak, *Eur. Polym. J.*, 2011, **47**, 730–734.
14 P. Kwiatkowski, J. Jurczak, J. Pietrasik, L. Mueller and K. Matyjaszewski, *Macromolecules*, 2008, **41**, 1067–1069.
15 M. J. Evans and M. Polanyi, *Trans. Faraday Soc.*, 1935, **31**, 875–894.
16 T. Asano and W. J. le Noble, *Chem. Rev.*, 1978, **78**, 407–489.
17 R. van Eldik, T. Asano and W. J. le Noble, *Chem. Rev.*, 1989, **89**, 549–688.

18 A. Drljaca, C. D. Hubbard, R. van Eldik, T. Asano, M. V. Basilevsky and W. J. le Noble, *Chem. Rev.*, 1998, **98**, 2167–2289.
19 V. D. Kiselev, M. S. Shikhaab, G. G. Iskhakova and A. I. Konovalov, *Russ. J. Gen. Chem.*, 2002, **72**, 98–104.
20 L. V. McAdams and J. A. Gannon, in *Encyclopedia of Polymer Science and Engineering*, ed. H. F. Mark, N. M.Bikales, C. G.Overberger and J. I.Kroschwitz, John Wiley and Sons, New York, 1986, vol. 6, p. 322.
21 F. Ricciardi, W. A. Romanchick and M. M. Joullie, *J. Polym. Sci., Part A: Polym. Chem.*, 1983, **21**, 1475–1490.
22 G. Levita, A. Livi, P. A. Rolla and C. Culicchi, *J. Polym. Sci., Part B: Polym. Phys.*, 1996, **34**, 2731–2737.
23 E. Tombari, C. Ferrari, G. Salvetti and G. P. Johari, *J. Phys.: Condens. Matter*, 1997, **9**, 7017–7037.
24 D. A. Wasylyshyn and G. P. Johari, *J. Polym. Sci., Part B: Polym. Phys.*, 1997, **35**, 437–456.
25 D. A. Wasylyshyn and G. P. Johari, *J. Polym. Sci., Part B: Polym. Phys.*, 1999, **37**, 3071–3083.
26 G. Galonne, S. Capaccioli, G. Levita, P. A. Rolla and S. Corezzi, *Polym. Int.*, 2001, **50**, 545–551.
27 J. Mijovic and B. D. Fitz, *Dielectric Spectroscopy of Reactive Polymers: Application Note Dielectrics 2*, Novocontrol, Hundsangen, Germany, vol. 591, 1998.
28 G. P. Johari, *J. Chem. Soc. Faraday Trans.*, 1994, **90**, 883–888.
29 R. Casalini, S. Corezzi, A. Livi, G. Levita and P. A. Rolla, *J. Appl. Polym. Sci.*, 1997, **65**, 17–25.
30 D. S. Achilias, *J. Therm. Anal. Calorim.*, 2014, **116**, 1379–1386.
31 M. T. Viciosa, J. Quiles Hoyo, M. Dionisio and J. L. Gomez Ribelles, *J. Therm. Anal. Calorim.*, 2007, **90**, 407–414.
32 H. F. Lu and J. N. Hay, *Polymer*, 2001, **42**, 9423–9431.
33 A. T. Lorenzo, M. L. Arnal, J. Albuerne and A. J. Muller, *Polym. Test.*, 2007, **26**, 222–231.
34 M. G. Parthun and G. P. Johari, *J. Chem. Phys.*, 1995, **103**, 440–450.
35 I. T. Smith, *Polymer*, 1961, **2**, 95–108.
36 K. Horie, H. Hiura, M. Souvada, I. Mita and H. Kambe, *J. Appl. Polym. Sci. A: Polym. Chem.*, 1970, **8**, 1357.
37 M. R. Kamal, *Polym. Eng. Sci.*, 1974, **14**, 23.
38 S. Sourour and M. R. Kamal, *Thermochim. Acta*, 1976, **14**, 41.
39 M. Avrami, *J. Chem. Phys.*, 1939, **7**, 1103–1112; 1940, 8, 212–224; 1941, 9, 177–184.
40 V. Schetitino and R. Bini, *Chem. Soc. Rev.*, 2007, **36**, 869–880.
41 M. G. Lu, M. J. Shim and S. W. Kim, *Mater. Sci. Commun.*, 1998, **56**, 193.
42 S. W. Kim, M. G. Lu and M. J. Shim, *Polym. J.*, 1998, **30**, 90.
43 M. G. Lu, M. J. Shim and S. W. Kim, *J. Therm. Anal. Calorim.*, 1999, **58**, 701–709.
44 C. Yiyun, C. Dazhu, F. Rongqiang and H. Pingsheng, *Polym. Int.*, 2005, **54**, 495–499.
45 S. V. Muzumdar and L. J. Lee, *Polym. Eng. Sci.*, 1996, **36**, 943–952.
46 M. Pollard and J. L. Kardos, *Polym. Eng. Sci.*, 1987, **27**, 829.
47 X. Weibing, H. Pingsheng and C. Dazhu, *Eur. Polym. J.*, 2003, **39**, 617–625.
48 S. Havriliak and S. Negami, *J. Polym. Sci., Part C: Polym. Symp.*, 1966, **14**, 99–117.
49 M. Tarnacka, M. Dulski, S. Starzonek, K. Adrjanowicz, E. U. Mapesa, K. Kaminski and M. Paluch, *Polymer*, 2015, **68**, 253–261.
50 S. Corezzi, D. Fioretto and P. Rolla, *Nature*, 2002, **420**, 653.

A4. Following Kinetics and Dynamics of DGEBA-aniline Polymerization in Nanoporous Native Alumina Oxide Membranes - FTIR and Dielectric Studies.

Autorzy: M. Tarnacka, M. Dulski, S. Starzonek, K. Adrjanowicz, E. U. Mapesa, K. Kaminski, M. Paluch

Referencja: *Polymer* 2015, **68**, 253-261

Mój udział w poniższym artykule polegał na zaplanowaniu i koordynowaniu eksperymentu, wykonaniu pomiarów dielektrycznych, analizie otrzymanych wyników i ich dyskusji oraz przygotowaniu artykułu. Natomiast wkład pozostałych autorów pracy wyglądał następująco:

- dr Mateusz Dulski wykonał pomiary IR oraz przeanalizował otrzymane wyniki,
- Szymon Starzonek pomógł w przygotowaniu próbek,
- dr Karolina Adrjanowicz brała udział w dyskusji otrzymanych wyników,
- dr Emmanuel U. Mapesa brał udział w edycji powstającego manuskryptu pod względem językowym.
- dr hab. Kamil Kamiński brał udział w dyskusji wyników oraz korekcji treści manuskryptu,
- prof. dr hab. Marian Paluch brał udział w dyskusji wyników.

Polymer 68 (2015) 253–261

Contents lists available at ScienceDirect

Polymer

journal homepage: www.elsevier.com/locate/polymer

Following kinetics and dynamics of DGEBA-aniline polymerization in nanoporous native alumina oxide membranes – FTIR and dielectric studies

Magdalena Tarnacka [a, b, 1], Mateusz Dulski [b, c, 1], Szymon Starzonek [a, b, 1], Karolina Adrjanowicz [d], Emmanuel U. Mapesa [e], Kamil Kaminski [a, b, *, 1], Marian Paluch [a, b, 1]

[a] Institute of Physics, University of Silesia, Uniwersytecka 4, 40-007 Katowice, Poland
[b] Silesian Center of Education and Interdisciplinary Research, University of Silesia, 75 Pulku Piechoty 1A, 41-500 Chorzow, Poland
[c] Department of Material Sciences, University of Silesia, 75 Pulku Piechoty 1A, Chorzow 41-500, Poland
[d] NanoBioMedical Centre, Adam Mickiewicz University, ul. Umultowska 85, 61-614 Poznan, Poland
[e] Institute Experimental Physics I, University of Leipzig, Linnestr. 5, 04103 Leipzig, Germany

ARTICLE INFO

Article history:
Received 3 April 2015
Received in revised form
10 May 2015
Accepted 12 May 2015
Available online 19 May 2015

Keywords:
Step-growth polymerization
Confined geometry
Reaction kinetics

ABSTRACT

Fourier Transform Infrared and Broadband Dielectric Spectroscopies were applied to follow kinetics as well as molecular dynamics upon step-growth polymerization of bisphenol-A diglycidyl ether (DGEBA) with aniline both in bulk and in anodic aluminum oxide (AAO) membranes. For the first time the dynamics and kinetics of a curing epoxy system under confinement were analyzed and compared with the reaction in the bulk. As it turned out, polymerization is faster under confinement, compared to the analogous reaction carried out in the bulk system at the same temperature conditions. Additionally, the reaction speeds up with the degree of confinement. Furthermore, it was found that the initial step of the polymerization is significantly reduced or even suppressed in nanochannels; this is evident from the observation that kinetic curves do not follow sigmoidal shape that is characteristic for the autocatalytic type of chemical reactions. FTIR data showed unquestionably that the rate of reaction is slower at the surface of the pores with respect to the polymerization at the core of nanochannels. This finding is in tandem with Monte Carlo simulation reporting lower reactivity of the functional units close to the pore walls. Moreover, we found out that the activation barrier for the polymerization remains unchanged under confinement. Finally, dielectric measurements revealed that there is a characteristic change in the slope of segmental relaxation times plotted as a function of the time of reaction under confinement, a phenomenon whose comprehension demands further investigation.

1. Introduction

The effect of confined geometry on molecular dynamics, phase transitions and the crystallization behavior of different materials has been investigated for years by many research groups [1–4]. Generally, a decrease in the glass transition or melting temperature is observed in 1D and 2D confinement upon approaching the nanometer scale [5–11]. However, experimental and simulation studies have also revealed some counterexamples that exhibit enhancement of both transitions with respect to the bulk values [12,13]. One of the key determinant factors here seems to be the strength of the intermolecular interactions between the surface matrix and the guest molecules. If those interactions are weak, a decrease in the freezing point can be observed. On the other hand, once they are strong, the opposite scenario is expected with the magnitude of the shift strongly depending on the size of the confining environment [14]. According to the Gibbs–Thomson approach, the shift of the melting temperature under confinement is linearly correlated to the diameter of the pores [5]. Moreover, previous studies have also indicated that crystallization of the

* Corresponding author. Institute of Physics, University of Silesia, Uniwersytecka 4, 40-007 Katowice, Poland.
E-mail address: kamil.kaminski@us.edu.pl (K. Kaminski).
[1] These authors contributed equally.

http://dx.doi.org/10.1016/j.polymer.2015.05.022
0032-3861/

very labile compounds can be effectively suppressed in different nanoporous materials [5,11,15,16]. This springs from the fact that in some cases the pore diameter is smaller than the critical nucleus size that triggers nucleation and the crystal growth process. Hence, formation of the crystal can be completely eliminated. This observation may be of exceptional importance in view of potential pharmaceutical applications of these materials as drug carriers.

Another promising application of nanoporous materials is to control and produce a variety of two dimensional unique polymer morphologies well defined on the nanometric length scale that otherwise cannot be obtained via standard methods of synthesis. These macromolecules can be further used in nano-engineering, as miniaturized sensors, magnetic labels, tissue implants etc. [17–19].

The majority of studies devoted to the polymerization process are focused on the basic structural properties of the recovered polymers. Surprisingly, only a few of them are dedicated to monitor in situ polymerization of monomers confined in nanochannels [20–23]. Several investigations focused on the radical polymerization of standard monomers such as styrene [24] or acrylates [25–28] revealed that the reaction proceeds much faster in the nanocavities when compared to bulk polymerization. This enhancement of the reaction pace was shown to be correlated to the pore diameter. The same observation was made for the step-growth polymerization of bisphenol-M dicyanate ester [29]. Furthermore, Quingxiu et al. [30] investigated the effect of surface chemistry (native and silanized pores) on the curing kinetics of this system. They have demonstrated that polymerization is much faster in the native controlled pore glasses due to the catalytic nature of the hydroxyl group. Uemura et al. [25] have studied the impact of confinement on the molecular weight and stereostructure of polymers recovered after radical polymerization of vinyl monomers in porous coordination materials. They reported that macromolecules of much higher molecular weight and lower PDI were obtained. Additionally, in some cases, it was possible to control, to some extent, the tacticity of obtained polymers. Giussi et al. have also made similar observations for the case of radical polymerization of styrene [24].

Since almost all studies – except those employing radical pyrolysis reactions [31] – have indicated, with respect to bulk polymerization, that the same reaction under confinement is much faster, and that polymers of higher M_n can be produced, concerted efforts have been aimed at understanding the microscopic origin of these findings. Some authors have suggested that the rate of termination is probably significantly suppressed due to a decrease in chain diffusivity for reactions carried out in geometrical confinement. This effect seems to be especially significant in the direction perpendicular to the pore walls [32]. Such predictions were further reinforced in some way by Monte Carlo studies that revealed an inverse scaling of the polymer chain diffusivity with confinement size to the second power [33]. Note worthily, these computations showed monomer diffusion not to be affected at all by the confinement.

This paper presents studies of the kinetics and dynamics of a curing system under confinement. FTIR data revealed that reaction proceeds much faster in pores. Also, kinetic curves follow an exponential trend suggesting strong reduction of the initial part of the step growth polymerization. We also found that the reaction close to the pore walls is slightly slower than at the center of the nanochannels. This is due to reduced reactivity of the functional groups caused by the interaction with hydroxyl groups attached to the pore walls, as reported recently from Monte Carlo simulation [33]. Additionally, our FTIR studies indicated that the activation barrier for the polymerization stays constant. As a final point of our investigations, the dynamics of the curing system under confinement was examined for the first time. Using broadband dielectric spectroscopy, we had the possibility to follow the real time progress of segmental relaxation as the reaction proceeded. We report that its evolution is completely different from that observed for bulk polymerization, and intuitively attribute this to changes in density caused by strong interactions between pore walls and the curing system. Furthermore, we observe a broadening of the segmental relaxation with decreasing pore diameter and assign this phenomenon to the increasing interactions between the curing system and pore walls with decreasing pore diameter.

2. Experimental section

Bisphenol-A diglycidyl ether (known as EPON 828 or DGEBA) and aniline of purity higher than 99% were supplied from the Sigma Aldrich. These two compounds were mixed in the molar ratio 1:1 (see Scheme 1).

2.1. Infiltration procedure

Anodic aluminum oxide (AAO) membranes, having dimensions ranging from 150 to 18 nm, were purchased from Synkera Technologies, Inc. Prior to filling, the membranes were dried in an oven at 423 K to remove any volatile fractions from the nanochannels. After cooling, they were placed in a solution made of DGEBA and aniline, mixed in the molar stoichiometric ratio. Then, the whole system was maintained at T = 288 K in vacuum (10^{-2} bar) for 12 h to let both compounds flow into the nanocavities. The temperature of infiltration was chosen after a series of trial measurements. We had to balance between viscosity (that increases significantly with lowering temperature) and progress of the reaction (which increases with temperature). At the selected infiltration conditions, the progress of reaction was relatively small, even after 12 h. Basing on the analysis of the integral intensities of NH_2 vibration and the band at around 3056 cm^{-1}, monomer conversion was estimated to be equal to 2–4% after filing for each sample.

2.2. Dielectric measurements

Isobaric measurements of the dielectric permittivity $\varepsilon^*(\omega) = \varepsilon'(\omega) - i\varepsilon''(\omega)$ at ambient pressure were performed using an impedance analyzer (Novocontrol Alpha) over a frequency range from $1\cdot10^{-2}$ to $3\cdot10^{6}$ Hz. AAO templates filled with DGEBA and aniline were placed between two stainless-steel electrodes (diameter: 10 mm) and mounted inside a cryostat. During measurement each sample was maintained under dry nitrogen gas flow. The temperature was controlled by a Quatro Cryosystem using a nitrogen gas cryostat, with stability better than 0.1 K. The time dependent dielectric measurements of the curing system were performed at two different temperatures, T = 293 and 323 K.

2.3. Infrared measurements

Time-dependent infrared data for bulk and pores were carried out using Agilent Cary 660 FTIR spectrometer equipped with a standard source and a DTGS Peltier-cooled detector. The bulk material prepared as a thick film (~5 μm) was placed between two parallel ZnSe windows. Isothermal measurements for bulk and pores were performed using a heating stage with an accuracy of ±0.1 K. Bulk infrared spectra were accumulated in the 500–4000 cm^{-1} range while spectra for pores were collected from 2500 to 4000 cm^{-1} due to strong Al_2O_3 absorption in the

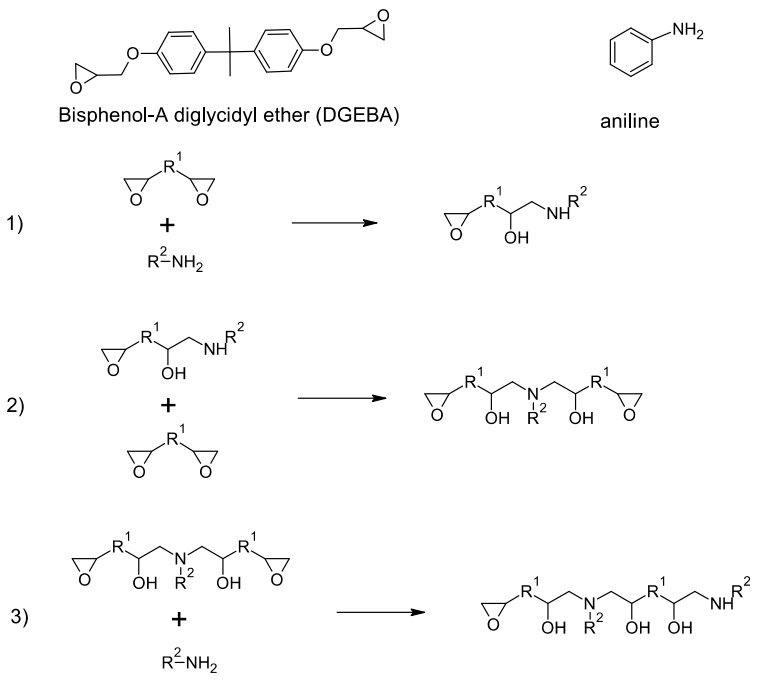

Scheme 1. The chemical structures of DGEBA, aniline and polymerization scheme between an epoxide and amine groups.

low-frequency range. All spectra were recorded with a spectral resolution of 4 cm^{-1} and 16 scans.

3. Results and discussion

In the literature, there are only a handful of studies on the ring opening polymerization or especially epoxy amine curing reaction under confinement. This mainly due to the fact that usually after mixing of the compounds, reaction proceeds very fast making it impossible to fill the membranes in reasonable time. Consequently, not much can be deduced from the experimental data on the mechanism as well as kinetics of such reaction. Interestingly, we found one epoxy amine system that undergoes polymerization very slowly, over one week at room temperature. So we got enough time to fill the membranes. Simultaneously, the progress of the reaction was kept low upon filling. Hence, an exceptional opportunity to study kinetics as well as dynamics of this specific reaction under confinement for the first time was given.

In order to probe the impact of confinement on the speed of step growth polymerization, first the bulk kinetics was evaluated by means of FTIR spectroscopy. Fig. 1 illustrates infrared spectra obtained upon polymerization of aniline and DGEBA at T = 323 K. One can see that during the reaction, absorbance as well as the positions of some bands undergoes continuous changes. The intensity of the bands associated with hydroxyl (ν_{OH}) and secondary amine (ν_{NH2}) stretching vibrations, in the 3300–3500 cm^{-1} and 3410–3470 cm^{-1} range, respectively, as well as bands originating from the vibration within epoxy rings (ν_{C-O-C}) between 970 and 1010 cm^{-1} significantly changed. The deconvolution of each mentioned wavenumber region was done to precisely grasp the structural changes occurring during polymerization. It should be expected that the intensity of bands connected to amine and epoxide moieties decreases while that from hydroxyl units increases. Hence, the reaction kinetics can be evaluated based on the analysis of integral intensities (I) of these bands. It is worth noting that each analyzed band was renormalized with respect to the vibration of methyl group located in the 2800–3000 cm^{-1} region that stays constant in the course of the reaction. Note that the analysis of amine/epoxy bands provides information of the monomers concentration or conversion, as well.

To show kinetic curves of the reaction measured at four different temperatures (in the range 323–353 K) on one graph, normalized integral intensities of the considered bands are rescaled accordingly to the following equation:

$$\alpha_m = \frac{I(0) - I(t)}{I(0) - I(\infty)}, \quad (1)$$

where $I(0)$ and $I(\infty)$ are the initial and final values of the integral intensities measured during the polymerization progress, while α_m denotes maximum monomer conversion. It should be added that α_m was determined from the analysis of the integral intensities of the amine as well as oxirane units. Deconvolution of the data enabled precise estimation of the real amine/epoxy band positions and their integral intensities at the beginning and at the end of the process, which were further used to recalculate the degree of monomer conversion. However, due to the very weak intensity of the band connected to the vibrations of the epoxide ring and the overlapping of the band connected to the vibration of amine with the one corresponding to the hydroxyl groups, such analysis may yield adulterated results as discussed in literature [34–38]. Therefore, complementary analysis with the use of calorimetry was done. Interestingly, very good agreement (within negligible percent disparity) between monomer conversion estimated from FTIR and DSC measurements was obtained (see panel (e) in Fig. 2).

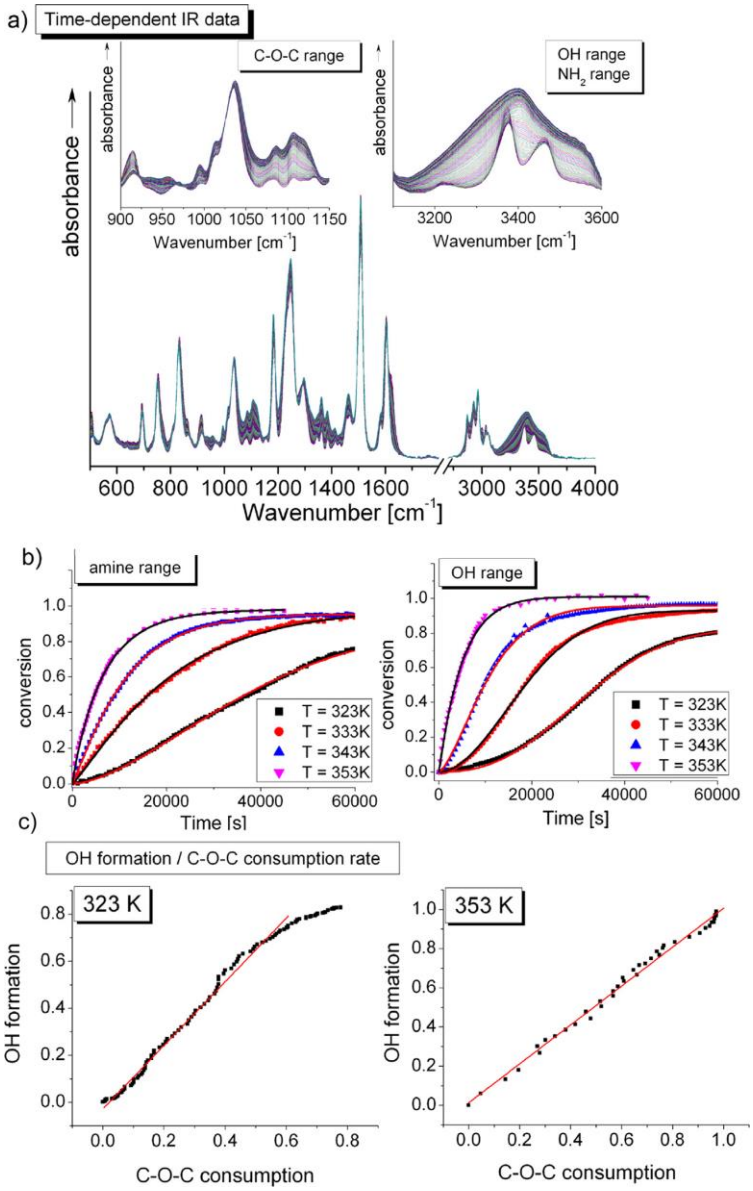

Fig. 1. Panel (a) presents time-dependent infrared spectra for bulk material in the spectral range (400–4000 cm^{-1}) with insets illustrating epoxy group (900–1150 cm^{-1}) and hydroxyl and amine groups region (3100–3600 cm^{-1}) upon polymerization. Panel (b) shows kinetic curves based on the integral intensity analysis of amine, epoxy (*left panel*), hydroxyl (*right panel*) bands for bulk material. Red lines are the best Avrami fits of the data. Panel (c) presents formation of OH moieties plotted *vs* consumption of C–O–C group at indicated temperatures. (For interpretation of the references to color in this figure legend, the reader is referred to the web version of this article.)

In Fig. 1 (b), kinetic curves constructed for the reaction carried out at four temperatures are shown. It is seen that they follow a sigmoidal shape for the reaction carried out at lower temperatures – characteristic for autocatalytic reactions. It is worth mentioning that this pattern is very often observed for the curing of epoxy/amine systems. According to the current knowledge, formation of the hydroxyl units in oligomers governs the first part of the step growth polymerization (initialization). Once they are produced, they act as a catalyst and propel the pace of the reaction [39]. Interestingly, with increasing temperature, kinetic curves follow an exponential trend, indicating significant reduction of the first step of polymerization. Our data presented in Fig. 1(b) reveals also another interesting finding: the consumption rate of amine moieties is slightly faster than the one determined for the production of hydroxyl units. This discrepancy becomes more evident at lower temperatures. Interestingly, linear dependency between both rates is found when plotted against each other (see panel (c) in Fig 1). This is a strong suggestion that the integral analysis of vibrations

assigned to primary amine and hydroxyl moieties can be used to follow kinetics of the polymerization reaction. Note also that the observed difference in the shape of kinetic curves presented in Fig. 1 (panels (b) and (c)) is likely due to the fact that either the mechanism of reaction follows different steps, or the intermolecular interactions between monomers and oligomers are significantly altered upon formation of the polymer. Hence, effectively, the integral position as well as intensity of the hydroxyl vibration band is affected.

To analyze kinetic curves, several models have been proposed. Smith et al. considered 3rd order reaction mechanism of this type of polymerization [40]. On the other hand, Horie and coworkers proposed a model – considering the autocatalytic role of the hydroxyl group generated during chemical reaction (autocatalysis) – which has been used and validated in many epoxy/amine systems at different temperatures [41]. According to this approach, reaction can be modeled with the use of the following equation:

$$d\alpha/dt = (k_1 + k_2\alpha^m)(1-\alpha)^n, \quad (2)$$

where α denotes conversion, k_1 and k_2 are rate constants, while m and n are the kinetic exponents of the reactions.

However, to study kinetics of the polymerization between DGEBA and aniline we have chosen the Avrami model [42], which also predicts the sigmoidal character of the reaction [43] and provides insight into the overall constant rate of reaction. It should be added that this model is commonly applied to describe various solid state chemical reactions [43–45]. The validity of this approach has been verified in numerous cases where the curing reaction is similar to that herein studied [46–48]. There is also another reason to use the Avrami model instead of Eq. (2). As it will be shown later on, the autocatalytic character of the polymerization seems to be lost in pores. Hence, the application of the autocatalytic model is not reasonable. On the other hand, the Avrami model can be used to describe kinetics of polymerization in bulk as well as under confinement. Hence, any uncertainties in determination of constant rates are model independent since the same equation was used to fit both bulk and confinement data. Therefore, experimental data presented in Fig. 2 (panels (a) and (b)) were fitted to the following equation:

$$\frac{\alpha}{\alpha_m} = 1 - \exp(-kt^n), \quad (3)$$

where α and α_m is monomer conversion and maximum monomer conversion, k is a constant rate of reaction and n is the Avrami exponent that is related to the mechanism of crystallization, or eventually, chemical reaction. As demonstrated in Fig. 2 (panels (c) and (d)), the Avrami model describes experimental data well, albeit with some slight deviation in the plateau regime. Therefore constant rates of the reaction (depicted by filled symbols in Fig. 2(f)) can be easily evaluated. We also observed that constant rates obtained from analysis of the integral intensity of the epoxy, hydroxyl, as well as amino moieties vibrations are fairly the same, yielding complementary information on the progress of polymerization. This holds in spite of the fact that some discrepancies in the consumption and formation rates of amine, epoxide and hydroxyl moieties, respectively, are noted. It should also be added that almost the same constant rates were obtained from complementary DSC measurements (data not shown). This information is crucial in the context of the analysis performed for the curing reaction in AAO pores.

Additionally, the activation barrier for the bulk reaction was determined from the Arrhenius equation:

$$k = k_0 \exp(E_a/RT), \quad (4)$$

where k_0 is a pre-exponential factor, E_a is the activation barrier and R is the universal gas constant. Interestingly, it was found that the activation energies obtained from the analysis of amine and epoxy integral intensities data are both equal to 54 kJ/mol (panel (f) in Fig. 2). This is in excellent agreement with the one evaluated from calorimetry, $E_a = 51$ kJ/mol (panel (f) in Fig. 2).

Having described in detail the kinetics of the bulk polymerization, we now turn our attention to the reaction carried out under geometrical constraints. As a first reference, FTIR spectra of the empty annealed membranes with pore diameter d = 150 nm and 35 nm were measured (panels (a) and (b) in Fig. 2). For the empty pores only bands associated with the stretching vibration of the hydroxyl moieties attached to the pore walls are detected. On the other hand, after filling the membranes with DGEBA and aniline, additional bands originating from the NH_2 stretching vibration (~3450 cm^{-1}) as well as due to the CH stretching vibrations such as $\nu(CH_3$-asym/sym), $\nu(CH_2$-asym/sym) and ν(CH) (2800–3200 cm^{-1} wavenumber region) can be found. Unfortunately, due to strong infrared absorption by AAO in the low-frequency range (400–1800 cm^{-1}), no information about epoxy ring vibration can be obtained. Hence, to study kinetics of the step growth polymerization, only bands connected to the stretching vibration of the NH_2 unit were used. Fig. 2(a) presents FTIR spectra obtained upon polymerization of DGEBA and aniline in AAO pores (d = 150 nm and 35 nm) at T = 323 K. In each case, the spectrum of empty membrane was subtracted from the ones measured upon reaction. According to our data, significant changes in the integral intensities of the amine (I_{NH2} decreases) and hydroxyl moieties (I_{OH} increases) are noticed. The intensities of the other bands originating from the $\nu(CH_3)$, $\nu(CH_2)$ and ν(CH) groups remain generally unchanged except of the ones observed around 3056 cm^{-1} that are assigned to the vibration of methylene moieties attached to the oxirane units. To study the progress of the reaction, infrared spectra were rescaled with respect to the most intense CH stretching band and then the integral intensity analysis of the band due to the vibration of the amine group was done.

Again, in order to display all kinetic curves on one graph, data were rescaled accordingly to Eq. (1) (see panels (c) and (d) in Fig. 2). It should be stressed that the maximum degree of monomer conversion for each reaction was determined using similar protocol of data analysis as in case of the bulk measurements (see panel (e) in Fig. 2). However, due to overlapping of the vibration of hydroxyl and amine moieties at high conversion in pores, precise determination of maximum degree of monomer conversion basing on the latter band can be strongly underestimated. Hence, we decided to apply an alternative way of analysis. A few years ago, there was quite hot debate on how to analyze mid-infrared data to get reliable information on progress of polymerization and monomer conversion. It was demonstrated that analysis of the integral intensity of the methylene band at around 3056 cm^{-1} (well visible in pores) provides the most valuable information on monomer conversion [49,50]. Thus, detailed analysis of this band enabled calculation of monomer conversion that was shown to be slightly lower with respect to the bulk reaction (see panel (e) in Fig. 2).

Kinetic curves reveal a very important finding concerning the mechanism of the reaction in pores (presented in panels (c) and (d) of Fig. 2). It is clear that in contrast to the bulk data, kinetic curves constructed for the reaction performed in AAO membranes (d = 150 nm and 35 nm) follow an exponential trend suggesting that the initial step of polymerization is suppressed. It is worth mentioning that there exists a view that this missing part of the reaction is strongly related to the formation of hydroxyl moieties at

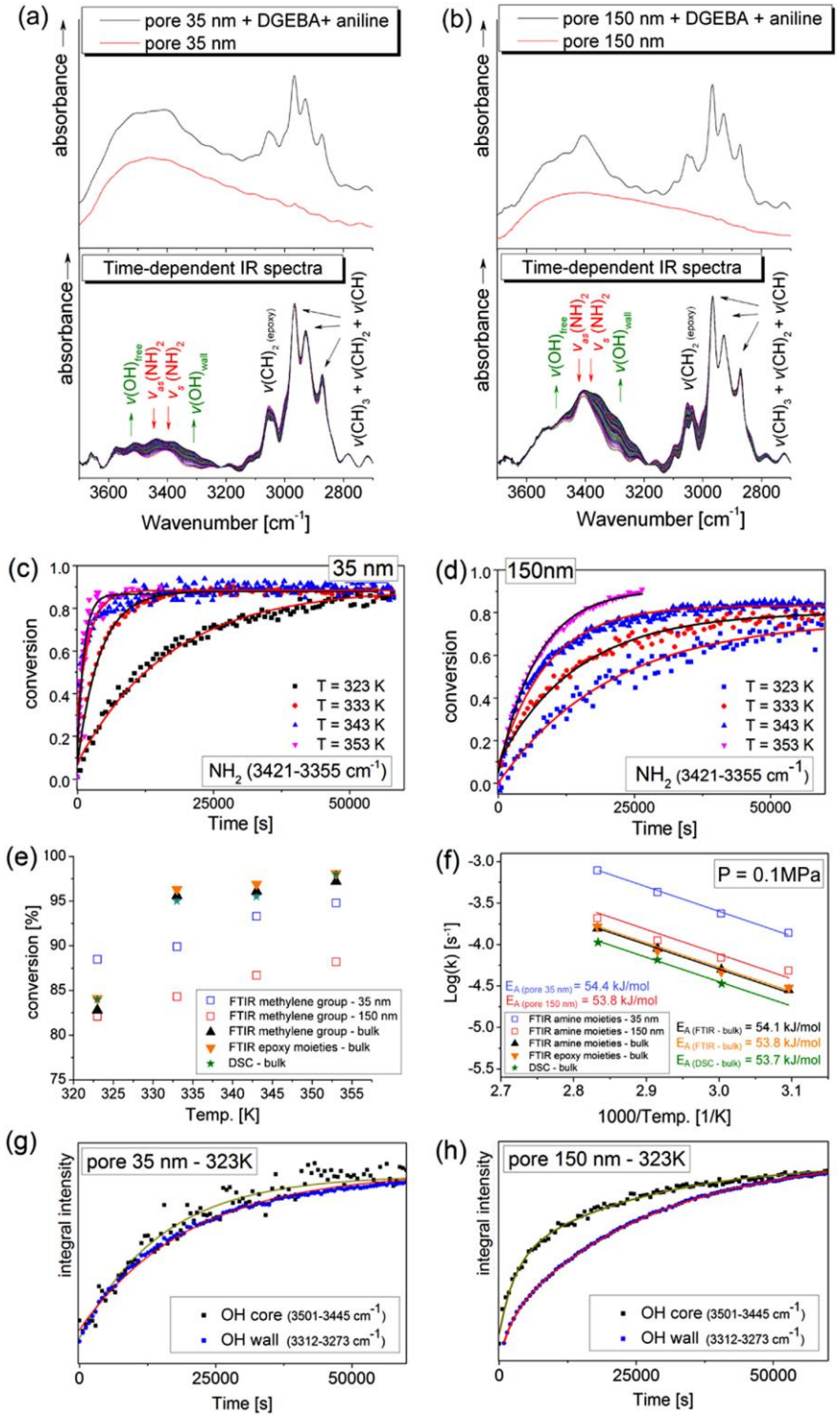

Fig. 2. Panels (a) and (b) each present FTIR spectra of an empty AAO membrane and one loaded with DGEBA and aniline as well as time-dependent multi spectra of Al_2O_3 pore with DGEBA and aniline after subtraction of the background (data for 35 nm and 150 nm pores). Panels (c) and (d) illustrate kinetic curves based on the integral intensity

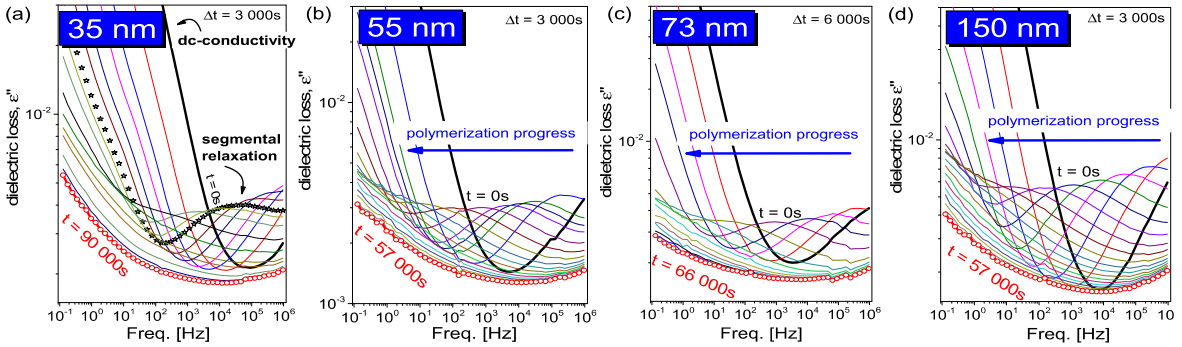

Fig. 3. Loss spectra obtained upon polymerization of DGEBA and aniline in AAO templates (with pore sizes indicated in nm) at T = 323 K, p = 0.1 MPa.

the ends of oligomers in the curing system that catalyze further progress of the polymerization. That notwithstanding, there are already OH units attached to the pore walls which should result in the reduction or even complete suppression of this slow part of the polymerization. Consequently, speeding up of the overall kinetics of the step growth polymerization with respect to the bulk conditions can be observed. This supposition is consistent with the experimental observation that polymerization of bisphenol-M dicyanate ester proceeds faster in the native pores when compared to silanized ones [30].

In the next step, kinetic curves (panels (c) and (d) of Fig. 2) were analyzed with the use of the Avrami equation, with n = 1 (exponential functions). As can be seen, these fits describe kinetic data quite well enabling calculation of the constant rates of the reactions which are depicted as open symbols in panel (f) of Fig. 2. Interestingly, the constant rates for the reaction at large pores (d = 150 nm) are slightly faster (≈1.5 times) than the ones evaluated for the bulk conditions while in case of smaller nanochannels (d = 35 nm), the reaction proceeds even much faster (≈5 times). The application of the Arrhenius law (Eq. (4)) enabled calculation of the activation barrier for the polymerization reaction which is unaffected under confinement; its variation is within experimental uncertainty (see panel (f) in Fig. 2).

Finally, FTIR spectra revealed another very interesting aspect of the polymerization under confinement that has been previously studied only at the theoretical level [32,33]. Infrared data provides information on the hydroxyl groups attached to the walls as well as those formed at the center of nanochannels. This enabled us to study kinetics of the step growth polymerization at these two locations. Thus, kinetic curves for both cases in different pore sizes were constructed (see panels (g) and (h) in Fig. 2). It is observed that in larger nanochannels, at least production rates of hydroxyl moieties at the pore walls proceeds slower at lower temperatures. This can be attributed to the decrease in the reactivity of the functional moieties caused by strong interactions between monomers and hydroxyl groups attached to the pore walls. Interestingly at higher temperatures as well as for the smaller pore sizes, this effect becomes negligible.

Hence, our kinetic studies using FTIR spectroscopy delivered valuable information on kinetics of the step growth polymerization under confinement. It is apparent that due to the presence of hydroxyl moieties attached to the pore walls, the autocatalytic character of the reaction is lost. This in turn has an impact on the overall kinetics of the polymerization in AAO pores. Nonetheless, confinement by itself is as much important since the kinetics of polymerization is significantly affected by pore size.

4. Molecular dynamics

In Fig. 3 dielectric loss spectra recorded upon polymerization of DGEBA and aniline in AAO membranes (of pore diameters ranging from 150 to 35 nm) at T = 323 K are presented. The loss spectra clearly portray two identifiable molecular processes. The first one, appearing at lower frequencies is characterized by the constant slope ($\varepsilon'' \approx \omega^{-1}$) and it is related to the dc-conductivity (charge transfer) while the second one, seen at higher frequencies is the segmental relaxation. It should be noted that both processes shift to lower frequencies with progress of polymerization due to the increase in viscosity induced by the growing chains of the newly formed polymers. Since segmental relaxation times are proportional to the viscosity, one can get information on the dynamics of growing chains from the evolution of this process. Notably, we also made a series of dielectric measurements for the reaction carried out at T = 293 K and a similar scenario as described above was observed.

Dielectric data presented in Fig. 3 reveals the following two: in the course of each reaction, the segmental relaxation moves out of the experimental window – a clear sign that the curing systems undergo vitrification (just as observed in bulk samples).

In the next step, dielectric loss spectra were analyzed with the use of Havriliak–Negami (HN) function (with a conductivity term) [51]:

$$\varepsilon(\varpi)'' = \frac{\sigma_{dc}}{\varepsilon_0 \varpi} + \frac{\Delta\varepsilon}{[1 + (i\varpi\tau_{HN})^{\alpha}]^{\beta}}, \quad (5)$$

where α and β are the shape parameters representing the symmetric and asymmetric broadening of given relaxation peaks, $\Delta\varepsilon$ is the dielectric relaxation strength, τ_{HN} is the HN relaxation time, ε_∞

analysis of the amine band for 35 nm and 150 nm pores. Red solid lines represents the best Avrami fits with n = 1. Panel (e) shows conversion rate based on the integral analysis of the band at 3056 cm^{-1} for bulk, 35 nm, 150 nm pores in comparison with FTIR analysis of epoxy group and DSC data. Panel (f) presents the constant rates plotted *vs* reciprocal temperature. Solid lines are the best fits to Equation (4). Panels (g) and (h) show the integral intensity analysis for the core OH and wall hydroxyl moieties for 35 nm and 150 nm pores, respectively. Solid lines are Avrami fits with n = 1. (For interpretation of the references to color in this figure legend, the reader is referred to the web version of this article.)

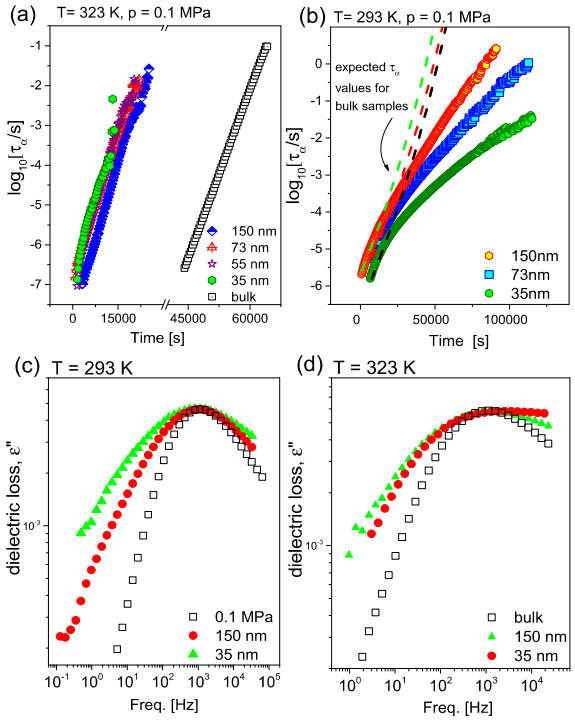

Fig. 4. Panels (a) and (b) present the evolution of segmental relaxation times upon polymerization of DGEBA and aniline at two indicated temperatures in AAO templates with different pore diameters. Dashed lines denote the time-dependence of segmental relaxation times expected for the bulk polymerization. Panels (c) and (d) illustrate the comparison of the distribution of relaxation times of the segmental relaxation process measured for the polymerization carried out under confinement at ambient pressure.

is the high frequency limiting permittivity, and ω is the angular frequency ($\omega = 2\pi f$). In panels (a) and (b) of Fig. 4, the evolution of the segmental relaxation times (τ_α) upon polymerization carried out at T = 323 K and T = 293 K in AAO membranes is presented. It should be mentioned that the value of τ_α was estimated from τ_{HN}, as presented in Ref. [52]. We observe that in each case, segmental relaxation moves into the experimental window much faster as compared to the bulk polymerization. However, once segmental relaxation time reaches $\tau_\alpha = 10^{-7}$s, further evolution of this process under confinement seems to be comparable to the bulk conditions, at least at T = 323 K. We must mention that we did not measure the evolution of segmental relaxation times for the bulk reaction carried out at T = 293 K due to the time required for such measurements (≈7 days).

In addition, it is worthy to note that we also observed rather untypical time dependence of segmental relaxation time τ_α for the measurements carried out at T = 293 K under confinement (see panel (a) in Fig. 4): a clear change in slope in the time dependence of segmental relaxation times is detected. We recall that usually an exponential or linear behavior is observed for this kind of reaction performed in bulk [53–55]. Hence, our experimental finding must be solely a characteristic feature of the polymerization carried out in AAO membranes. We speculate that this effect might be due to changes in density. Notably, our recent studies of small-molecule glass formers confined in uniaxial nanoporous alumina membranes found a similar trend in the structural relaxation times [56]. However, to get a deeper insight into this issue, further studies (e.g. on free volume by Positron Annihilation Spectroscopy) are necessary.

As a final point, dielectric loss peaks of the segmental relaxation process obtained upon polymerization of DGEBA and aniline at indicated conditions are compared (see panels (c) and (d) in Fig. 4). A systematic broadening of this process under confinements is observed. This effect is extremely pronounced on the low frequency (long time) part of the segmental relaxation. We attribute it mainly to the interactions, which seem to be quite strong, between the formed polymers and pore walls. Similar observations are reported for simple glass forming liquids and polymers confined in pores made from different materials [13,57,58]. This observation is in line with reports showing that due to strong interactions between pores, or more precisely hydroxyl groups attached to the nanochannels, and polymerizing systems, the character as well as speed of the curing is enhanced in native porous AAO membranes.

5. Conclusions

In this paper, kinetic and dynamics of step growth polymerization under different conditions have been investigated by infrared and broadband dielectric spectroscopies for the first time. We found that the speed of reaction is significantly enhanced in pores with respect to the bulk measurements. We have also demonstrated that the first step, usually related to the formation of short oligomers with OH moieties at the ends, characteristic for this kind of polymerization might be suppressed under confinement However, it should be stressed herein that we cannot rule out that this part of reaction occurred upon filling of the membranes. Although one should remember that the degree of monomer conversion was estimated to stay in the range 2–4 % after infiltration procedure. In addition we showed that the rate of production of hydroxyl moieties is slower at the surface of the nanochannels. This was attributed to the strong interaction between curing system and pore walls. Further dielectric investigations supported this observation. Moreover, a clear change in slope in the time dependence of the segmental relaxation times in AAO pores upon DGEBA and aniline polymerization was observed for the first time. We think that this might be related to some variation in density as shown by some of us in case of salol confined in AAO membranes. However, this point must be verified in the future.

Conflict of interest

The authors declare no financial conflict of interest.

Author contributions

The manuscript was written through contributions of all authors. All authors have given approval to the final version of the manuscript.

Acknowledgments

K.K., K.A. and M.T gratefully acknowledge financial support from the Polish National Science Centre within the program Sonata entitled “High pressure polymerization. The kinetic studies” based on decision DEC-2012/05/D/ST4/00326. M.D. is also thankful for the financial support of the NCN grants based on decision DEC-2012/07/N/ST5/02221. E.U.M. appreciates funding from the German Research Foundation (SPP 1369).

References

[1] Ha J-M, Wolf JH, Hillmyer MA, Ward MD. J Am Chem Soc 2004;126:3382.

[2] Jiang Q, Ward MD. Chem Soc Rev 2014;43:2066.
[3] Grigoriadis C, Duran H, Steinhart M, Kappl M, Jürgen Butt H, Floudas G. ACS Nano 2011;5:9208.
[4] Duran H, Steinhart M, Butt H-J, Floudas G. Nano Lett 2011;11:1671.
[5] Jackson CL, McKenna GB. Chem Mater 1996;8:2128.
[6] Park J-Y, McKenna GB. Phys Rev B 2000;61:6667.
[7] Zhang J, Liu G, Jonas J. J Phys Chem 1992;96:3478.
[8] Zheng W, Simon SL. J Chem Phys 2007;127:194501.
[9] Kremer F, Schonhals A. Dielectric relaxation spectroscopy; fundamentals and applications. Berlin: Springer; 2003.
[10] Koppensteiner J, Schranz W, Puica MR. Phys Rev B 2008;78:054203.
[11] Bras AR, Merino EG, Neves PD, Fonseca IM, Dionisio M, Schönhals A, et al. J Phys Chem C 2011;115:4616.
[12] Alcoutlabi M, McKenna GB. J Phys Condens Matter 2005;17:R461.
[13] Mapesa EU, Tarnacka M, Kamińska E, Adrjanowicz K, Dulski M, Kossack W, et al. RSC Adv 2014;4:28432.
[14] Alba-Simionesco C, Coasne B, Dosseh G, Dudziak G, Gubbins KE, Radhakrishnan R, et al. J Phys Condens Matter 2006;18:R15.
[15] Beiner M, Rengarajan GT, Pankaj S, Enke D, Steinhart M. Nano Lett 2007;7:1381–5.
[16] Rengarajan GT, Enke D, Steinhart M, Beiner M. J Mater Chem 2008;18:2537.
[17] Martin CR. Science 1994;266:1961.
[18] Azzaroni O, Lau KHA. Soft Matter 2011;7:8709.
[19] Serghei A, Zhao W, Miranda D, Russell TP. Nano Lett 2013;13:577.
[20] Comotti A, Bracco S, Mauri M, Mottadelli S, Ben T, Qiu S, et al. Angew Chem 2012;51:10136.
[21] Scelta D, Ceppatelli M, Santoro M, Bini R, Gorelli FA, Perucchi A, et al. Chem Mater 2014;26:2249.
[22] Reddy CS, Arinsteina A, Zussman E. Polym Chem 2011;2:835.
[23] Zetterlund PB. Polym Chem 2011;2:534.
[24] Giussi JM, Blaszczyk-Lezak I, Cortizo MS, Mijangos C. Polymer 2013;54:6886.
[25] Uemura T, Ono Y, Kitagawa K, Kitagawa S. Macromolecues 2008;41:87.
[26] Ng SM, Ogino S, Aida T, Koyano KA, Tatsumi T. Macromol Rapid Commun 1997;18:991.
[27] Zhao H, Simon SL. Polymer 2011;52:4093.
[28] Begum F, Simon SL. Polymer 2011;52:1539.
[29] Li Q, Simon SL. Macromolecules 2008;41:1310.
[30] Li Q, Simon SL. Macromolecules 2009;42:3573.
[31] Kidder MK, Buchanan AC. J Phys Chem C 2008;112:3027.
[32] Baschnagel J, Binder K. J Phys I Fr 1996;6:1271.
[33] Cui T, Ding JD, Chen JZY. Phys Rev E 2008;78:061802.
[34] Dannenberg H, Harp WR. Anal Chem 1956;28:81.
[35] Mijovic J, Andjelic S. Macromolecules 1995;28:2787.
[36] Mijovic J, Andjelic S, Yee CFW, Bellucci F, Nicolais L. Macromolecules 1995;28:2797.
[37] Poisson N, Lachenal G, Sautereau H. Vib Spectrosc 1996;12:237.
[38] Xu LS, Schlup JR. J Appl Polym Sci 1998;67:895.
[39] Yousefi A, Lafleur PG, Gauvin R. Polym Compos 1997;18:157.
[40] Smith IT. Polymer 1961;2:95.
[41] Horie K, Hiura H, Sawada M, Mitta I, Kambe H. J Polym Sci A 1970;8:1357.
[42] Avrami M. J Chem Phys 1939;7:1103. 1940; 8: 212; 1941; 9: 177.
[43] Schettino V, Bini R. Chem Soc Rev 2007;36:869.
[44] Kossack W, Kipnusu WK, Dulski M, Adrjanowicz K, Madejczyk O, Kaminska E, et al. J Chem Phys 2014;140:215101.
[45] Wlodarczyk P, Kaminski K, Dulski M, Haracz S, Paluch M, Ziolo J. J Non-Cryst Solids 2010;356:738–42.
[46] Lu MG, Shim MJ, Kim SW. J Therm Anal Calorim 1999;58:701–9.
[47] Muzumdar SV, Lee LJ. Polym Eng Sci 1996;36:943–52.
[48] Yiyun C, Dazhu C, Rongqiang F, Pingsheng H. Polym Int 2005;54:495–9.
[49] Mijovic J, Andjelic S. Polymer 1996;37:1295–303.
[50] Nikolic G, Zlatkovic S, Cakic M, Cakic S, Lacnjevac C, Rajic Z. Sensors 2010;10:684–96.
[51] Havriliak S, Negami S. J Polym Sci C 1966;14:99–117.
[52] Alvarez F, Alegria A, Colmonero J. Phys Rev B 1991;44:7306.
[53] Johari GP. J Chem Soc Faraday Trans 1994;90:883.
[54] Eloundou JP. Eur Polym J 2002;38:431.
[55] Corezzi S, Fioretto D, Rolla P. Nature 2002;420:653–6.
[56] K. Adrjanowicz, K. Kolodziejczy, W.K. Kipnusu, M. Tarnacka, E.U. Mapesa, A. Pazdzierniok, et al. submitted to The Journal of Physical Chemistry C.
[57] Tress M, Erber M, Mapesa EU, Huth H, Muller J, Serghei A, et al. Macromolecules 2010;43:9937.
[58] Tress M, Mapesa EU, Kossack W, Kipnusu WK, Reiche M, Kremer F. Science 2013;314:1371.

3. Podsumowanie i dalsze perspektywy badawcze

Celem niniejszej pracy doktorskiej było opracowanie odpowiedniej metody analizy danych dielektrycznych uzyskanych w warunkach wysokiego ciśnienia oraz charakterystyka kinetyki różnych reakcji polimeryzacji w warunkach podwyższonego ciśnienia. W przypadku polimeryzacji jonowej glicydolu pokazano, że wzrost ciśnienia (aż do 800 MPa) powoduje (*i*) wzrost szybkość reakcji [podobnie jak wzrost temperatury], (*ii*) eliminacje reakcji pobocznych [takich jak m.in. makrocyklizacja, deprotonacja] oraz ostatecznie również (*iii*) powstawanie polimeru o wyższych masach cząsteczkowych.

Również w przypadku reakcji polimeryzacji żywic epoksydowych z udziałem różnych anim pierwszorzędowych nasze badania wykazały, że ciśnienie bardzo mocno przyspiesza reakcję, jednakże w wąskim zakresie ciśnień. Powyżej pewnego progowego ciśnienia polimeryzacja stawała się wolniejsza. Miało to związek z całkowitą zmianą mechanizmu reakcji. W ciśnieniach wyższych niż 300 MPa zarówno lepkość, jak i gęstość była na tyle duża, że dyfuzja stawała się czynnikiem kontrolującym całkowicie przebieg reakcji.

Zaproponowana przez nas nowa metoda analizy danych dielektrycznych została z powodzeniem zweryfikowana za pomocą dodatkowych pomiarów z wykorzystaniem techniki IR oraz DSC, dając w przypadku wszystkich stosowanych technik porównywalne wartości stałych szybkości reakcji oraz energii aktywacji. Ponadto otrzymane wyniki pokazały, że wartość objętości aktywacji procesu znacząco zależy od rodzaju użytej w reakcji aminy. Obliczone ΔV zawierały się w przedziale od -38 do -18 cm^3/mol – najwyższa wartość objętości aktywacji została uzyskana dla układu z aminą aromatyczną (aniliną), a najwyższa dla aminy alifatycznej (2- etylohelksyloaminy). Ponadto zaobserwowano, że wartość ΔV bardzo silnie zależy również od warunków procesu. W przypadku układu z 2- etylheksylaminą ΔV= - 38cm^3/mol oraz -46 cm^3/mol dla reakcji prowadzonej w ciśnieniu atmosferycznym, odpowiednio w T=293 K i w T=313 K. Oszacowane wartości objętości aktywacji znacznie różnią się między sobą, co w pewien sposób kwestionuje przyjmowanie jednej wartości tego parametru dla konkretnych typów reakcji, jak powszechnie postępuę się w literaturze naukowej poświęconej tej tematyce. Nasze badania jednoznacznie wykazały, że objętość aktywacji jest funkcją warunków termodynamicznych i może się zmieniać w bardzo szerokim zakresie.

Innym niezwykle intersującym wątkiem naszych badań są reakcje polimeryzacji prowadzone w układach ograniczonych przestrzennie. Zostało przedstawione, że reakcja poliaddycji DGEBY i aniliny zachodzi znacznie szybciej w uniaksjalnych porach wykonanych z tlenku glinu. Pomiary z wykorzystaniem spektroskopii w podczerwieni i dielektrycznej rzuciły nowe światło na zagadnienie polimeryzacji w porach. Wskazaliśmy, że reakcja ta nie ma już charakteru autokatalitycznego. Dodatkowo zaobserwowaliśmy, że szybkość reakcji wzrasta wraz ze zwiększeniem ograniczenia geometrii próbki (czyli wraz ze zmniejszeniem średnicy membran aluminiowych). Za pomocą spektroskopii w podczerwieni udało nam się również rozróżnić 2 typy molekuł znajdujących się w tych układach: molekuły znajdujące się przy ściankach oraz znajdujące się wzdłuż osi kanałów. Ponadto dalsza analiza wykazała jednak, że układy te charakteryzują się: (*i*) wysokim stopniem konwersji oraz (*ii*) stałą energia aktywacji procesu niezależnie od stopnia ograniczenia geometrii próbek równą 54 kJ/mol.

Natomiast w ramach dalszej pracy naukowej chciałabym skupić się na wpływie wysokiego ciśnienia oraz dwuwymiarowego ograniczenia przestrzennego na: (*i*) poliaddycję innych wybranych układów aminowo-epoksydowych, (*ii*) polimeryzację przebiegającą z otwarciem pierścienia laktonowego na przykładzie wybranych laktonów (m.in. δ-walerolakton, ε-kaprolakton) oraz (*iii*) polimeryzację rodnikową monomerycznych cieczy jonowych. Ponadto chciałabym określić wpływ badanych warunków reakcji na podstawowe własności fizykochemiczne, takie jak: rozkład mas cząsteczkowych, temperaturę zeszklenia, przewodnictwo stałoprądowe, morfologię i strukturę otrzymanych makrocząsteczek. Dodatkowo za pomocą zebranych danych chciałabym stworzyć model umożliwiający przewidywanie szybkości reakcji i objętości aktywacji (ΔV) w różnych warunkach termodynamicznych oraz precyzyjne planowanie reakcji syntezy przy minimalnym prawdopodobieństwie zachodzenia reakcji ubocznych współtowarzyszących przemianie głównej.

Należy jednak podkreślić fakt, że obecnie w literaturze można znaleźć bardzo niewiele prac poświęconych kinetyce reakcji prowadzonych zarówno w warunkach podwyższonego ciśnienie, jak również w nanoukładach. Dlatego też dalsze badania nad przebiegiem polimeryzacji we wspomnianych warunkach niewątpliwie w znaczący sposób wzbogacą obecny stan wiedzy, a w dalszej perspektywie będą mogły posłużyć do zaprojektowania nowych, innowacyjnych i niekonwencjonalnych metod syntezy

pozwalających na swobodne otrzymywanie polimerów niezbędnych w nieustannym rozwoju przemysłu oraz nanotechnologii.

Dodatkowo chciałabym również zgłębić wątek przejść fazowych oraz dynamiki molekularnej w fazie przechłodzonej i szklistej substancji mało- i wielkocząsteczkowych w układach ograniczonych przestrzennie (jedno i dwuwymiarowo), które wierzę, że pozwolą na dokładniejsze zrozumienie zjawisk obserwowanych w reakcjach polimeryzacji prowadzonych w analogicznych układach. Dotychczasowe dane literaturowe pokazują dużą heterogeniczność oraz anizotropię upakowania substancji w układach ograniczonych przestrzennie, czego konsekwencją jest istnienie nieidentycznych frakcji molekuł o zróżnicowanej dynamice molekularnej. Należy wspomnieć, że nasz badania pozwoliły na rozróżnienie dwóch frakcji (przyściankowej oraz rdzeniowej), których dynamika jest ściśle związana z obserwowanym przejściem szklistym [54]. Ponadto najnowsze pomiary wskazują, że obserwowana różnica mobilności molekuł umieszczonych w uniaksjalnych porach jest niewątpliwie związana z generowaniem się ujemnych ciśnień w układzie [57].

W przyszłości nasz zespół badawczy planuje również przeprowadzić pionierskie badania nad układami reagującymi w porach w warunkach podwyższonego ciśnienia. Oczekujemy, że poprzez kombinację obydwu parametrów możliwe będzie stworzenie pełniejszego obrazu obserwowanych zjawisk oraz zwiększenie kontroli nad przebiegiem procesu syntezy. Mamy wielką nadzieję, że planowane przez nas systematyczne dalsze badania znacząco pogłębią obecny stan wiedzy oraz umożliwią dynamiczny rozwój nanotechnologii poprzez syntezę materiały o całkowicie kontrolowanej morfologii tzw. nanodrutów, nanowłókien, o unikalnych własnościach fizykochemicznych.

Spis literatury

[1] Glossary of Basic Terms in Polymer Science, *Pure & Appl. Chem*. 1996, **68**, 2287-2311.

[2] Z prac Komisji Nomenklatury Makromolekularnej IUPAC. Słownik Podstawowych Terminów w Nauce o Polimerach, *Polimery* 1998, **43**, 637-644.

[3] W. Przygocki, A. Włochowicz, *Fizyka Polimerów*, PWN, Warszawa 2001

[4] A. Kreślak, *Przemysł polimerów*, Ministerstwo Środowiska, Warszawa 2005

[5] A. Stolarzewicz, *Metody syntezy polimerów i ich charakterystyka*, UŚ, Katowice 2005

[6] E. Bortel, *Polimery* 2002, **9**, 591-676.

[7] P. M. Kazmaier, K. A. Moffat, M. K. Georges, R. P. N. Vergin, G. K. Hamer, *Macromolecules* 1995, **28**, 1841.

[8] W. Davenport, L. Michalak, E. Malstrom, M. Mate, B. Kurdi, C. J. Hawker, G. G. Barclay, R. Sinta, *Macromolecules* 1997, **30**,7929.

[9] M. K. Georges, R. P. N. Veregin, P. M. Kazmaier, G. K. Hamer, *Macromolecules* 1993, **26**, 2987.

[10] J. S. Wang, K. Matyjaszewski, *J. Am. Chem. Soc.* 1995, **117**, 5614.

[11] K. Matyjaszewski , J. H. Xia , *Chem. Rev.* 2001, **101**, 2921.

[12] N. V. Tsarevsky , K. Matyjaszewski , *Chem. Rev*. 2007, **107,** 227.

[13] J. Chiefari, Y. K. Chong, F. Ercole, J. Krstina, J. Jeffery, T. P. T. Le, R. T. A. Mayadunne, G. F. Meijs, C. L. Moad, G. Moad, E. Rizzardo, S. H. Thang, *Macromolecules* 1998, **31**, 5559–5562.

[14] M. Destarac, D. Charmot, X. Franck, S. Z. Zard, *Macromolecular Rapid Communications* **2000, 21**, 1035–1039.

[15] G. Moad, E. Rizzardo, S. H. Thang, *Australian Journal of Chemistry* 2005, **58**, 379–410.

[16] D. Chelazzi, M. Ceppatelli, M. Santoro, R. Bini, and V. Schettino, *Nature Mat*. 2004, **3**, 470.

[17] M. Citroni, M. Ceppatelli, R. Bini, V. Schettino, *Science* 2002, **295**, 85505.

[18] S. W. Benson, *J. Chem. Phys.* 1967, **46**, 4920

[19] M. Citrini, M. Ceppatelli, R. Bini and V. Scettino, *J. Phys. Chem. B* 2007**, 111**, 3910–3917

[20] J. L. Binder, K. C. Eberly, G. E. P. Smith, Jr., *J. Polym. Sci.* 1959, **38**, 229

[21] *Chemia polimerów t. 1,* praca zbiorowa pod redakcją Z. Florjańczyka i S. Penczka, Oficyna Wydawnicza Politechniki Warszawskiej, Warszawa 2001

[22] J. Fournier, G. Williams, C. Duch and G. A. Aldridge, *Macromolecules* 1996**, 29**, 7097–7107

[23] F. Ricciardi, W. A. Romanchick and M. M. Joullie, *J. Polym. Sci. Part A: Polym. Chem*. 1983, **21**, 1475–1490

[24] G. Levita, A. Livi, P. A. Rolla and C. Culicchi, *J. Polym. Sci. Part B: Polym. Phys*. 1996, **34**, 2731–2737

[25] E. Tombari, C. Ferrari, G. Salvetti and G. P. Johari, *J. Phys.: Condens. Matter* 1997, **9**, 7017–7037

[26] K. Adrjanowicz, D. Zakowiecki, K. Kaminski, L. Hawelek, K. Grzybowska, M.Tarnacka, M. Paluch, and K. Call, *Mol. Pharm.* 2012, **9**, 1748–1763

[27] M. Tarnacka, K. Adrjanowicz, E. Kaminska, K. Kaminski, K. Grzybowska, K. Kolodziejczyk, P. Wlodarczyk, L. Hawelek, G. Garbacz and A. Kocot, M. Paluch, *Phys. Chem. Chem. Phys.* 2013,**15**, 20742-2075

[28] G. Galonne, S. Capaccioli, G. Levita, P. A. Rolla, S. Corezzi, *Polym. Int.* 2001, **50**, 54

[29] E. Kaminska, M. Tarnacka, P. Włodarczyk, K. Jurkiewicz, K. Kołodziejczyk, M. Dulski, D. Haznar-Garbacz, L. Hawelek, K. Kaminski, A. Wlodarczyk, and M. Paluch, *Mol. Pharm*. 2015, **12**, 3007–3019

[30] P. Wlodarczyk, K. Kaminski, M. Paluch, J. Ziolo, *J. Phys. Chem. B* 2009, **113**, 4379

[31] P. Wlodarczyk, K. Kaminski, S. Haracz, M. Dulski, M. Paluch, J. Ziolo, M. Wygledowska-Kania, *J. Chem. Phys*. 2010, **132**, 19510.

[32] Z. Wojnarowska, P. Wlodarczyk, K. Kaminski, K. Grzybowska, L. Hawelek, M. Paluch, *J. Chem. Phys*. 2010, **133**, 094507

[33] J. Mijovic and B. D. Fitz, *Dielectric Spectroscopy of Reactive Polymers: Application Note Dielectrics 2*, Novocontrol, Hundsangen, Germany, vol. 591, 1998

[34] F. Kremer, A. Schonals, Eds., *Dielectric Relaxation Spectroscopy. Fundamentals and Applications*, Springer-Verlag, Berlin, 2002

[35] M. Avrami, *J. Chem. Phys*. 1939, **7**, 1103; 1940, **8**, 212; 1941, **9**, 177

[36] K. Horie, H. Hiura, M. Souvada, I. Mita and H. Kambe, *J. Appl. Polym. Sci. A: Polym. Chem*. 1970, **8**, 1357

[37] M. R. Kamal, *Polym. Eng. Sci.* 1974, **14**, 23

[38] A. Yousefi, P. G. Lafleur, R .Gauvin, *Polymer Composities* 1997, **18**, 157-168

[39] T. Asano and W. J. le Noble, *Chem. Rev*. 1978, **78,** 407–489

[40] R. van Eldik, T. Asano and W. J. le Noble, *Chem. Rev*. 1989, **89**, 549–688

[41] A. Drljaca, C. D. Hubbard, R. van Eldik, T. Asano, M. V. Basilevsky and W. J. le Noble, *Chem. Rev.* 1998, **98**, 2167–2289

[42] V. D. Kiselev, M. S. Shikhaab, G. G. Iskhakova, A. I. Konovalov, *Russ. J. Gen. Chem*. 2002**, 72,** 983104

[43] D. A. Wasylyshyn and G. P. Johari, *J. Polym. Sci. Part B: Polym. Phys*. 1997, **35**, 437–456.

[44] D. A. Wasylyshyn and G. P. Johari, *J. Polym. Sci. Part B: Polym. Phys*. 1999, **37**, 3071–3083.

[45] G. P. Johari, *J. Chem. Soc. Faraday Trans.* 1994, **90**, 883–888.

[46] http://www.synkerainc.com/products-services/unikera-ceramic-membranes/unikera-standard

[47] A. Comotti, S. Bracco, M. Mauri, S. Mottadelli, T. Ben, S. Qiu, et al. *Angew. Chem.* 2012, **51**, 10136.

[48] D. Scelta, M. Ceppatelli, M. Santoro, R. Bini, F. A. Gorelli, A. Perucchi, *Chem. Mater.* 2014, **26**, 2249.

[49] C. S. Reddy, A. Arinsteina, E. Zussman, *Polym. Chem*. 2011, **2**, 835.

[50] J. M. Giussi, I. Blaszczyk-Lezak, M. S. Cortizo, C. Mijangos, *Polymer* 2013, **54**, 6886.

[51] Q. Li, S. L. Simon, *Macromolecules* 2008, **41**, 1310.

[52] Y. Chai, T. Salez, J. D. McGraw, M. Benzaquen, K. Dalnoki-Veress, E. Raphaël, J. A. Forrest, *Science* 2014, **343**, 994

[53] Z. Fakhraai and J. A. Forrest, *Science* 2008, **319**, 600

[54] K. Adrjanowicz, K. Kolodziejczyk, W. K. Kipnusu, M. Tarnacka, E. U. Mapesa, E. Kaminska, S. Pawlus, K. Kaminski and M. Paluch, *J. Phys. Chem. C* 2015, **119**, 14366–14374

[55] E. U. Mapesa, M. Tarnacka, E. Kaminska, K. Adrjanowicz, M. Dulski, W. Kossack, M. Tress, W. K. Kipnusu, K. Kaminski and F. Kremera, *RSC Adv.* 2014, **4**, 28432–28438

[56] M. Tress, E.U. Mapesa, W. Kossack, W.K. Kipnusu, M. Reiche, F. Kremer, *Science* **2013**, 314, 1371-137

[57] K. Adrjanowicz, K. Kaminski, K. Koperwas, M. Paluch, *Phys. Rev. Lett*. 2015, **115**, 265702